Acta Universitatis Tamperensis 2255

MINNA AMPUJA

BMP4 in Breast Cancer Growth and Metastasis with Insights into Transcriptional Regulation

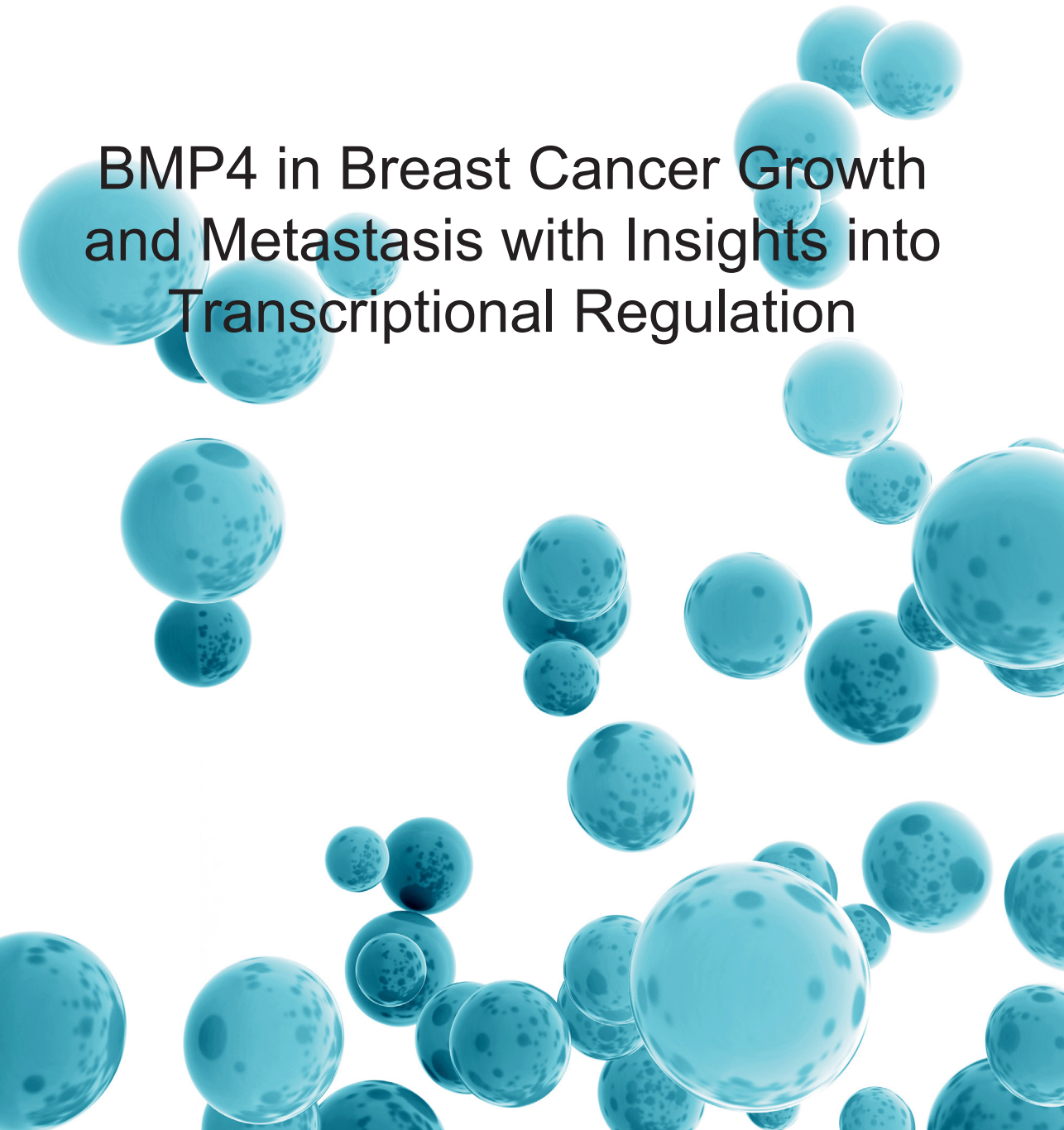

MINNA AMPUJA

BMP4 in Breast Cancer Growth and Metastasis with Insights into Transcriptional Regulation

■

ACADEMIC DISSERTATION
To be presented, with the permission of
the Board of the Faculty of Medicine and Life Sciences
of the University of Tampere, for public discussion
in the auditorium F114 of the Arvo building,
Lääkärinkatu 1, Tampere,
on 24 Febryary 2017, at 12 o'clock.

UNIVERSITY OF TAMPERE

MINNA AMPUJA

BMP4 in Breast Cancer Growth and Metastasis with Insights into Transcriptional Regulation

Acta Universitatis Tamperensis 2255
Tampere University Press
Tampere 2017

UNIVERSITY
OF TAMPERE

ACADEMIC DISSERTATION
University of Tampere, Faculty of Medicine and Life Sciences
BioMediTech Institute
Fimlab Laboratories
Finland

Supervised by
Professor Anne Kallioniemi
University of Tampere
Finland
PhD Emma-Leena Alarmo
University of Tampere
Finland

Reviewed by
Docent Erkki Hölttä
University of Helsinki
Finland
Docent Katri Koli
University of Helsinki
Finland

Cover design by
Mikko Reinikka

Acta Universitatis Tamperensis 2255
ISBN 978-952-03-0349-5 (print)
ISSN-L 1455-1616
ISSN 1455-1616

Acta Electronica Universitatis Tamperensis 1756
ISBN 978-952-03-0350-1 (pdf)
ISSN 1456-954X
http://tampub.uta.fi

Suomen Yliopistopaino Oy – Juvenes Print
Tampere 2017

Contents

List of original communications

This thesis is based on the following communications, which are referred to by the corresponding Roman numerals.

I Ampuja M, Jokimäki R, Juuti-Uusitalo K, Rodriguez-Martinez A, Alarmo EL, Kallioniemi A. BMP4 inhibits the proliferation of breast cancer cells and induces an MMP-dependent migratory phenotype in MDA-MB-231 cells in 3D environment. BMC Cancer 2013;13:429.

II Ampuja M, Alarmo EL, Owens P, Havunen R, Gorska AE, Moses HL, Kallioniemi A. The impact of bone morphogenetic protein 4 (BMP4) on breast cancer metastasis in a mouse xenograft model. Cancer Lett 2016; 375:238-44.

III Ampuja M*, Rantapero T*, Rodriguez-Martinez A*, Palmroth M, Alarmo EL, Nykter M, Kallioniemi A. Integrated RNA-seq and DNase-seq analyses identify phenotype-specific BMP4 signaling in breast cancer. BMC Genomics 2017;18:68.

* Equal contribution

The publication No. III will also be used in the doctoral thesis of Tommi Rantapero

Abbreviations

BAMBI	BMP and activin membrane-bound inhibitor
BLI	bioluminescence imaging
BMP	bone morphogenetic protein
BMPR1A	BMP receptor type 1A
bp	base pair
BRE	BMP response element
CAF	cancer-associated fibroblast
ChIP	Chromatin immunoprecipitation
CBFB	Core binding factor β
DEG	differentially expressed gene
DHS	DNase hypersensitivity site
DNase-seq	DNase I hypersensitive sites sequencing
ECM	Extracellular matrix
EMT	Epithelial-to-mesenchymal transition
FBS	Fetal bovine serum
G-CSF	Granulocyte colony-stimulating factor

GDF	Growth and differentiation factor
GFP	Green fluorescent protein
GO	gene ontology
H&E	Hematoxylin and eosin
HIF1A	Hypoxia-inducible factor 1α
IHC	Immunohistochemistry
IF	Immunofluorescence
MAPK	Mitogen-activated protein kinase
MH	MAD homology
MMP	Matrix metalloproteinase
NGS	next-generation sequencing
PEG	poly(ethylene glycol)
PI	Propidium iodide
PWM	Position weight matrix
qRT-PCR	quantitative reverse transcription polymerase chain reaction
rhBMP4	recombinant human BMP4
RNA-seq	RNA sequencing
SBE	SMAD-binding element
siRNA	Small interfering RNA

SMAD	Sma- and Mad-related protein
SMURF	Smad ubiquitination regulatory factor/SMAD specific E3 ubiquitin protein ligase
TCGA	The Cancer Genome Atlas
TGF-β	Transforming growth factor β
TF	Transcription factor
TFBS	Transcription factor binding site
TRAP	Tartrate-resistant acid phosphatase
TSS	Transcription start site

Abstract

Breast cancer is the most common cancer in women worldwide. The bone morphogenetic proteins (BMPs) are signaling molecules that are often aberrantly regulated in cancer. BMP4 has previously been shown to reduce the proliferation of breast cancer cells and in some cases increase their migration. However, these studies have been done using standard 2D culture. The aim of this study was to characterize the effect of BMP4 on breast cancer cells in 3D culture and using an in vivo model, as well as to study BMP4 target genes and signaling pathway regulation.

Several different breast cancer cell lines were grown in both the synthetic PEG gel and biologically-derived Matrigel. BMP4 inhibited the proliferation of cells in both materials. The growth inhibition was examined more closely in Matrigel, showing that the effect was partly due to p21 induction. In addition, in response to BMP4 MDA-MB-231 breast cancer cells in Matrigel formed large, branching structures, indicative of increased migration/invasion. This reaction was dependent on matrix metalloproteinases.

The migration/invasion effect promoted by BMP4 was examined in more detail by using a mouse model and following the effects of BMP4 on metastasis formation. The mice were injected intracardially with MDA-MB-231 cells and treated with BMP4 or vehicle control. The mice treated with BMP4 had slightly more bone metastases, but less adrenal gland metastases compared to the vehicle group. The activation of BMP signaling, epithelial-to-mesenchymal transition, as well as blood vessels and cancer-associated fibroblasts were studied from the metastases. However, there were no differences between the treatment groups. Interestingly, in both groups osteoclast marker staining was found among the cancer cells.

In order to study BMP4 signaling, MDA-MB-231 and T-47D breast cancer cells were treated with BMP4 or vehicle and differences in gene expression (RNA-seq) and in regulatory regions of the genome (DNase-seq) were analyzed. RNA-seq data showed that the responses of the cell lines to BMP4 were different, although there were also common BMP4 target genes, which were also target genes in additional cell lines when tested with qPCR. Enrichment analysis revealed that in MDA-MB-231 cells, which react to BMP4 with increased migration, motility-related genes were enriched. Correspondingly, in T-47D cells, which respond with reduced

proliferation, genes related to development and signaling were enriched. Similar results were obtained when analyzing enrichment of chromatin regions that were opened due to BMP4 treatment. Moreover, based on the open chromatin regions, three transcription factors (MBD2, CBFB and HIF1A) were chosen for functional analyses using siRNA and validated as BMP4 downstream regulators. Of these, MBD2 was mainly an activator in both cell lines, CBFB in T-47D cells and HIF1A acted as a repressor in MDA-MB-231 cells.

Taken together, BMP4 inhibits proliferation and increases migration in both 2D and 3D culture, but more studies are needed to clarify the role of BMP4 in metastasis formation, particularly in bone metastases. The effects of BMP4 are reflected in gene expression and chromatin openness. Additionally, depending on the effects different transcription factors seem to regulate BMP4 target genes.

Tiivistelmä

Rintasyöpä on maailmanlaajuisesti naisten yleisin syöpä. Luun morfogeneettiset proteiinit (bone morphogenetic protein, BMP) ovat signalointimolekyylejä, jotka ovat usein syövässä poikkeavalla tavalla säädeltyjä. BMP4:n on aiemmin näytetty hidastavan rintasyöpäsolujen kasvua ja joissakin tapauksissa samalla lisäävän niiden migraatiokykyä. Nämä tutkimukset on kuitenkin tehty standardimallisessa 2D kasvatuksessa. Tämän tutkimuksen tavoitteena oli tutkia BMP4:n vaikutusta rintasyöpäsoluihin 3D- ja in vivo -malleissa, sekä lisäksi tutkia BMP4-reitin kohdegeenejä ja signaalinsäätelyä.

Usean eri rintasyöpäsolulinjan soluja kasvatettiin sekä synteettisessä PEG geelissä että biologisesta lähteestä saadussa Matrigeelissä. BMP4 hidasti solujen kasvua molemmissa materiaaleissa. Kasvun laskua tutkittiin lähemmin Matrigeelissä ja efektin todettiin johtuvan osittain p21 induktiosta. Lisäksi MDA-MB-231 rintasyöpäsolut Matrigeelissä muodostivat BMP4:n vaikutuksesta isoja haarautuvia rakenteita, jotka viittaavat lisääntyneeseen migraatioon/invaasioon. Tämä reaktio oli matriksin metalloproteinaaseista riippuvainen.

BMP4:n aiheuttamaa migraatio/invaasioefektiä tutkittiin tarkemmin käyttämällä hiirimallia ja seuraamalla BMP4:n kykyä vaikuttaa metastaasien muodostukseen. Hiirten sydämiin injektoitiin MDA-MB-231 soluja ja niitä käsiteltiin BMP4:llä tai vehikkelikontrollilla. BMP4-käsitellyissä hiirissä oli jonkin verran enemmän luumetastaaseja, mutta vähemmän lisämunuaismetastaaseja kuin vehikkeliryhmässä. Metastaaseista tutkittiin BMP signaloinnin aktivoitumista, kasvua, epiteeli-mesenkymaalitransitiota sekä verisuonia ja syöpään liittyviä fibroblasteja (cancer-associated fibroblasts). Eroa ryhmien välillä ei kuitenkaan ollut. Mielenkiintoista oli että molemmissa ryhmissä löytyi osteoklastimarkkerin värjäytymistä syöpäsolujen joukosta.

BMP4:n signaloinnin tutkimusta varten MDA-MB-231 ja T-47D rintasyöpäsoluja käsiteltiin BMP4:llä tai vehikkelillä ja analysoitiin geenien ilmentymiseroja (RNA-seq) ja genomissa olevia säätelyalueita (DNaasi-seq). RNA-seq data osoitti solulinjojen olevan keskenään hyvin erilaisia, vaikka myös yhteisiä BMP4 kohdegeenejä löytyi. Rikastumisanalyysi paljasti, että MDA-MB-231 soluissa, jotka reagoivat BMP4:ään lisääntyneellä migraatiolla, liikkumiseen liittyvät geenit olivat rikastuneet. Vastaavasti

T-47D soluissa, joissa tapahtuu kasvun hidastuminen BMP4:n vaikutuksesta, kehitykseen ja signalointiin liittyvät geenit olivat rikastuneet. Samanlaiset tulokset saatiin kun analysoitiin BMP4:n aiheuttamien avoimen kromatiinin alueiden rikastumista. Lisäksi avoimen kromatiinin analysoinnin avulla valittiin kolme transkriptiotekijää, MBD2, CBFB ja HIF1A, joiden validoitiin funktionaalisten siRNA-kokeiden perusteella olevan BMP4-reitin alavirran säätelijöitä. Näistä MBD2 toimi säätelyn aktivaattorina molemmissa solulinjoissa, CBFB T-47D soluissa ja HIF1A toimi repressorina MDA-MB-231 soluissa.

Yhteenvetona BMP4:llä on kasvua vähentäviä ja migraatiota lisääviä vaikutuksia sekä 2D että 3D kasvatuksissa, mutta lisätutkimuksia tarvitaan selventämään BMP4:n osuutta metastaasien muodostuksessa, erityisesti luumetastaaseissa. BMP4:n aiheuttamat muutokset heijastuvat geenien ilmentymiseen ja kromatiinin aukeamiseen. Lisäksi muutoksista riippuen eri transkriptiotekijät vaikuttavat säätelevän BMP4:n kohdegeenejä.

1 Introduction

Cancer is a malignant form of cell growth, which starts with one cell, where a mutation favorable to unlimited cellular growth occurs. Other changes follow the first one, finally leading to full-blown cancer. Oncogenes are normal growth-promoting genes that are abnormally activated in cancer cells and provide the cells with a growth advantage over other cells (Croce, 2008; Lee and Muller, 2010). Growth-restricting tumor suppressor genes limit the proliferation of cells, and inactivating mutations or rearrangements in them are critical to cancer cells (Oliveira et al., 2005). In addition, cancer progression can be affected by molecules that are aberrantly expressed, but do not harbor any mutations. An example of this is the transforming growth factor β (TGF-β), which has been found to have a bidirectional role, where it inhibits cancer progression in pre-malignant cells but promotes it in advanced cancer (Massague, 2012). Additionally there can be other changes, such as alterations in non-coding RNAs and epigenetics (Stratton et al., 2009).

The distinction between benign and malignant cells is the ability of malignant cells to metastasize. Many steps are required for cancer cells to leave the site of their origin and then colonize a distant site in the body. First the cells must be able to degrade the surrounding extracellular matrix (ECM) and locally invade the tissue (Lu et al., 2011; Lu et al., 2012). The cells then intravasate into blood vessels, where they have to survive the conditions in circulation (Nguyen et al., 2009). In a distant site in the body, they attach to the surface of the blood vessel and extravasate into the tissues there (Reymond et al., 2013). In the destination sites, they must then survive and start proliferating, finally forming a metastasis (Nguyen et al., 2009; Valastyan and Weingberg, 2011).

Cancer is the second leading cause of death worldwide, only behind cardiovascular disease (Global Burden of Disease Cancer Collaboration et al., 2015). In women, breast cancer is the most common cancer type worldwide (Ferlay et al., 2015). Most of breast cancers are sporadic, but 5-10% are hereditary with BRCA1 and BRACA2 mutations accounting for most of the risk (Claus et al., 1996; Martin and Weber, 2000). Other known risk factors include female gender, age, obesity, early menarche, late menopause, nulliparity, and late age at first birth (Singletary, 2003).

Breast cancer is a heterogeneous disease. Historically it has been classified based on histology into ductal adenocarcinomas, lobular adenocarcinomas and other more rare types. However, the histological differences are not indicative of the origin of the cancer, as all breast cancers are thought to originate in the terminal ductal lobular unit of the breast (Weigelt et al., 2010). Breast cancers can also be categorized based on hormonal status (Payne et al., 2008; Weigelt and Reis-Filho, 2009). Hormone-receptor positive cancers express estrogen and/or progesterone receptors (Lim et al., 2012). HER2 positive cancers express the human epidermal growth factor receptor 2 (HER2/ERBB2) (Payne et al., 2008). Triple-negative breast cancers lack the expression of these receptors and are the subtype with the poorest prognosis (Bianchini et al., 2016). Microarray studies have yielded yet another classification tool. Based on gene expression patterns, breast cancers can be divided into five categories: luminal subtype A, luminal subtype B, basal-like, ERBB2+ and normal breast-like (Sorlie et al., 2003). Similarly to other solid cancers, the grade (appearance) and stage (size and invasiveness) of the breast cancer remain important aspects in determining prognosis and treatment (Rakha et al., 2010).

As in most cancer types, breast cancer patients die of metastatic disease (Redig and McAllister, 2013). Breast cancer metastasizes mostly to lungs, bone and liver (Weigelt et al., 2005). Despite advances in diagnosis and treatment, breast cancer is still the leading cause of morbidity and mortality among all the cancers in women (Redig and McAllister, 2013). The purpose of this study was to examine the effect of the growth factor bone morphogenetic protein 4 (BMP4) on breast cancer cells in in vitro and in vivo models and to characterize the regulation of BMP4 signaling in breast cancer cells.

2 Literature review

2.1 3D and in vivo models in cancer

Much of basic research is done using cell lines, which are cultured in 2D on cell culture plastics. Although very feasible, fast and cheap, this is not a very natural environment for the cells. To overcome this problem, cell lines have been grown in 3D culture that better mimics the physiological conditions (Hartung, 2014). Studies can also be done using model animals, which offer the complexity of a living body for experimentation. However, 3D models are a growing field and an attractive alternative to animal models for both ethical and economical reasons (Antoni et al., 2015).

2.1.1 3D models

There are several ways to provide a more physiological environment for the cells (Benien and Swami, 2014). The simplest method is to force the cells to grow in aggregates without any other structural support (Figure 1A). The cells can also be cultured inside a synthetic or biological gel (Figure 1B) or a rigid scaffold (Figure 1C). The most complex models include organ-on-a-chip and bioreactors (Figure 1D).

The aggregate model of cell culture creates an environment where cells aggregate to form a 3D structure. When the cells cannot attach to a substrate they remain floating and form collective masses. This type of culture can be achieved for example with low adhesion surfaces or the hanging drop method depicted in Figure 1A (Achilli et al., 2012).

Some manufacturing methods, such as 3D printing, are used to produce preformed scaffolds for the cells (Carletti et al., 2011). Depending on the manufacturing method, scaffolds with different properties are created (Carletti et al., 2011). For example strength and stability may vary. The cells are then allowed to enter the porous structure and proliferate within (Knight and Przyborski, 2015).

3D culture gels are formed from naturally-derived or synthetic materials (Figure 1B). One of the most common biological gelling substances used in 3D culture is Matrigel. Matrigel is an extract of the basement membrane of Engelbreth-Holm-Swarm (EHS) mouse sarcoma cells (Kleinman and Martin, 2005). It contains a mixture of proteins and growth factors. The most common constituents are collagen IV and laminin, and the growth factors present include transforming growth factor β (TGF-β), epidermal growth factor (EGF) and fibroblast growth factor (FGF) (Hughes et al., 2010). A version of Matrigel with reduced growth factor content is also available for applications where a more defined composition is desired (Kleinman and Martin, 2005). Below room temperature, Matrigel is in a liquid form, but forms a gel when the temperature is higher, providing a 3D matrix for the cells (Figure 1). Matrigel is capable of providing physiological clues to the cells, for example normal mammary epithelial cells in Matrigel have been shown to form acini, with a hollow lumen and apicobasal polarization (Debnath et al., 2003). In contrast, breast cancer cells grow in more disorganized patterns forming e.g. grape-like and stellate structures (Kenny et al., 2007). Thus the advantage of Matrigel, in addition to providing the cells a 3D environment, is its constituents, which make the gel bioactive and capable of being remodeled by the cells. However, the composition of Matrigel is not clearly defined or controlled and there is variation between different batches (Hughes et al., 2010).

In addition to Matrigel, collagen I- and alginate-based gels are common biological 3D substances (Wang et al., 2014a). Collagen I is the most abundant structural protein in the connective tissues of bone and dermis (Vigier and Fülöp, 2016). Alginate is a polysaccharide found from algae (Carletti et al., 2011). Other materials that are used include agarose, chitosan and silk (Carletti et al., 2011).

For a controlled composition, synthetic hydrogels are often used. They are cross-linked polymers, e.g. poly(ethylene glycol) (PEG), poly(vinyl alcohol) (PVA) and poly(acrylic acid) (PAA) (Ruedinger et al., 2015). They have a defined composition, but are typically not as bioactive as biological gels (Ruedinger et al., 2015). To make them more biocompatible, the gels can be modified to have cross-links that are cleaved by proteolytic enzymes such as matrix metalloproteinases (MMPs) (Song et al., 2014). Furthermore, additional molecules, such adhesion peptides (e.g. RGD) and growth factors, may be added to the gels prior to gelling (Ruedinger et al., 2015). The gelling of the hydrogel can be achieved through different means, such as enzymatic cross-linking or through physical manipulation (such as UV light) (Ruedinger et al., 2015).

A relatively new method is the organ-on-a-chip model, which mimics a functional unit of a living organ, consisting of micro-sized channels that are lined by cells (Esch et al., 2015). In addition, fluid flow conditions are controlled in the chip in order to better represent physiological conditions (Skardal et al., 2016). Similarly, in a bioreactor environmental factors such as pH, nutrient supply and waste removal is controlled (Haycock, 2011). In a rotating bioreactor a continuous rotary motion keeps the cells afloat (Haycock, 2011; Benien and Swami, 2014). Other bioreactor models are based on e.g. hollow fibers and spinner flasks (Haycock, 2011).

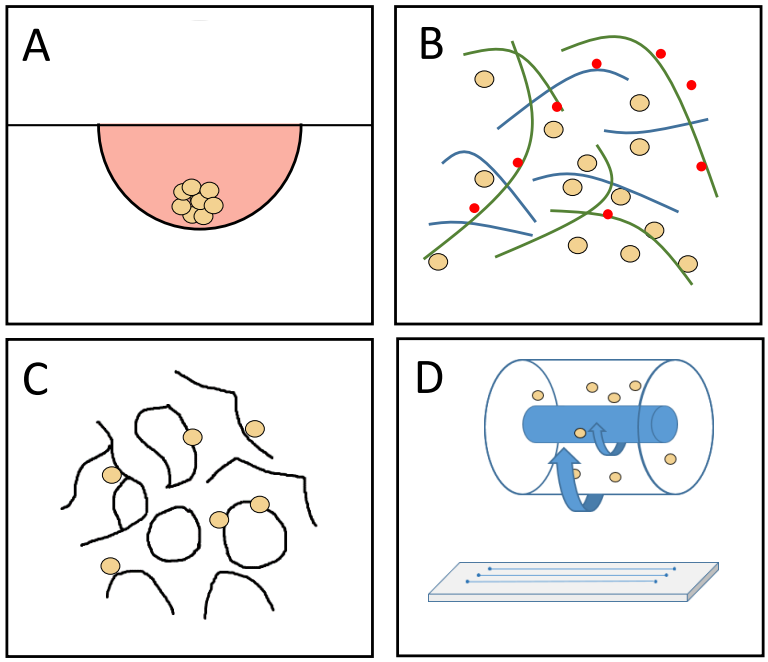

Figure 1. 3D culture methods. A, In the hanging drop culture, cells form aggregates in suspended drops of liquid. B, In 3D gels cells grow inside a matrix containing a mesh of structural proteins or polymer chains (colored lines). Other molecules, such as growth factors, may be present (red dots). C, Scaffolds provide a ready-made 3D environment for cells. D, In the bioreactor (top) microgravity is mimicked. Organ-on-a-chip (bottom) is a miniaturized in vitro version of in vivo interactions.

In addition to cues provided by biologically active molecules, in 3D culture it is possible to culture more than one type of cell simultaneously. This 3D co-culture method is used to mimic physiological conditions where multiple cell types interact. For example, adding human dermal fibroblasts (HDF) to MCF-7 breast cancer cells improved the growth of the cells in collagen, floating spheroids and alginate (Stock

et al., 2016). Endothelial and immune cells have also been co-cultured with tumor cells (Katt et al., 2016).

Taken together, the different 3D methods provide different benefits and drawbacks. The synthetic gels and scaffolds provide consistent quality, along with the hanging-drop method which is often used in high-throughput methods due to its simplicity (Tung et al., 2011). However, these methods provide only the 3D architecture. Biological materials also provide other cues to the cells and are more easily reorganized by the cells, although modifications to the synthetic gels and scaffolds can improve their biocompatibility (Zhu, 2010). In organ-on-a-chip models and bioreactors the nutrient and waste flow of the actual tissue is mimicked, but these methods are more costly compared to the others.

2.1.2 In vivo models

Although in vitro models have been created for replacing many tests done with animals, animal models are still needed for observing the effects of systemic interactions on the variables studied. Mouse models are the most commonly used in cancer research (Cekanova and Rathore, 2014) and they include transgenic animals, chemically/physically induced tumor models and xenograft models.

Transgenic mice have a modified genome. Using the modern CRISPR-Cas9 or other gene-editing tools, the mice are engineered to e.g. lack or overexpress a particular gene and the impact of this manipulation on tumor formation can then be followed (Markossian and Flamant, 2016). All the cells of the mice are modified but by using a tissue-specific promoter, the gene can be expressed or silenced only at a certain tissue (Markossian and Flamant, 2016). Generation of a transgenic mouse is time-consuming, but tumor progression can be followed in its entirety and the mice remain immunocompetent, an important aspect when the most physiological environment is needed (Richmond and Su, 2008).

Human cancer cells, either primary cells/tissues or cell lines, can be planted into mice to establish a xenograft model which requires immunocompromised mice. Immunocompetent mice can be used only when mouse cancer cells are transplanted into a mouse with a similar genetic background (a syngeneic model) (Teicher, 2006). An orthotopic xenograft model is established by injecting the cancer cells to a location in the mouse body which corresponds to the location the cells were originally derived from (Khanna and Hunter, 2005). This model has the advantage of the cells being in the same kind of environment that they initially evolved in. The

cells can also be injected subcutaneously, under the skin, in which case the size of the primary tumor is easily measured and its growth readily followed (Tomayko and Reynolds, 1989). However, in these models metastasis from the primary site is a slow process (Saxena and Christofori, 2013). In order to establish a metastatic model, the cells can be injected into circulation, either into the tail vein, or intracardially, into the heart (Saxena and Christofori, 2013). This mimics the circumstances of a cancer that has already been able to invade into the bloodstream. Because the intravasation step of the metastatic process is skipped, this model produces metastases rapidly compared to the other methods (Jung, 2014). In order to follow the growth of the metastases, the cells can be manipulated prior to implantation so as to give a signal which can be followed (Khanna and Hunter, 2005). Commonly, the cells are manipulated to express a fluorescent protein, for instance Green fluorescent protein (GFP, fluorescence), or the luciferase enzyme (bioluminescence) (Khanna and Hunter, 2005). The excited GFP produces light, which can be detected. If the luciferase system is used, luciferin, which is the substrate of the enzyme, is first injected into the bloodstream of the mice. The luciferase enzyme produces bioluminescent light as it catalyzes luciferin into oxyluciferin (Zinn et al., 2008). Similarly as with GFP, the light produced gives away the location of the cells.

In addition to transgenic and xenograft models, a mouse cancer model can also be created by an exogenous agent, for example radiation or chemicals (Frese and Tuveson, 2007). There are also mouse strains that spontaneously develop cancer (Frese and Tuveson, 2007). However, these models develop cancer with inconsistent timing and penetrance, and are not suitable for all cancers (Frese and Tuveson, 2007).

In breast cancer, orthotopic mouse models can be established by injecting the cells into the mammary fat pad. There is usually a high latency in metastasis development from orthotopic sites, but metastatic orthotopic models of breast cancer have been established (Kuperwasser et al., 2005; Iorns et al., 2012; Saxena and Christofori, 2013). Mice genetically engineered to develop breast cancer recapitulate many of the features of human breast cancer (such as similar molecular lesions, which have similar morphologic patterns) (Hennighausen, 2000). However, there are some differences in morphology and hormone dependency (Hennighausen, 2000).

Although animal models have the advantage of offering a naturally physiological design, there are also drawbacks to using animals in research. Depending on the animal model, performing experiments may take a long time and require sophisticated facilities, thus increasing the cost of experimentation. In addition, the results from animal models do not always translate to humans (Mak et al., 2014).

Finally, ethical considerations limit the usability of animal models and other methods are preferred when possible (Ferdowsian and Beck, 2011).

2.2 High-throughput methods to determine gene expression and chromatin state

Modern sequencing methods (often called next-generation sequencing, NGS) allow for a wealth of information to be gathered from the state of the chromatin and its expression. The expression levels of genes can be studied using RNA-seq (Wang et al., 2009) and open chromatin regions can be identified with DNase-seq (Song and Crawford, 2010). In addition, there are other methods, such as chromatin immunoprecipitation and sequencing (ChIP-seq) for transcription factor binding site (TFBS) recognition, which will not be discussed here.

2.2.1 RNA-seq

Using RNA-seq the whole transcriptome of a cell can be characterized. With this method, a library is formed from the fragmented cDNA sequences of expressed transcripts. The library is then sequenced using either single-end sequencing (sequenced from one end of the fragmented sequence) or paired-end sequencing (sequenced from both ends) (Wang et al., 2009). The reads that are thus produced are usually lined with a reference genome in order to reveal the identity of the transcript (Finotello and Di Camillo, 2015). The number of reads in turn reflects the expression levels (Oshlack et al., 2010). Thus from a given sample it is possible to find out what transcripts are present and what is their level of expression.

Compared to previously used hybridization-based techniques for high-throughput gene expression analyses, RNA-seq is a more direct method with a lower background (Wang et al., 2009). Furthermore, with RNA-seq it is possible to detect e.g. fusion genes and de novo transcripts, without prior information about the sequence (Wang et al., 2009; Kumar et al., 2016). It is thus not surprising that RNA-seq has become the favored method in transcriptomics (Conesa et al., 2016).

2.2.2 DNase-seq

Gene expression is regulated by transcription factors (TFs) binding to promoter and enhancer regions in the genome (Tsompana and Buck, 2014). During this event, the chromatin is opened for TF access (Tsompana and Buck, 2014). Using DNase-seq, it is possible to identify these open regions that indicate the presence of binding sites for regulatory control.

The technique is based on digestion of DNA by the DNase I enzyme. DNase I is able to access only open chromatin regions (called DNase hypersensitivity sites, DHSs), which the enzyme then cleaves (Song and Crawford, 2010). After optimization of the extent of cleavage by DNase I, fragments of 100 to 1000 bp of DNA are isolated, processed into a library and sequenced (Song and Crawford, 2010). As with RNA-seq, the sequencing reads are aligned to the genome and stacked reads form peaks to the regions where the chromatin is open (Strino and Lappe, 2016).

Even before NGS techniques were developed, DNase I-based cleavage of chromatin was used on a smaller scale to identify TFBSs (Neph et al., 2012). Nowadays, DNase-seq offers a method to gather information about the chromatin across the whole genome. However, follow-up studies are needed to ascertain biological function for the open regions discovered (Song and Crawford, 2010).

2.3 Bone morphogenetic proteins

2.3.1 Structure and function

Bone morphogenetic proteins (BMPs) are a family of growth factors, some of which are known by the name growth and differentiation factor (GDF). Their actions were brought to light by Urist (1965) in 1960s, in an attempt to find factors capable of inducing bone formation, although he first used the term bone morphogenetic protein years later (Urist and Strates, 1971). By the end of 1980s, several different BMPs had been found (Wozney, 1989) and to date, around 20 members are known (Carreira et al., 2015). One of the members, BMP4, is focused on in the following sections.

BMPs are a part of the transforming growth factor β (TGF-β) superfamily. The members are all structurally similar, with a cystine knot formation containing seven

cysteine residues (Rider and Mulloy, 2010). Six of the residues form intramolecular disulfide bridges, and one cysteine is involved in an intermolecular bond allowing dimerization of the monomeric proteins (Rider and Mulloy, 2010). BMPs can exist as homo- or heterodimers, and in some cases heterodimers have been shown to be more active (Valera et al., 2010; Sun et al., 2012). BMPs also possess an N-terminal signal peptide and a prodomain, which are cleaved upon secretion into the extracellular space (Mulloy and Rider, 2015). The prodomain may still remain associated with the mature polypeptide, influencing its binding to other molecules of the extracellular matrix (ECM) (Sengle et al., 2011). BMPs may also be glycosylated prior to secretion into the ECM (Rider and Mulloy, 2010). Based on structure and function, BMPs can be divided into subfamilies, including BMP2 and 4; BMP5, -6, 7, 8a and 8b; BMP9 and 10; and GDF5, -6 and 7 family (Miyazono et al., 2010). Although no crystal structure has been solved for BMP4, many research groups have studied the structure of its closest homolog BMP2. Scheufler et al. (1999) were the first to crystallize the protein and discover its similarity to other TGF-β superfamily members.

Although inducing bone formation was the first function attributed to BMPs, many other roles were found as more BMPs were discovered (Katagiri and Watabe, 2016). BMPs are now recognized as important developmental regulators, taking part in determining body axes as well as the formation of individual organs and organ systems such as hair follicle, kidney, tooth and skeletal muscle development (Niehrs, 2010; Katagiri and Watabe, 2016). In addition, in the adult body they are involved in maintaining tissue homeostasis, in processes such as vascular remodeling and skeletal stability (Khan et al., 2016; Garcia de Vinuesa et al., 2016). BMP4 specifically regulates e.g. limb development, adipogenesis and tooth development (Vainio et al., 1993; Selever et al., 2004; Bowers and Lane, 2007; Jia et al., 2013). It is also expressed in a wide variety of adult tissues and has been found to be involved in skeletal repair, ovarian steroidogenesis, neurogenesis, hematopoietic stem cell function and regulation of insulin metabolism in the adult body (Nakase and Yoshikawa, 2006; Goulley et al., 2007; Otsuka, 2010; Alarmo et al., 2013; Xu et al., 2013; Khurana et al., 2013). Bmp4 knock-out mice are embryonically lethal and heterozygotes are viable but with abnormalities, such as craniofacial malformations (Winnier et al., 1995; Dunn et al., 1997). Due to the critical roles of BMPs in development and in the adult body, it is not surprising that defects in BMP regulation may contribute to various diseases, including cancer, skeletal disorders and cardiovascular diseases (Wang et al., 2014b).

2.3.2 Signaling pathway

BMPs signal by binding to their receptors on target cells and initiating a signaling cascade that culminates in altered expression of BMP target genes. Three common type I (BMPR1A, BMPR1B and ACVR1) and three type II (BMPR2, ACVR2A and ACVR2B) serine/threonine kinase receptors are used by the BMP ligands, as they bind as dimers to two type I and two type II receptors (Miyazono et al., 2010). Of the type I receptors, BMP4 preferentially binds to BMPR1A and BMPR1B (ten Dijke et al., 1994). The receptor complex with both receptor types may be pre-formed or alternatively ligand binding brings the receptor-ligand complex together (Yadin et al., 2016). The type II receptor kinase domain is constitutively active and phosphorylates the type I receptor, thereby initiating the downstream signaling cascade (Figure 2, Yadin et al., 2016).

The intracellular mediators of BMP signaling are the SMAD molecules. Receptor-regulated SMADs (R-SMADs: SMAD1/5/9) bind to the activated receptor complex and are phosphorylated by the type I receptors (Massague et al., 2005). In the cytoplasm they then bind to the common SMAD, SMAD4, which is shared by the TGF-β and BMP signaling pathways. The complex thus formed translocates to the nucleus, where it binds to the promoters of BMP target genes and either activates or represses transcription in concert with other transcription factors (Figure 2, Miyazono et al., 2005).

The BMP signaling pathway is regulated at multiple levels. In the extracellular space, BMP antagonists bind BMPs and prevent them from binding to their receptors (Rider and Mulloy, 2010). The antagonists have different binding specifities, e.g. Noggin binds to BMP2 and -4 with high affinity and to BMP7 with a moderate affinity (Zimmerman 1996). At the cell membrane decoy or pseudoreceptors, co-receptors or other membrane-bound molecules may regulate BMP signaling (Raju et al., 2003; Bragdon et al., 2011; Brazil et al., 2015). For example, the pseudoreceptor BMP and Activin Membrane Bound Inhibitor (BAMBI), binds BMPs but lacks the kinase domain, leading to formation of a non-functional receptor complex (Onichtchouk et al., 1999). Intracellularly the action of R-SMADs is opposed by the Smad ubiquitination regulatory factors (SMURFs) and the inhibitory SMADs. The SMURFs target SMADs to ubiquitin-mediated destruction (Zhu et al., 1999). The inhibitory SMADs compete with SMADs for receptor binding (SMAD7) or with SMAD1 for SMAD4 binding (SMAD6) (Massague et al., 2005).

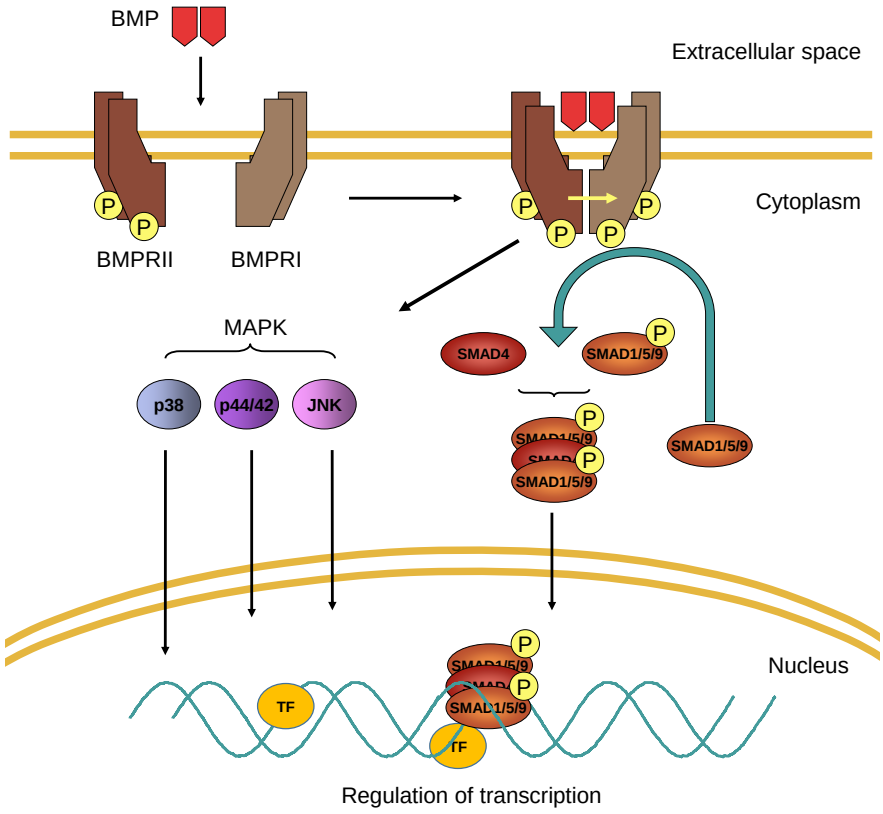

Figure 2. BMP signaling pathway. BMPs bind to their receptors and activate the canonical SMAD signaling pathway or alternatively the MAPK pathway. In the nucleus other transcription factors (TFs) are involved in BMP target gene regulation.

In addition to the canonical signaling pathway described above, BMPs may exert their effects through the MAP kinase pathways (Figure 2, Bragdon et al., 2011). Furthermore, there is extensive signaling crosstalk with other pathways. For example, the Notch and Wnt pathways have been found to regulate BMP signaling (Miyazono et al., 2005).

2.3.3 BMP target genes and their regulation

2.3.3.1 Transcription factors

In order to regulate transcription, SMAD4 complexed with R-SMADs binds to the promoters of BMP target genes at specific locations containing short SMAD binding elements (SBEs, GTCT/AGAC) as well as longer, GC-rich sequences (Morikawa et al., 2013). However, the binding affinity of SMADs alone is low (Massague et al., 2005). Therefore it is believed that other transcription factors (TFs) are required to interact with SMADs for adequate induction or repression of genes (Blitz and Cho, 2009). Both transcriptional activators and repressors have been found to interact with SMADs (Table 1). SMADs contain a linker region and two MAD homology (MH) domains. It is the MH1 domain that is responsible for binding to DNA (Morikawa et al., 2013), whereas interaction with TFs may happen through either the MH1 or MH2 domains (Massague et al., 2005). To date, transcription factors interacting with SMAD1/5/9 have mostly been identified using cells of various normal tissues (Table 1). Although not included in Table 1, transcription factors have also been studied in non-vertebrate models such as Drosophila.

Table 1. Transcription factors that regulate BMP target genes and interact with SMAD1/5/9 or 4 (only vertebrates included).

TF	Cell line/type/organism	TF type	Ref
ATF2	Mouse carcinoma/cardiomyocytes (p19cl6)	Activator	Monzen et al., 2001
β-catenin	Transgenic mice	Activator	Hu and Rosenblum, 2005
CBP	Human keratinocyte (HaCaT), mouse myoblast (C2C12) cells	Activator	Ghosh-Choudhury et al., 2006; Pouponnot et al., 1998
CIZ	murine osteoblastic cell line (MC3T3E1)	Repressor	Shen et al., 2002
CREBZF	Prostate cancer cells (PC-3)	Repressor	Lee et al., 2012
Dach1 (chick)	C2C12 and monkey kidney fibroblast cells (COS-7) cells	Repressor	Kida et al., 2004

E4F1	C2C12 cells	Repressor	Nojima et al., 2010
FOS, FOSB	Normal human osteoblastic cells, MC3T3-E1	ND	Lai and Cheng, 2002
GATA (4/5/6)	FVB mouse embryo, chick embryos, p19cl6, Mouse fibroblast (C3H/10T1/2), monkey kidney cells (CV-1)	Activator	Lee et al., 2004; Brown et al., 2004
GCN5	breast cancer cells (MCF-7)	Activator	Kahata et al., 2004
Gli3, truncated	Mink cells (R1B/L17)	Repressor	Liu et al., 1998
Hic-5	primary rat prostate fibroblasts, PC-3	Repressor	Shola et al., 2012
HIPK2	C2C12 cells	Repressor	Harada et al., 2003
HIVEP1	Xenopus	Activator	Yao et al., 2006
Hoxc-8	Mouse fibroblast (C3H/10T1/2)	Repressor	Shi et al., 1999
JUNB	Normal human osteoblastic cells, MC3T3-E1	ND	Lai and Cheng, 2002
mZnf8	Monkey kidney cells (COS-M6), mouse embryonal carcinoma cells (P19)	Repressor	Jiao et al., 2002
Nkx3.2	C3H10T1/2, COS-7, breast cancer cells (MDA-MB-468), and colorectal adenocarcinoma cells (SW480.7)	Repressor	Kim and Lassar, 2003
OAZ	Xenopus	Activator	Hata et al., 2000
p300	HaCaT	Activator	Pouponnot et al., 1998
p53	Immortalized mammary epithelial cells	Repressor	Balboni et al., 2015
p63	Immortalized mammary epithelial cells	Activator	Balboni et al., 2015
p65	Mouse embryonic fibroblasts	Repressor	Hirata-Tsuchiya et al., 2014

RUNX2	C2C12, C3H/10T1/2, cervical cancer cells (HeLa), mouse embryonic calvarial tissue cell line, chick chondrocytes	Activator	Hanai et al., 1999; Lee et al., 2000; Leboy et al., 2001; Bae et al., 2001; Afzal et al., 2005; Phimphilai et al., 2006; Javed et al., 2008
RUNX3	COS7	Activator*	Hanai et al., 1999
SIP1	Human embryonic kidney cells (HEK293T), monkey kidney fibroblast cells (COS1), yeast, Xenopus, C2C12 cells	Repressor	Verschueren et al., 1999; Tylzanowski et al., 2001; Conidi et al., 2013
SERTAD 1	Mouse primary cardiomyocytes	Activator	Peng et al., 2013
Smad6	COS-1 cells, mink lung epithelial cells (Mv1Lu)	Repressor	Bai et al., 2000
SMIF	Mv1Lu	Activator	Bai et al., 2002
Ski	Xenopus, bone marrow stromal cells (mouse)	Repressor	Wang et al., 2000
Sox5	Xenopus embryos	Activator	Nordin and LaBonne, 2014
Tcf4	Transgenic mice	Activator	Hu and Rosenblum, 2005
Tob	C2C12	Repressor	Yoshida et al., 2000
XBP1	Xenopus	Activator/ Repressor	Cao et al., 2006
YY1	1, HaCaT, C2C12, murine mammary epithelial cells (NMuMG), Mv1Lu, COS-7, human embryonic kidney (293T) cells, MDA-MB-468, human hepatoma (HepG2) cells, 2, chick embryos, P19, transgenic mice	1, Repressor, 2 Activator	Kurisaki et al., 2003; Lee et al., 2004
ZEB1	C2C12	Activator	Postigo, 2003

*tested only with TGF-β stimulation, ND = not determined

Of the SMAD-interacting TFs in vertebrate models, one of the most studied transcription factors is RUNX2 (Table 1, Ito et al., 2015). As a transcriptional activator, it interacts with SMADs and together with BMPs is important in inducing many factors critical to bone formation (Rahman et al., 2015). Transcriptional repressors, on the other hand, inhibit the transcriptional induction of gene expression. SIP1 is an example of a well-studied repressor of BMP signaling (Table 1). In C2C12 cells it interacts with Smad1/5 and represses the expression of alkaline phosphatase, which is implicated in osteogenesis induction (Tylzanowski et al., 2001).

Only a few studies on TFs involved in BMP signaling have been done in cancer cells. CREBZF was found to be a repressor in prostate cancer cells (Lee et al., 2012) and GCN5 a repressor in MCF-7 breast cancer cells (Liu et al., 1998). Nkx3.2 and YY1 TFs were identified as BMP target gene regulators in the MDA-MB-468 breast cancer cells (Kim and Lassar, 2003; Lee et al., 2004). Other studies have mostly used mouse, Xenopus or human kidney, osteoblast or other mesenchymal cells (Table 1). Many of the identified transcription factors have only been studied in one or a few different cell lines. Additionally, the BMP used in the stimulation of the signaling pathway varies depending on the study, with most using either BMP2 or BMP4. To date, any large-scale screenings of the TFs involved in BMP target gene regulation have not been performed. Thus is it is difficult to know whether these transcription factors are general mediators of BMP response or act in conjunction with a particular BMP or in a specific tissue or developmental stage.

2.3.3.2 Target genes

Some BMP target genes are well-known and have been meticulously characterized. The most prominent of these include the Inhibitor of differentiation genes (ID1-3) (Hollnagel et al., 1999; Miyazono et al., 2005). IDs regulate differentiation of cells both during development and in the adult body, and their deregulation is associated with tumorigenesis (Lasorella et al., 2014). BMPs also induce the expression of inhibitors of BMP signaling in a negative feedback loop, a mechanism for keeping expression levels steady (Paulsen et al., 2011). For example, BMP antagonists, inhibitory SMADs and BAMBI have been shown to be activated due to BMP treatment (Gazzerro et al., 1998; Paulsen et al., 2011).

Several studies have been done on a genome-wide scale to look for BMP target genes. Fei et al. (2010) searched for target genes in embryonic stem cells using ChIP-chip and ChIP-seq with SMAD antibodies, which identify promoters of BMP- and

TGF-β-regulated genes. An expression array was done after BMP9 and BMP4 treatment of endothelial cells (HUVECs) and pulmonary artery cells (PASMCs) (Morikawa et al., 2011) and revealed target genes common to both cell lines (such as SMAD6 and ID1-3) as well as individual target genes. Genander et al. (2014) found common BMP target genes as well as individual genes when looking at hair follicle stem cell lineages. BMP2 target genes in osteoblasts were divided into multiple expression profiles by de Jong et al. (2004). A meta-analysis of microarray data on BMP target genes in bone revealed some genes that may be common target genes in bone, such as Lox, Klf10 and Gpr97 (Prashar et al., 2014). Rodriguez-Martinez et al. (2011) identified BMP4 and BMP7 target genes in breast cancer cells, employing multiple cell lines and time points. These studies show that BMPs have many common target genes but that there are both tissue-specific and BMP-specific responses as well. However, large scale studies on BMP target genes have not been done in any other cancer type apart from breast cancer (Rodriguez-Martinez et al., 2011). To gain a more complete view of BMP target genes, large-scale screenings are needed.

2.3.4 BMP4 and cancer

Due to their role as developmental regulators, BMPs have also been linked to cancer progression (Alarmo and Kallioniemi, 2010; Singh and Morris, 2010; Wang et al., 2014b). As aberrant signaling is frequent in cancer (McCleary-Wheeler et al., 2012; Giancotti, 2014), the expression and function of BMPs and the BMP pathway have been studied in many cancer types. The results show that the effect is dependent on the specific BMP, cancer type and context (Singh and Morris, 2010; Alarmo and Kallioniemi, 2010; Ehata et al., 2013). For example, in breast cancer, most of the BMPs studied have been shown to reduce proliferation (Alarmo and Kallioniemi, 2010; Ye et al., 2010; Chen et al., 2012; Hu et al., 2013; Lian et al., 2013; Zhang et al., 2013). In contrast, the effects of BMPs on breast cancer cell migration and metastasis seem to be dependent on the BMP in question with e.g. BMP2 inhibiting and BMP6 inducing migration (Alarmo and Kallioniemi, 2010; Ye et al., 2010; Zhang et al., 2013; Ren et al., 2014).

The expression of BMP4 is tissue-specific; tumors from squamous epithelial cells had strong granular staining and some tissues had only weak and moderate staining (Alarmo et al., 2013). There was also variation in expression between different histological subtypes of some cancers. Indeed, the expression of BMP4 has been

suggested as a prognostic marker in some cancers, for example glioma, hepatocellular carcinoma and serous ovarian carcinoma (Laatio et al., 2011; Guo et al., 2012b; Wu and Yao, 2013). In addition, different polymorphisms in the BMP4 gene have been suggested as potentially relevant to cancer progression. For example, colorectal cancer risk was associated with BMP4-rs4444235 polymorphism in a meta-analysis of several studies (Li et al., 2012).

The function of BMP4 in cancer has been studied with both in vitro and in vivo models (Table 2, Kallioniemi, 2012). Both inhibition and promotion of proliferation, as well as varying effects on migration have been observed (Table 2). In some studies, BMP4 also had an effect on other phenotypes, such as differentiation, apoptosis, survival and drug resistance of cancer cells (Table 2). However, it seems that BMP4 often acts as a suppressor of proliferation and inducer of cell differentiation, although there are studies that have found opposite effects (Table 2). BMP4 also more often induces migration and invasion than suppresses them (Table 2). The effects of tumor suppressive reduced proliferation and tumor promoting increased migration have been noted, even within one cancer cell type (Alarmo and Kallioniemi, 2010; Ehata et al., 2013). However, many BMP4 studies have only used one or a few cell lines and the manipulation method of BMP4 levels have also been variable, thus making comparisons between different studies difficult. More studies are needed in order to form more comprehensive conclusions.

Table 2. The effect of BMP4 on the behavior of cancers from different tissues. The studies have been done using in vitro models, unless otherwise indicated.

Cancer type	Manipulation*	Effect	Reference
Basal cell carcinoma	8–833 ng/ml	Reduced cell growth	Sneddon et al., 2006
Bladder cancer	100 ng/ml	Inhibited growth in one cell line, no effect in one cell line, inhibited growth in one cell line when forced expression of BMPR2 was used	Kim et al., 2004
Brain tumors	5 ng/ml	Increased growth and decreased apoptosis	Iantosca et al., 1999
	100 ng/ml	Decreased proliferation and induced differentiation, in vivo	Piccirillo et al., 2006
	100 ng/ml	Decreased proliferation, in vivo	Zhao et al., 2008
	30 ng/ml	Increased proliferation	Johnson et al., 2009
	100 ng/ml	Inhibited proliferation and increased apoptosis	Zhou et al., 2011
	BMP4 containing nanoparticles	Improved survival, in vivo	Mangraviti et al., 2016
	Silencing	Reversed multidrug resistance	Liu et al., 2013
	10-200 ng/ml	Increased proliferation	Paez-Pereda et al., 2003
	50-200 ng/ml	Reduced proliferation	Giacomini et al., 2006
Breast cancer	100 ng/ml	Reduced proliferation, increased migration	Ketolainen et al., 2010
	50-100 ng/ml	Reduced migration and invasion, no effect on viability	Shon et al., 2009

	Overexpression	Inhibited proliferation and promoted migration and invasion	Guo et al., 2012a
	Silencing	Increased proliferation and decreased migration/invasion	Guo et al., 2012a
	2.5 ng/ml	Increased invasion	Cyr-Depauw et al., 2016
	100 ng/ml	Increased invasion	Pal et al., 2012
	100 ng/ml	Stimulation of mammary fibroblasts enhanced breast cancer cell invasion	Owens et al., 2013
	Overexpression	Inhibited metastasis, in vivo	Cao et al., 2014
Colorectal/ Colon cancer	Dose unknown	Inhibited growth	Whissell et al., 2014
	100 ng/ml	Inhibited growth, increased apoptosis, G1 cell cycle arrest (in vitro), loss of tumorigenicity (in vivo)	Nishanian et al., 2004
	100 ng/ml	Reduced tumor formation, in vivo	Lombardo et al., 2011
	Overexpression	Induced migration, invasion, apoptosis and resistance to serum starvation	Deng et al., 2007a
	Overexpression	Increased survival and decreased apoptosis after heat treatment	Deng et al., 2007b
	Overexpression	Increased migration and invasion in Smad4-deficient cells	Deng et al., 2009
Gastric cancer	Overexpression	Increased proliferation and invasion	Ivanova et al., 2013
	Silencing	Inhibited proliferation and migration	Ivanova et al., 2013

	30 ng/ml	Inhibited proliferation, induced cell cycle arrest	Shirai et al., 2011
Head and neck cancer	Knockdown	Reduced migration and invasion	Yang et al., 2013
Hepatocellular cancer	10 - 100 ng/ml	Promoted differentiation, inhibited self-renewal, tumorigenic capacity	Zhang et al., 2012b
	Silencing	Reduced migration, invasion and anchorage-independent growth, no effect on proliferation	Maegdefrau et al., 2009
	10 ng/ml	Increased proliferation and migration	Chiu et al., 2012
Leukemia/ lymphoma	Dose unknown	Increased proliferation (reduced in one cell line), suppressed clonogenicity	Takahashi et al., 2012
	Silencing	Decreased colony formation	Zhao et al., 2013
Lung cancer	Knockdown	Suppressed growth, migration (in vitro), metastasis (in vivo)	Kim et al., 2015
	10 – 300 ng/ml	Decreased clonogenic growth	Fang et al., 2014
	100 ng/ml	Induced senescence, inhibition of proliferation and invasion (in vitro, in vivo)	Buckley et al., 2004
	Overexpression	Induced senescence	Su et al., 2009
Melanoma	Antisense-BMP4, BMP antagonist	Reduced migration and invasion, no change in proliferation and anchorage-independent growth	Rothhammer et al., 2005
Myeloma	50 ng/ml	Induced G1 arrest and/or apoptosis	Hjertner et al., 2001
	20 ng/ml	Induced apoptosis	Holien et al., 2012
Ovarian cancer	10 ng/ml	Induced motility	Theriault and Nachtigal, 2011

	10 ng/ml	No effect on proliferation, decreased cell density and increased spreading in long-term culture	Shepherd and Nachtigal, 2003
	10 ng/ml	Increased adhesion, invasion, induced EMT	Theriault et al., 2007
Pancreatic cancer	250 ng/ml	Reduced proliferation, increased migration	Virtanen et al., 2011
	300 ng/ml	Induced EMT and invasiveness or no effect	Gordon et al., 2009
	50 ng/ml	Induced EMT and migration	Hamada et al., 2007
Prostate cancer	BMP4 blocking antibody	Inhibited osteogenic differentiation	Lee et al., 2011
	1-100 ng/ml	Inhibited proliferation, or no effect	Brubaker et al., 2004
	Dose unkown	No effect on proliferation or invasion	Dai et al., 2005
	1-500 ng/ml	No effect on proliferation, migration or invasion	Feeley et al., 2005
	20 ng/ml	Inhibited proliferation	Shaw et al., 2010
Retinoblastoma	40 ng/ml	Increased apoptosis, no effect on proliferation	Haubold et al., 2010

* Manipulation of BMP4 expression through BMP4 treatment, silencing or overexpression

3 Aims of the study

The aim of this study was to expand the previous data concerning the effects of BMP4 on breast cancer, by employing two different study models that are more physiological compared to standard cell culture. In addition, BMP4 target genes and their regulation was studied with integration of next-generation sequencing (NGS) analyses. The specific aims of this dissertation were:

1. To examine the effects of BMP4 on breast cancer cells in 3D culture (Study I)

2. To characterize the impact of BMP4 on breast cancer metastasis formation using an in vivo mouse model (Study II)

3. To decipher BMP4 signaling regulation at the chromatin and transcriptomic levels (Study III)

4 Materials and methods

4.1 Cell culture (I, II, III)

The breast cancer cell lines (BT-474, HCC1954, MCF-7, MDA-MB-231, MDA-MB-361, MDA-MB-436 and T-47D), the immortalized breast epithelial cell line (MCF-10A) and the embryonic kidney cell line (293T) were obtained from ATCC (Manassas, VA, USA). They were maintained according to ATCC directions except for MCF-10A, which was cultured as previously described (Debnath et al., 2003). All cell lines were authenticated and regularly checked for mycoplasma infection.

4.2 BMP4 treatment (I, II, III)

Recombinant human BMP4 was purchased from R&D Systems (Minneapolis, MN, USA). Either prior to or during the experiments, the cells and animals were treated with BMP4 and vehicle (BMP4 dilution solution, 4 mM HCl with 0.01% BSA) was used as control. The details of treatment can be found in the appropriate sections.

4.3 3D Matrigel assay (I, II)

Cells were cultured on growth-factor reduced Matrigel (Corning, Corning, NY, USA) using the overlay method by Debnath et al., (2003). In brief, 4-chambered Lab-Tek chamber slides (Nalge Nunc International, Rochester, NY, USA) or 24-well plates were first coated with Matrigel. Cells (Table 3) suspended in 2.5 % Matrigel solution containing BMP4 (100 ng/ml) or vehicle were added on Matrigel-coated wells. Medium with BMP4 or vehicle was replaced every two to three days and the cells were allowed to grow up to 17 days.

Table 3. Concentration of cells in Matrigel and PEG gel.

Cell line	Concentration in Matrigel (cells/ml)	Concentration in PEG gel (cells/ml)
BT-474	6.0×10^4	-
MCF-10A	2.4×10^4	1.4×10^5
MDA-MB-231	2.0×10^4	1.0×10^5
MDA-MB-361	1.2×10^5	4.0×10^5
T-47D	2.0×10^4	8.0×10^4

4.4 3D PEG gel assay (I)

Poly(ethylene glycol) (PEG) gel with RGD peptides and MMP-degradable crosslinks was obtained from QGel (Lausanne, Switzerland). Briefly, QGelTM MT 3D Matrix powder was mixed with 400 µl of Buffer A, followed by addition of 100 µl of cell suspension (Table 3), containing 100 ng/ml BMP4 or vehicle. Drops of 40 µl applied into a disc caster were allowed to gel for 30 min at 37 °C, before they were removed and placed on 24-well plates containing 1 ml of medium per well. The cells were allowed to grow up to 18 days.

4.5 Western blot (I)

The cells were collected 24 hours or 5 days (2D culture) and 4 or 7 days (3D Matrigel assay) after the first addition of BMP4. For dissolving the Matrigel, cold PBS with 5mM EDTA was used and the cells were kept on ice for 15 min. The cell-Matrigel solution was then collected, kept on ice for an additional 30 min and centrifuged for 15 min at 3300 × g, at 4 °C. Cells from both 2D and 3D culture were then lysed into RIPA-buffer (1% PBS, 1% non-idet P-40, 0.5% sodium deoxycholate, and 0.1% SDS) containing cOmplete Mini Protease Inhibitor Cocktail (Roche, Basel, Switzerland) and PhosStop Phosphatase Inhibitor Cocktail (Roche), incubated on ice for 20 min and centrifuged for 10 min, at 10 000 g and 4 °C. Protein concentration was measured using the Bradford reagent (Sigma–Aldrich, St. Louis, MO, USA).

A total of 50 µg of protein per sample was loaded onto SDS-PAGE gels. The proteins were transferred to a PVDF membrane following electrophoresis. The

primary antibodies are listed in Table 4. Proteins were detected using the BM Chemiluminescence Western Blotting kit (Roche) according to manufacturer's instructions. For all antibodies except for Cyclin B2, anti-mouse/rabbit secondary antibody (1:5000, Roche) was used. Cyclin B2 was detected with anti-goat secondary antibody (1:5000, Santa-Cruz Biotechnology, Dallas, TX, USA). The membranes were stripped and probed with β-tubulin (Sigma-Aldrich) as a loading control.

Table 4. Antibodies used in Western blot.

Antibody	Manufacturer	Dilution	Clonality
Cdc2	Santa Cruz Biotechnology	1:1000	rabbit polyclonal
p-Cdc2 (Thr14/Tyr15)	Santa Cruz Biotechnology	1:200	rabbit polyclonal
Cdk4	Santa Cruz Biotechnology	1:1000	rabbit polyclonal
Cyclin B1	Santa Cruz Biotechnology	1:200	rabbit polyclonal
Cyclin B2	Santa Cruz Biotechnology	1:100	goat polyclonal
Cyclin D1	Santa Cruz Biotechnology	1:200	rabbit polyclonal
GTF2H1	Abcam	1:1000	mouse monoclonal
p15	Santa Cruz Biotechnology	1:200	rabbit polyclonal
p16	Santa Cruz Biotechnology	1:100	mouse monoclonal
p21	Santa Cruz Biotechnology	1:100	rabbit polyclonal
p27	Santa Cruz Biotechnology	1:500	rabbit polyclonal

4.6 Cell proliferation and cell cycle assays (I)

The cells were incubated with medium containing 10% alamarBlue reagent (Invitrogen, Carlsbad, CA, USA) for 1 hour (MCF-10A 2D culture) or 4 hours (3D culture). Fluorescence (excitation wavelength 560 nm, emission wavelength 590 nm) was measured from the collected medium using Tecan infinite F200 Pro plate reader (Tecan, Männedorf, Switzerland). Additionally, the number of cells in standard 2D culture was counted using the Z1 Coulter Counter (Beckman Coulter, Brea, CA, USA) at indicated time points.

For cell cycle analysis, MCF-10A cells were cultured on 24-well plates and analyzed 3 and 5 days after the first addition of BMP4. The cells were stained with propidium iodide (PI) as described (Parssinen et al., 2008). Briefly, the cells were harvested and resuspended in hypotonic staining buffer containing PI. The stained

nuclei were analyzed and the cell cycle distribution determined using the Accuri C6 flow cytometer (BD Biosciences, San Jose, CA, USA) and ModFit LT 3.0 (Verity software house, Topsham, ME, USA), respectively.

4.7 In vivo mouse experiment (II)

4.7.1 Virus production and transduction

Lentiviral plasmid vector pHIV-Luciferase (pHIV-Luc) containing the firefly luciferase as a reporter gene was purchased from Addgene (Cambridge, MA, USA). Plasmid identity was verified by sequencing and the plasmid DNA was purified using GenElute Endotoxin-free Plasmid Maxiprep kit (Sigma-Aldrich). A total of 7 μg of plasmid DNA was used to generate lentiviruses in 293T cells as instructed in the Lenti-X Tet-On Advanced Inducible Expression System (Clontech, Mountain View, CA, USA). A total of 8.0×10^4 MDA-MB-231 cells were transduced with the virus in normal medium in the presence of 8 μg/ml polybrene. After 24 h the transduction medium was replaced with normal medium. Luciferase expression was verified using Luciferase Assay System (Promega, Madison, WI, USA) and luminescence was measured with Luminoskan Ascent (Thermo Fisher Scientific, Waltham, MA, USA).

4.7.2 Mice and BMP4 treatment

All mice experiments were performed by Pharmatest Services Ltd (Turku, Finland) that holds the ethical approval of the National Committee for Animal Experiments (license number ESAVI 2077-04 10 07-2014). MDA-MB-231/Luc cells were treated with BMP4 or vehicle for seven days with fresh medium changed every three days. At day 0, the cells (2×10^5 cells in 0.1 ml of PBS) were inoculated into the left cardiac ventricle of female athymic nude mice (athymic nude Foxn1nu, Harlan, The Netherlands). Mice were given 100 μg/kg of BMP4 (in a concentration of 20 μg/ml in PBS with pH of 3.8) or vehicle through tail vein injection thrice a week for seven weeks, starting at day 0 (Figure 3). Animals were monitored daily and weighed before each BMP4/vehicle dose. Appearances of any clinical signs were noted. Four mice died or were sacrificed following complications of cell inoculation and one mouse due to a dosing-related complication. Due to exclusion of these animals, 10 mice

were left in the BMP4 group and 11 in the vehicle group. There was no statistical difference in the weight of the animals between the groups.

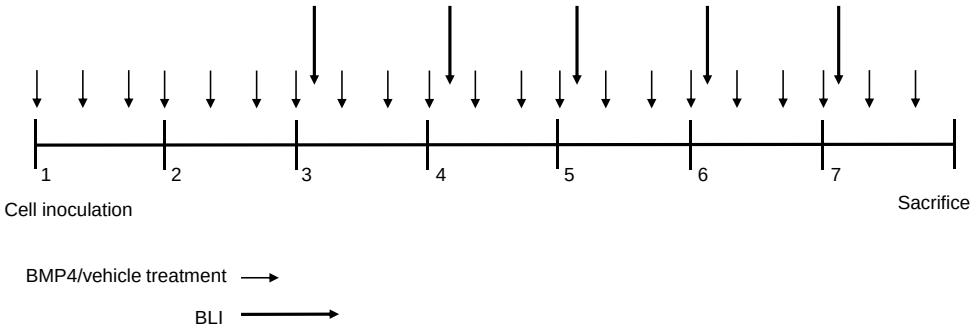

Figure 3. Time line of the in vivo experiment. Mice were injected intracardially at the start of week 1, and sacrificed at the end of week 7. BLI = Bioluminescence imaging.

4.7.3 Bioluminescence imaging (BLI) and sample collection

The metastases were detected by imaging the bioluminescence emitted by the MDA-MB-231/Luc cells, using IVIS Lumina imaging system (PerkinElmer, Waltham, MA, USA). 100 mg/kg of D-luciferin (Gold Biotechnology, St Louis, MO, USA) was intraperitoneally administered and the animals were imaged under anesthesia, within 10–30 minutes after luciferin application. From week 3 until sacrifice at 7 weeks after inoculation, imaging was performed weekly. At the end of the study, gross necropsy was performed on all mice. Samples from all tissues with metastases and corresponding control tissues with no metastases were collected. Fixation of the tissues was done in 10% formalin, bone tissues were decalcified with EDTA, and all the samples were embedded on paraffin (BiositeHisto, Tampere, Finland). Tissue sections cut from the paraffin blocks were deparaffinized and rehydrated. Hematoxylin and eosin (H&E) staining was performed using routine procedures.

4.8 Staining protocols

4.8.1 Immunofluorescence

4.8.1.1 Immunofluorescence staining of 3D assay (I)

The MCF-10A cells in Matrigel and PEG gel were fixed in 4% paraformaldehyde for 1 hour at 37 °C and permeabilized with 0.1% Triton-X100 for 45 min at room temperature followed by blocking with 3% BSA for 1.5 hours at 37 °C. The samples were incubated with mouse monoclonal anti-α6 integrin antibody (1:300, Abcam, Cambridge, UK) for 1.5 hours at 37 °C. The secondary goat anti-mouse Alexa Fluor 488 (1:200, Invitrogen) was used analogously. The slides were stained with DAPI (Invitrogen) and mounted with Vectashield (Vector Laboratories, Burlingame, CA, USA).

4.8.1.2 Immunofluorescence staining of mouse tissues (II)

The slides were cut, baked and deparaffinized. Antigen retrieval was performed using citrate buffer. Antibodies were diluted in 12% BSA. Primary antibodies (Table 5) were incubated 20-30 min at room temperature. Goat anti-chicken, anti-rabbit or anti-mouse Alexa Fluor 488 secondary antibodies (at a dilution of 1:200, all from Thermo Fisher Scientific) were incubated for 20-30 min at room temperature. The slides were mounted in SlowFade +DAPI (Invitrogen).

4.8.2 Immunohistochemistry (II)

The slides were cut, baked and deparaffinized. Antigen retrieval was performed using citrate buffer and the samples treated with 3% H2O2 for 10 minutes. Blocking was done for 1 hour at room temperature using goat or rabbit serum or Normal antibody Diluent (ImmunoLogic, Duiven, the Netherlands), which were also used for antibody dilutions. M.O.M. kit (Vector laboratories) was used with mouse antibodies. Primary antibodies (Table 5) were incubated overnight at 4 °C. Biotinylated goat anti-rabbit and biotinylated rabbit anti-rat (both at a dilution of 1:100, from Vector laboratories) or Simple Stain MAX PO (MULTI) Universal

Immunoperoxidase polymer (Nichirei biosciences, Tokyo, Japan) secondary antibodies were incubated for 1 hour at room temperature. DAB based detection was used to visualize target proteins. The slides were counterstained with hematoxylin and mounted in AquaPolyMount (Polysciences, Inc.,Warrington, PA, USA) or dehydrated and mounted in DPX Mountant (VWR, Radnor, PA, USA).

Table 5. Antibodies used in immunofluorescence and immunohistochemistry.

Antibody	Application	Manufacturer	Dilution	Clonality
α-SMA	IF	Sigma-Aldrich	1:500	Mouse monoclonal
Keratin 5	IF	BioLegend	1:500	Rabbit polyclonal
Keratin 14	IF	BioLegend	1:500	Rabbit polyclonal
Ki67	IHC	Leica Biosystems	1:200	Mouse monoclonal
MECA32	IHC	BD Biosciences	1:100	Rat monoclonal
p-SMAD1/5/9	IHC	Cell signaling technology	1:200	Rabbit polyclonal
Vimentin	IF	BioLegend	1:500	Chicken polyclonal

Abbreviations: IF, immunofluorescence; IHC, immunohistochemistry

4.8.3 Bone stainings (II)

To visualize bone and cartilage, the tissues were stained with Toluidine blue. TRAP (tartrate-resistant phosphatase) staining for osteoclasts was carried out by incubation in naphthol AS-BI phosphate solution (cat N-2125, Sigma Aldrich). The color reaction was achieved using sodium nitrate and pararosaniline dye (cat P-3750, Sigma Aldrich).

4.9 Image analysis (I, II)

Images for IF slides were taken with Zeiss Axio Imager M2 microscope (Carl Zeiss, Oberkochen, Germany) connected to an ApoTome slider module (Carl Zeiss). 3D cell culture, IHC, H&E and bone staining images were captured with an Olympus microscope (Olympus, Tokyo, Japan) connected to Surveyor software (Objective Imaging, Cambridge, UK). Quantification of Ki67 data was performed using the NIH ImageJ software (http://rsbweb.nih.gov/ij/docs/examples/stained-sections/index.html) by calculating the percentage of positively stained areas within the tumor masses. The areas from 3D culture images were also calculated using ImageJ.

4.10 qRT-PCR (I, III)

After 14 days of BMP4 treatment in the Matrigel, BT-474 and MDA-MB-231 cells were harvested as described above for Western blot. Samples used in other analyses are described below, under the relevant sections. RNA was extracted using RNeasy Mini kit (Qiagen, Hilden, Germany) or Nucleospin RNA Plus (Macherey-Nagel, Düren, Germany) according to the manufacturer's instructions. The RNA was then reverse transcribed using SuperScript III First-Strand Synthesis System for RT-PCR (Invitrogen) with random hexamers according to the manufacturer's protocol. LightCycler equipment with gene-specific primers (Sigma-Aldrich) and either LightCycler FastStart DNA Master SYBR Green I assay (Roche) or Universal Probe Library (UPL) probes (Roche) with LightCycler Taqman Master was used (Table 6). The expression levels were normalized using phosphoglycerate kinase 1 (PGK1) or hypoxanthine phosphoribosyltransferase 1 (HPRT1) housekeeping genes.

Table 6. Primers used for qPCR analyses.

Gene	Primer sequences (5'-3')	Probe
*3D Matrigel assay (**Study I**)*		
ADAM17	F: TTTGAGACTGCCCAGAAGAAG	79
	R: GCGGGCACTCACTGCTAT	
MMP1	F: CAGAGATGAAGTCCGGTTTTTC	26
	R: GGGGTATCCGTGTAGCACAT	
MMP2	F: TGCTGGAGACAAATTCTGGA	60
	R: GATGGCATTCCAGGCATC	

MMP3	F: CCAGGTGTGGAGTTCCTGAT	72
	R: CATCTTTTGGCAAATCTGGTG	
MMP7	F: GCTGACATCATGATTGGCTTT	72
	R: TCTCCTCCGAGACCTGTCC	
MMP9	F: ATCCGGCACCTCTATGGTC	43
	R: CTGAGGGGTGGACAGTGG	
MMP14	F: GCCTTGGACTGTCAGGAATG	37
	R: AGGGGTCACTGGAATGCTC	
*DHS cleavage assay (**Study III**)*		
LB2M	F: CAGAAGTTCTCCTTCTGCTAGGT	-
	R: TGGAGAAGGGAAGTCACGGA	
LGUSB	F: CGTCGGTTGTCAGAGAAGT	-
	R: CCTGCAACACCAAGAGGGA	
LNegC9	F: AACCCCAAGGCATCCAAACA	-
	R: TTCTCTGCCTGCCAAAGTCC	
LNegC20	F: TTGCCTTGTTCCCAGCAGAA	-
	R: GCCACATAGCCTTCCAACCT	
*Fragment release assay (**Study III**)*		
sB2Mprom	F: CTGGCTTGGAGACAGGTGA	-
	R: CCCAGCCAATCAGGACAAGG	
sGUSBprom	F: CCAGAACAGAACCCCTGAGA	-
	R: CTCCTTGAAGAAACAGGGGGAT	
sPPIAprom	F: TCCGTCTATAGGCCAGATGC	-
	R: CCAATCGGGTCTGCGACTT	
sNegC2	F: GCCAGTTCATGCTGTCTACCA	-
	R: CGCAGTTCAGCAAAGGGAAG	
sNegC9	F: AGTGTGTTCAGAGTTGGAAGGA	-
	R: AGACTGGAAGACAGGGAGAA	
sNegC20	F: AACAGGTGGAAAGAGCCACA	-
	R: TCACTCCACTGTTGTCCACT	
*BMP4 target genes (Study **III**)*		
AMIGO2	F: CCCCAGCACCGTTCAC	-
	R: ACGACATTATGGTCGCCTCTG	
ATOH8	F: GAGGGACGTGCCAAGAAG	12
	R: TCAGCGAGCTCACCTTGTC	
CGB	F: CTACTGCCCCACCATGACCC	-
	R: GGTAGTTGCACACCACCTGA	

DLL1	F: CTTCCCCTTCGGCTTCAC	2
	R: GGGTTTTCTGTTGCGAGGT	
DLX3	F: GAGCCTCCTACCGGCAATAC	26
	R: TCCTCCTTCACCGACACTG	
GATA2	F: CTACAGCAGCGGACTCTTCC	-
	R: ACTCCCGGCCTTCTGAACA	
ID2	F: ATATCAGCATCCTGTCCTTGC	5
	R: AAAGAAATCATGAACACCGCTTA	
IGFBP3	F: GGATAAGTATGGGCAGCCTCT	12
	R: TGAGCTCCACATTAACCTTGC	
LIN7B	F: GCTTTATGACACGCTGGACA	8
	R: GCTCCACTACCCTGGGATG	
NOG	F: TAGAGTTCTCCGAGGGCTTG	37
	R: CTCCGCAGCTTCTTGCTTAG	
PMEPA1	F: GCACAGTGTCAGGCAACGG	-
	R: AGATGGTGGGTGGCAGGTC	
SKIL	F: GAGGCTGAATATGCAGGACAG	13
	R: CTTGCCTATCGGCCTCAG	
SMAD6	F: GGGCCCGAATCTCCGC	-
	R: AGAATTCACCCGGAGCAGTG	
SMAD9	F: GCATTAACCCTTACCACTACCG	16
	R: GAGCTGGGGGTTATATTCACTG	
ZNF503	F: ATTTTGCACCCCGAGTACCT	8
	R: CTTCCCGATCTGCGAACA	
Transcription factors (Study III)		
CBFB	F: ATGGTATGGGCTGTCTGGAG	88
	R: TCAAAGGCCTGTTGTGCTAA	
HIF1A	F: GATAGCAAGACTTTCCTCAGTCG	64
	R: TGGCTCATATCCCATCAATTC	
MBD2	F: ACGAATGAATGAACAGCCACG	-
	R: TGGACCAACTCCTTGAAGACC	
SMAD4	F: TGTGTTACCATACAGAGAACATT	83
	R: GGGCATAGATCACATGAGGAA	

If UPL probe system was used, the probe number is indicated; otherwise, SYBR Green assay was used

Abbreviations: F, forward primer; R, reverse primer

4.11 Statistical analyses (I, II)

The difference between BMP4- and vehicle-treated samples in cell proliferation (2D and 3D cell culture) and area analysis (3D cell culture) was evaluated using the Mann–Whitney test with GraphPad Prism 4 (GraphPad Software, La Jolla, CA, USA). Using statistical software R (version 3.1.0 or newer, www.r-project.org), linear mixed-effects models and model contrasts were applied to evaluate the BLI data and body weight of mice. In addition, Kaplan–Meier method and the log-rank test was used for time to the first metastasis observation. A P-value of less than 0.05 was considered significant in all analyses.

4.12 Sequencing studies (III)

4.12.1 BMP4 treatment and sample collection

MDA-MB-231 and T-47D cells were treated with BMP4 (100 ng/ml) and vehicle for 3 h. For RNA-seq, total RNA was extracted from the cells using the Absolutely RNA miRNA kit (Agilent Technologies, Santa Clara, CA, USA) according to the manufacturer's instructions. RNA quality was controlled using Agilent 2100 Bioanalyzer (Agilent Technologies).

For DNase-seq the nuclei were isolated from the treated cells as previously described (Song and Crawford, 2010). DNase I digestion was carried out according to the protocol by Ling and Waxman (2013). Briefly, the digestion reaction was optimized and confirmed by the qPCR-based DNase hypersensitive site (DHS) cleavage assay with positive control primers in known DHSs in the promoters of housekeeping genes and negative control primers in intergenic insensitive sites (Table 6). Based on the optimization, 40 units of DNase I for 15 min was selected for the final protocol consisting of DNase I treatment followed by phenol-chloroform extraction and size fractionation of the DNA fragments by sucrose gradient ultracentrifugation. The most enriched fraction was identified by the qPCR-based fragment release assay using positive control primers located inside known DHSs in the promoters of housekeeping genes and negative control primers in gene-free regions of different chromosomes (Table 6). The DNA fragments from this fraction were used in the subsequent library construction and sequencing. As an input control undigested DNA from both cell lines was utilized.

4.12.2 Deep sequencing

All library construction and deep sequencing steps were performed at BGI (Shenzhen, China) according to their standard practice. Briefly, the RNA for RNA-seq was fragmented and synthesized into cDNA. The synthesized fragments were connected to adapters and amplified by PCR. For DNase-seq, sequencing adapters were added and 200-400 bp fragments selected. Both libraries were then sequenced using Illumina HiSeq 2000.

4.12.3 RNA-seq analysis

RNA-seq reads were aligned and normalized (Kim et al., 2013; Love et al., 2014). Log2 ratios were calculated between BMP4- and vehicle-treated samples for comparison between treatments. Genes that had a log2 ratio of 0.75 or greater were considered to be differentially expressed. In addition, the absolute difference in read counts between the two treatments was required to be at least 50. Gene enrichment of the differentially expressed protein-coding genes was performed with the DAVID 6.8 version (Huang da et al., 2009a; Huang da et al., 2009b). Fifteen differentially expressed genes (DEGs) were selected for further analysis using MDA-MB-231, T-47D, BT-474, MCF-7, MCF-10A, MDA-MB-361 and MDA-MB-436 cell lines treated with BMP4 or vehicle for 3, 6 and 24 h, before measurement of gene expression with qPCR (Table 6). Gene expression data from The Cancer Genome Atlas (TCGA), a dataset of 1212 breast cancer patients, was used to analyze association of the DEGs with survival. The difference in the survival times was tested using the logrank test and Benjamini-Hochberg correction was applied to the P-values. Further details can be found from the original publication (**Study III**).

4.12.4 DNase-seq analysis

Reads were analyzed using bowtie2 and DHSs were detected with DFilter (Langmead and Salzberg, 2012; Kumar et al., 2013). DHSs that were covered by less than 20 reads (in samples or input controls) or were located in ENCODE blacklisted regions (ENCODE Project Consortium, 2012) were omitted from further analysis. Additionally, DHSs with a distance of 100 bp or less between peaks were merged together and annotated from Gencode Genes version 19 using Bedtools (Quinlan and Hall, 2010). For comparison of the two treatments, DHS change scores (ΔDHS)

were calculated with a formula slightly modified from He et al. (2012). The DHSs with ΔDHS equal or greater than 0.20 were selected for enrichment analysis using GREAT version 3.0.0 (McLean et al., 2010) with default settings. In order to filter out generic ontology terms, categories with more than 1000 genes were excluded. Small categories, containing less than 10 genes, were also discarded. Transcription start sites (TSSs) from GENCODE transcripts corresponding to protein-coding genes were extended 1000 bases to both directions. For each gene, a weighted sum of the coverages of the TSSs over all the transcripts associated to it was calculated. The weight of each transcript's TSS was based on its estimated expression compared to total expression of the gene. The normalized expression values of the genes were linked to the corresponding TSSs. Detailed protocols can be found from the original publication (**Study III**).

4.12.5 Transcription factor binding site (TFBS) prediction, enrichment and TF silencing

DHSs in the promoter regions (2000 bp upstream of TSS) of upregulated genes in MDA-MB-231 and T-47D cell lines were scanned with Position Weight Matrices (PWMs), in order to find potential transcriptional regulators of BMP4 response. Due to the low signal-to-noise ratio in T-47D samples some DHS regions can be narrower or absent compared to untreated T-47D cell line samples from ENCODE DNase-seq datasets (Thurman et al., 2012; Natarajan et al., 2012). The promoter-associated DHSs were combined with the samples from ENCODE in order to increase the robustness of the analysis. The PWMs were retrieved from HOCOMOCO database (version 9) (Kulakovskiy et al., 2013), and the score calculated as previously described (Makeev et al., 2003). If the p-value was less than or equal to 0.001, the PWM was considered to be a match. Protocol details can be found from the original publication (**Study III**).

In order to find enriched TFBSs, DHSs of promoters from genes that were not upregulated by BMP4 were scanned for TFBSs and based on the results, the expected number of TFBSs were calculated for the promoter sets of upregulated genes of MDA-MB-231 and T-47D cells. The ratio of enrichment was then calculated by dividing the observed TFBSs by the number of expected TFBSs. For co-localization enrichment analysis, CAGACA, GTCT, CAGC, CGCC, GGCGCC and GCCGnCGC, previously reported as SMAD-binding elements (SBEs) (Kim et al., 1997; Jonk et al., 1998; Zawel et al., 1998; Nakahiro et al., 2010), were selected.

All TFBSs within 200 bp of a consensus motif were considered to be co-localized with the motif.

In order to silence selected TFs, 10 nM siRNA (siGENOME SMARTpool siRNAs, Dharmacon, Lafayette, CO, USA) and Interferin reagent (Polyplus-Transfection, Illkirch, France) or DharmaFECT (Dharmacon) were used for transfection of MDA-MB-231 and T-47D cells, according to manufacturer's instructions. ON-TARGETplus Non-targeting Control Pool was used as control (Dharmacon). Following 48 hours of transfection, the cells were treated with BMP4 or vehicle for 24h. RNA was then extracted for confirming TF knock-down (80% reduction in mRNA level was considered to be adequate) and for measuring BMP4 target gene expression (Table 6).

5 Summary of the results

5.1 The effects of BMP4 on breast cancer cell proliferation in 3D culture (I)

Previously BMP4 has been shown to reduce the proliferation of breast cancer cells in normal 2D culture (Ketolainen et al., 2010; Guo et al., 2012a). In this study, the persistence of this behavior was examined in 3D culture, which is a more physiological environment for cells. Ketolainen et al. (2010) found BMP4 to reduce growth of nine breast cancer cell lines to varying degrees. The endogenous expression of BMP4 in the cell lines was variable, with BT-474, MDA-MB-31 and T-47D having average expression values (Ketolainen et al., 2010). Other BMPs (BMP2 - 8) were expressed at a similar or lower level compared to BMP4 and BMP receptors were expressed by all nine cell lines (Alarmo et al., 2007). From the nine cell lines, MDA-MB-361, T-47D and MDA-MB-231 were included in this study. BT-474, which was first established to respond to BMP4 by reduced proliferation in 2D culture (70% reduction on day 6, $P<0.01$), was additionally included. In addition, the normal breast epithelial cell line MCF-10A was used as a reference and its growth was also shown to be inhibited by BMP4 in 2D culture (50% on day 6, $P<0.01$).

For 3D culture two different materials were used: the basement membrane extract Matrigel and the synthetic PEG gel. MCF-10A cells in Matrigel formed ordered acini structures, with a hollow lumen and basal localization of α6-integrin, a basal marker (Stewart and O'Connor, 2015). However, in PEG gel, the cells grew in more irregular structures with no polarization. BMP4 treatment reduced the growth of the MCF-10A cells in both Matrigel and PEG gel (Table 7). The breast cancer cell lines formed disordered structures in both materials. The proliferation of T-47D cells was inhibited by BMP4, in Matrigel as well as in PEG gel (Table 7). The proliferation of MDA-MB-361 and MDA-MB-231 cells were unaffected by BMP4 in Matrigel, but inhibition of growth can be seen in PEG gel (Table 7). BT-474 cells were only grown in Matrigel where the cells displayed a significant growth reduction in response to BMP4 (Table 7).

It has been previously shown that BMP4 induces a G1 cell cycle arrest in breast cancer cells (Ketolainen et al., 2010). G1 arrest was also confirmed to occur in MCF-

10A cells (G1 phase fraction 80% vs. 69% in BMP4- and vehicle-treated cells, respectively, on day 5 of treatment, $P < 0.05$). Further, known cell cycle regulator proteins were examined as possible mediators behind BMP4-induced inhibition of proliferation. Using Western blot, the effect of BMP4 (24 h treatment) on the expression of ten different cell cycle regulators was tested on 2D culture of MDA-MB-361 and T-47D cells. In both cell lines a change was seen in p21, phosphorylated CDC2 and Cyclins B1 and B2, with at least a 2-fold difference in one of the cell lines. p21 was selected for further analyses, both in 2D and 3D Matrigel. After 24 h of BMP4 treatment in 2D culture, p21 induction was seen in BT-474 and MDA-MB231 cells in addition to MDA-MB-361 and T-47D cells, as measured by Western blot analysis. In MCF-10A cells, p21 induction was seen after 5 days of treatment. In Matrigel, p21 induction was seen in all cell lines (after 4 or 7 days of treatment), except for MCF-10A, where no change was evident.

Table 7. The effect of BMP4 on breast epithelial and breast cancer cell growth. The proliferation percentage indicates the remaining level of proliferation (as measured by alamarBlue) compared to vehicle (100%). The area percentage indicates the area covered by the cells in BMP4 samples compared to vehicle (100%). Gray denotes statistically significant change between treatments ($P < 0.05$).

	Matrigel			PEG gel		
MCF-10A	*Day 7*	*Day 10*	*Day 14*	*Day 7*	*Day 9*	*Day 11*
Prol. (%)	52	83	59	43	22	31
Area (%)	48	63	60	49	62	84
T-47D	*Day 7*	*Day 10*	*Day 14*	*Day 7*	*Day 11*	*Day 14*
Prol. (%)	71	59	90	90	70	49
Area (%)	57	61	72	35	26	21
MDA-MB-361	*Day 10*	*Day 14*	*Day 17*	*Day 11*	*Day 14*	*Day 18*
Prol. (%)	93	75	94	85	78	72
Area (%)	139	113	112	52	69	56
MDA-MB-231	*Day 7*	*Day 10*	*Day 14*	*Day 7*	*Day 11*	*Day 14*
Prol. (%)	72	83	115	87	71	64
Area (%)	99*	145*	109*	74	64	74
BT-474	*Day 7*	*Day 10*	*Day 14*	*ND*	*ND*	*ND*
Prol. (%)	74	69	64	-	-	-
Area (%)	58	43	59	-	-	-

Prol. = Proliferation, ND = Not determined

* Due to the different cell morphologies between the treatments, area measurements may not accurately reflect growth of the cells.

5.2 BMP4-mediated effects on migration/invasion of MDA-MB-231 cells in 3D Matrigel culture (I)

Ketolainen et al. (2010) showed that in addition to the shared growth-inhibiting effect of BMP4, in three out of nine cell lines BMP4 induced migration as well. The most prominent induction of migration was found in MDA-MB-231 cells, also seen by Guo et al. (2012a). MDA-MB-231 was thus chosen for further study using 3D culture. In Matrigel BMP4 treatment caused a morphological change in the cells. Vehicle-treated cells formed dense aggregates of cells, whereas BMP4-treated cells grew in a stellate manner, with large branching structures (Figure 4). This behavior was reversed by addition of gremlin, a BMP antagonist. However, no change in morphology was apparent in PEG gel.

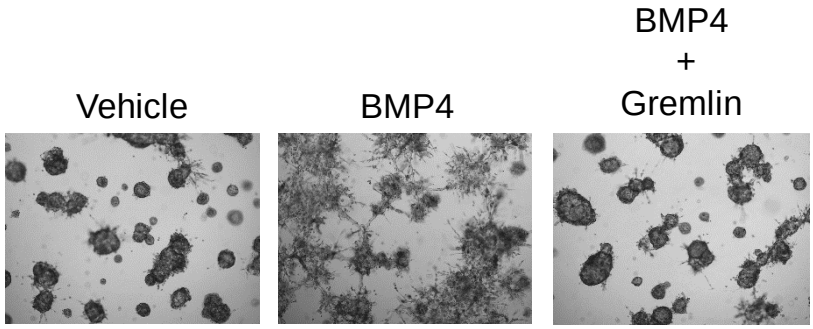

Figure 4. The effects of BMP4 and gremlin on MDA-MB-231 cells in Matrigel. The cells were treated with vehicle, BMP4 or gremlin together with BMP4. Representative images from day 14 are shown.

The migratory behavior exhibited by the cells upon BMP4 treatment may require the action of matrix metalloproteinases (MMPs). MDA-MB-231 cells in Matrigel were treated with a broad spectrum MMP inhibitor, Batimastat, along with BMP4 or vehicle. Batimastat alone caused a moderate reduction in proliferation of the cells. However, Batimastat was able to completely reverse the stellate phenotype caused by BMP4, resulting also in a reduction in the area covered by the cell structures.

Next, the expression of individual MMPs from the MDA-MB-231 cells were studied. RNA was extracted from the cells after 14 days of BMP4 and vehicle treatment in Matrigel and expression was measured by qPCR. No difference was seen in the expression of *ADAM17*, and *MMP2*, *MMP7* and *MMP9* were expressed

at levels that were too low for accurate assessment. However, there was a 19-fold increase in the expression of *MMP3* ($P < 0.05$) and a 3.7-fold increase in the expression of *MMP14* ($P < 0.05$) after BMP4 treatment. A 4.3-fold increase in *MMP1* expression was seen but the difference was not significant. Additionally, the expression of *MMP3* and *MMP14* was not induced by BMP4 in the non-stellate BT-474 cells.

5.3 The impact of BMP4 on breast cancer metastasis in vivo (II)

Previous studies have shown that BMP4 induced migration and invasion in MDA-MB-231 cells in 2D (Guo et al., 2012; Ketolainen et al., 2010) and 3D culture (as described above). Here the effect of BMP4 on MDA-MB-231 cells was examined in an in vivo model. The cells were first engineered to express luciferase and subsequent culturing in 3D Matrigel confirmed that the migratory behavior due to BMP4 persisted after the manipulation. BMP4- and vehicle pretreated MDA-MB-231/Luc cells were then injected intracardially, into the left ventricle of the nude mice. The mice were regularly injected with BMP4 or vehicle and metastasis followed by weekly bioluminescence imaging (BLI), from week three until sacrifice. The BMP4-treated mice developed metastases slightly earlier compared to vehicle-treated mice (Figure 5). However, the difference was not statistically significant. At end point, 13 metastases were found in the BMP4 group and 12 in the vehicle group (Figure 5), as confirmed by H&E and epithelial cell marker pancytokeratin immunohistochemistry (IHC) staining of the tissues. Most of the metastases occurred in bone, with the thigh bone (femur) being the most common site. There were more bone metastases in BMP4-treated mice (10 overall, 8 in thigh bone) compared to vehicle-treated (7 overall, 5 in thigh bone) (Figure 5). Noticeably, there were more adrenal gland metastases in the vehicle-treated mice compared to BMP4-treated (5 and 1, respectively). However, the numbers were too small to reach statistical significance in any of the cases.

For characterization of the tumors, IHC and immunofluorescence (IF) of the metastases collected at sacrifice were then performed using different markers. The stainings revealed active proliferation (as measured by Ki67 staining), and the presence of cancer-associated fibroblasts (CAFs, as measured by α-SMA staining) in both BMP4-treated and vehicle-treated mice. Staining for phosphorylated SMAD1/5/9 showed that BMP signaling was active in both treatment groups. Endothelial cell marker MECA-32 marker revealed that the tumor masses seemed

to contain deformed blood vessels, compared to the surrounding stroma, where normal blood vessels were seen. In addition, the tumor cells expressed the epithelial-to-mesenchymal transition (EMT) marker vimentin but not E-cadherin. However, no differences in these stainings were seen between the treatment groups.

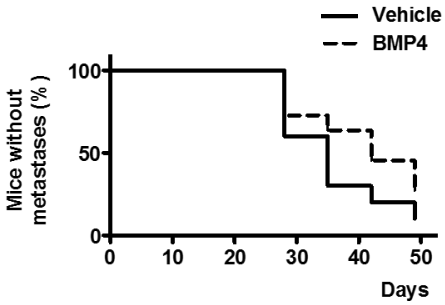

Number of	BMP4	Vehicle
Mice	10	11
Metastases	13	12
Soft tissue	3	5
Adrenal gland	1	5
Bone tissue	10	7
Femur	8	5
Metastasis/mouse (max)	2	3
Mice without metastasis	2	3

Figure 5. The impact of BMP4 on metastasis formation. On the left, the Kaplan–Meier plot shows the time to first metastasis. On the right, the metastases in BMP4 and vehicle group are categorized.

Since bone was the most common site of metastasis in both treatment groups, bone-specific stainings were employed for further characterization of the metastases. Toluidine blue was used for illustration of the cartilage and bone tissue in the epiphyseal plate of thigh bone metastases. The staining revealed that in some cases the tumor mass had invaded into the joint area through the epiphyseal plate. The osteoclast marker TRAP staining was found lining the epiphyseal plate, but also unexpectedly inside the tumor mass. Neither staining revealed any differences between the treatments.

5.4 Transcriptional regulation and chromatin landscape of breast cancer cells after BMP4 treatment (III)

BMP4 target genes and gene regulation were studied using RNA expression analysis (RNA-seq) and identification and mapping of open chromatin regions (DNase-seq), after BMP4 and vehicle treatment of MDA-MB-231 and T-47D cells. Using RNA-seq, 91 differentially expressed genes (DEGs) were found in MDA-MB-231 cells (59 upregulated and 33 downregulated genes) and 203 DEGs in T-47D cells (160

upregulated and 43 downregulated genes). Ten DEGs were common to both cell lines (*ATOH8*, *BDKRB2*, *BMF*, *GS1-124K5.4*, *ID1*, *ID2*, *ID3*, *SKIL*, *SMAD6*, and *SMAD9*), all of them upregulated. *ID1*, *ID2* and *ID3* are known BMP4 target genes, *SMAD9* a receptor-regulated SMAD and *SMAD6* an inhibitory SMAD. In T-47D, other BMP pathway-related genes were also upregulated, such as the BMP antagonist *NOG* and the pseudoreceptor *BAMBI*. In addition, 20 DEGs in MDA-MB-231 and 46 DEGs in T-47D, four of them shared (*ATOH8*, *ID3*, *SMAD6* and *SMAD9*) were associated with good or poor prognosis based on the The Cancer Genome Atlas (TCGA) database. DNase-seq data of the transcription start sites (TSSs) showed that in the majority of the DEGs, the chromatin openness did not increase upon to BMP4 stimulation. These data indicate that at this time point, changes in the chromatin status at TSS of the DEGs are not needed for transcription of the genes.

Gene ontology (GO) analysis was used for finding possible differences in the biological processes of the non-common DEGs. GO analysis using DAVID revealed that in MDA-MB-231 cell line migration-related categories were the most enriched, whereas in T-47D cells organ development and morphogenesis along with intracellular signaling were among the top GO terms.

For validation and expansion of the RNA-seq data, 15 DEGs compiled from both cell lines were selected for qPCR analysis based on their expression levels and cancer association as reported in the literature. In addition to MDA-MB-231 and T-47D, six other cell lines and time points of 3, 6 and 24 h of BMP4 treatment were used. The expression pattern of most of the genes was fairly similar across the cell lines and time points, except for MDA-MB-436 cells, where expression changed very little. In particular, the genes that were shared between MDA-MB-231 and T-47D (*ATOH8*, *ID2*, *SKIL*, *SMAD6* and *SMAD9*) were also consistently upregulated in the other cell lines and time points, whereas a little more variation was seen with the other selected DEGs.

Searching for DNase hypersensitive sites (DHSs) from the DNase-seq data of MDA-MB-231 cells revealed 89,830 peaks in the vehicle-treated sample and 97,349 peaks in the BMP4-treated sample. The corresponding numbers in T-47D were 68,000 and 73,881. For confirmation, peak detection of promoters from the T-47D cell line was compared with ENCODE data and the results were found to be consistent between the data sets. The overlapping DHSs from both treatment groups were then merged resulting in 106,154 peaks in MDA-MB-231 and 110,028 in T-47D. After the merging, 75% of the DHSs were shared between BMP4 and vehicle-treated samples in MDA-MB-231, while 9% of the DHSs were unique in the vehicle and 16% in the BMP4 sample. In T-47D cells, 27% of the DHSs were shared

while 34% were unique in the vehicle and 39% in the BMP4 sample. Annotation of DHSs to genomic features showed that in the vehicle-treated samples the distribution did not differ between the two cell lines. After BMP4 treatment, there was a shift to more DHSs in intronic and intergenic regions of both cell lines, accompanied with less DHSs in other genomic regions.

Enrichment analysis using GREAT was used to characterize the functional impact of BMP4-induced changes in the chromatin. With this analysis DHSs are assigned to putative gene regulatory regions. Consistently with the RNA-seq-derived DEGs, cell motility was one of the enriched categories in MDA-MB-231 cells, while e.g. different developmental processes were enriched in T-47D cells.

5.5 Transcription factors in BMP4 target gene regulation (III)

Using DNase-seq data from BMP4- and vehicle-treated MDA-MB-231 and T-47D cells, transcription factor binding sites (TFBSs) were searched for. The open chromatin regions of promoters in the upregulated genes were scanned for transcription factor motifs retrieved from the HOCOMOCO database. For the 401 individual TFs in the scan, an enrichment score was calculated in both cell lines. TFs that were not expressed based on RNA-seq data were excluded and 15 top enriched TFs from both cell lines were chosen as the most potential candidates for target gene regulation.

For experimental analysis we selected three TFs (MBD2, CBFB and HIF1A) that had 1) a motif with a quality category of A, B or C in the HOCOMOCO database, 2) relevant context to our model based on literature, 3) little or no other family members and 4) a high enough expression level for our experimental assay (> 1000 reads). Additionally, SMAD4 was used as a positive control. The three chosen TFs were also checked for SMAD4 binding site co-occurrence. MBD2 motif was found to be significantly co-localized with the GC-rich SMAD4 consensus motifs (CGCC, GCCGnCGC and GGCGCC; $P < 0.001$). Binding sites for CBFB and HIF1A in the DEGs were less frequent and although in several promoters SMAD bindings sites were co-localized with these factors, the associations were not significant.

The four TFs (SMAD4, CBFB, HIF1A, and MBD2) were silenced in MDA-MB-231 and T-47D cells to find out their impact on BMP signaling. After 48 hours of TF silencing, the cells were treated with BMP4 or vehicle for 24 hours before measurement of BMP4 target gene expression. For this purpose, the 15 target genes chosen for RNA-seq data validation and expansion were used (described above).

The results showed that SMAD4 silencing reversed the BMP4-mediated change of expression of all the tested target genes in both cell lines, with silencing of MBD2 reversing the change in most of the genes. On the other hand, HIF1A downregulation resulted in upregulation of the target genes in MDA-MB-231 cells, with an opposite effect or no change in T-47D cells. In MDA-MB-231, CBFB had variable effects, but it was mainly an activator of target genes in T-47D cells. Taken together, the effect of the TFs seemed to be cell line-specific.

6 Discussion

6.1 BMP4 functions as a key regulator of breast cancer cell growth in 3D environment

Previous studies have shown that BMP4 is able to inhibit the proliferation of breast cancer cells grown in standard 2D cell culture (Ketolainen et al., 2010; Guo et al., 2012a). However, 2D culture lacks many of the aspects that influence the behavior of cells in the body (Hartung, 2014). 3D culture methods aim to provide more physiological conditions for cell culture, providing e.g. a 3D environment and more complex cell-cell interactions. In **Study I**, breast cancer cells and one normal breast epithelial cell line (MCF-10A) were grown in two types of 3D materials, Matrigel (a biological gel) and PEG gel (a synthetic gel). MCF-10A cells in Matrigel formed round, hollow acini with polarization of the cells, corroborating previous findings using MCF-10A in Matrigel (Debnath et al., 2003). Also primary breast epithelial cells have been shown to form acinus-like structures in Matrigel (Petersen et al., 1992). The results thus suggest that Matrigel is a more physiological environment compared to PEG gel, where MCF-10A cells formed aggregates with no lumen and no polarization of the cells. The difference may be due to the many biological components of Matrigel, such as structural proteins and growth factors. For example, it has been shown that laminin is needed for the polarization of primary breast epithelial cells in collagen gels (Gudjonsson et al., 2002).

In contrast to MCF-10A, the breast cancer cell lines formed more disorganized structures in both materials. In Matrigel, T-47D grew in extensive raft-like formations, with BT-474 and MDA-MB-231 forming dense masses. These morphologies are mostly similar to what has been reported by Kenny et al. (2007). Large aggregates did not form in PEG gel, which may be due to the cells growing completely inside the matrix, in contrast to Matrigel where cells were grown near the surface (Debnath et al., 2003). Alternatively, Matrigel may provide a more growth-promoting matrix, as it has been shown to support the growth of MCF-7 breast cancer cells more than collagen, alginate or floating spheroid culture (Stock et al., 2016).

Previous studies have shown that BMP4 acts mainly as an inhibitor of proliferation in cancer cells, both in vitro and in vivo (Table 2). However, the effect of BMP4 seems to be context-dependent, as there is variation between and also within cancers from different tissues (Table 2). In **Study I,** the proliferation of all the cell lines tested in PEG gel was reduced after BMP4 treatment. In contrast, in Matrigel BMP4 inhibited the proliferation of two breast cancer cell lines and MCF-10A cells, while two breast cancer cell lines were unaffected (MDA-MB-231 and MDA-MB-361). In **Study II**, BMP4 did not inhibit proliferation (as measured by Ki67 staining) of metastases of MDA-MB-231 cells in mice, substantiating the results from Matrigel culture. Together with the fact that MCF-10A did not form acini in PEG gel, the results suggest that PEG gel does not offer an environment that suitably mimics the conditions in vivo. The effects of BMP4 in PEG gel matched those from 2D culture studies (Ketolainen et al., 2010; Guo et al., 2012a). In contrast, the effects in Matrigel were less extensive and in line with the observation that the behavior of cells may change in a 3D environment. For example, many anticancer drugs are not as effective in 3D culture (Smalley et al., 2006; Stock et al., 2016).

In **Study I**, the effect of BMP4 on proliferation was shown to be dependent on the cell cycle inhibitor p21. Its expression was induced in all the cell lines after BMP4 treatment in 2D culture. Previously BMP4 has been shown to induce p21 in gastric carcinoma cells and osteoblasts (Chang et al., 2009; Shirai et al., 2011). However, in breast cancer cells the effect of BMP4 on p21 has not been studied. Only BMP2 has previously been shown to induce p21 expression in breast cancer cells (Ghosh-Choudhury et al., 2000a; Ghosh-Choudhury et al., 2000b; Chen et al., 2012). In 3D Matrigel culture p21 was induced in all of the cell lines except MCF-10A. Even though growth reduction in MCF-10A 2D culture is apparent on day 3, p21 induction and G1 cell cycle arrest were evident only after 5 days of culture. In addition, p21 was induced even in the cells where no effect on proliferation was seen (MDA-MB-231 and MDA-MB-361). This suggests that p21 cannot solely explain the BMP4-induced inhibition of proliferation.

6.2 BMP4 is implicated in increased breast cancer cell migration/invasion in vitro and in vivo

BMP4 has been shown to inhibit the proliferation of many cancer types, including breast cancer, which makes it a potential subject for cancer therapy (Kallioniemi, 2012). However, in many cancer types BMP4 increased migration and/or invasion

(Table 2). In some breast cancer cell lines in 2D culture BMP4 has been shown to increase migration and invasion (Ketolainen et al., 2010; Guo et al., 2012a). As metastasis is the cause of death in most breast cancer patients (Redig and McAllister, 2013), the effect of BMP4 on the migration/invasion (**Study I**), metastatic ability (**Study II**) and transcriptional responses (**Study III**) of breast cancer cells was studied more closely.

The effect of BMP4 on transcription was studied in MDA-MB-231 cells, which respond to BMP4 with increased migration and invasion. In order to obtain a sufficient amount of material for the analysis, the expression of BMP4 target genes was measured after BMP4 treatment in normal 2D culture. Gene ontology (GO) analysis showed that motility-related pathways were enriched in BMP4 target genes. In addition, when putative regulatory regions of the genome were scanned from BMP4-treated MDA-MB-231 cells, some of the regions were also significantly associated with cellular motility. Previously migration-related terms have been shown to be enriched by BMP4 treatment in MDA-MB-361 breast cancer cells (Rodriguez-Martinez et al., 2011). Other efforts to study the transcriptional effects of BMP4 in more detail have focused on non-cancerous cells (Fei et al., 2010; Morikawa et al., 2011; Genander et al., 2014).

In order to expand on the results from 2D culture, in **Study I** MDA-MB-231 cells were grown in a more physiological environment using 3D culture. BMP4 did not have an effect on migration of the cells in the synthetic PEG gel. However, in Matrigel BMP4 induced a branching, stellate morphology indicative of increased migration, which was reversible by BMP antagonist gremlin. A broad spectrum MMP inhibitor Batimastat was able to reverse the stellate phenotype. MMPs are needed for breaking down of the physical barriers that restrict cancer cell invasion, although they may have other roles as well (Gialeli et al., 2011).

A more detailed analysis on the expression of seven individual MMPs from MDA-MB-231 cells in Matrigel showed that *MMP3* and *MMP14* expression was induced by BMP4 in MDA-MB-231 cells but not in the non-stellate BT-474 cells. In addition to increased invasion and EMT induction, MMP3 has previously been shown to increase growth factor bioavailability and MMP14 has been shown to participate in the induction of tumor angiogenesis and the proteolytic activation of TFG-β (Suzuki et al., 1997; Mu et al., 2002; Egeblad and Werb, 2002; Devy et al., 2009; Chen et al., 2013; Yan et al., 2015). However, there are no previous reports on the effects of BMPs on MMP3 or MMP14. BMP4 and BMP6 have been shown to inhibit *MMP9* expression in retinal pigment epithelial cells and MCF-7 breast cancer cells, respectively (Wang et al., 2011; Xu et al., 2012). However, one study found

BMP4 to induce *MMP2* and *MMP9* expression in breast cancer cells (Cyr-Depauw et al., 2016). In MDA-MB-231 cells BMP4 has been found to inhibit *MMP9* expression and either induce or not affect *MMP1* expression (Shon et al., 2009; Guo et al., 2012a). However, apart from **Study I**, the aforementioned studies have been done in standard 2D culture. Taken together, the induction of MMP expression by BMPs seems to be very context-dependent.

In **Study II**, the effect of BMP4 on MDA-MB-231 was studied in vivo using a mouse metastatic model with BMP4 or vehicle treatment. Although no significant difference was found, there was a trend toward earlier metastasis and more bone metastases in the BMP4-treated mice. However, the number of metastases was too small for statistical evaluation. Previously, the effect of BMP4 on breast cancer metastasis has only been studied using mouse mammary cancer cells showing BMP4-mediated reduction of metastasis formation (Cao et al., 2014). This reduction was shown to be caused by increased antitumor immunity resulting from BMP4-induced inhibition of granulocyte colony-stimulating factor (G-CSF) secretion (Cao et al., 2014).

The metastases in **Study II** were also stained with different markers. Staining for pSMAD/1/5/9 showed strong activation of BMP signaling but no difference was seen between the treatment groups, although dosing of BMP4 was comparable to other studies where BMP4 has been used (Buckley et al., 2004; Nishanian et al., 2004; Piccirillo et al., 2006; Buijs et al., 2007; Farnsworth et al., 2011; Klose et al., 2011; Tsuchida et al., 2014). Nevertheless, the signaling pathway is shared by many ligands of the BMP family (Rider and Mulloy, 2010) and it is likely that the possible additional effect of BMP4 cannot be seen on top of the basal BMP signaling level. α-SMA staining suggests that cancer-associated fibroblasts (CAF) are equally present in both treatment groups. CAFs are implicated in tumorigenesis, including metastasis formation, in breast cancer (Buchsbaum and Oh, 2016). MECA-32 staining showed possible deformed blood vessels in the tumor masses. As mesenchymal/myoepithelial-like cells, MDA-MB-231 expressed vimentin but not E-cadherin (Gordon et al., 2003). However, there were no differences between the treatment groups in any of the markers used.

Staining of the bone metastases from **Study II** showed that the cells in thigh bone formed metastases preferentially in the joint area. Sosnoski et al. (2012) showed that more cytokines are present in the joint area compared to the shaft (diaphysis), indicating that the cytokines may act as chemoattractants. In addition, metastases formed by MDA-MB-231 cells increased the cytokine presence in the joint area but not in the shaft (Sosnoski et al., 2012). Interestingly, osteoclast marker staining

(TRAP) was found in the tumor mass in **Study II**, suggesting that there may be osteoclasts in the tumor mass, or that the cells have started to express the TRAP enzyme (Adams et al., 2007; Shishido-Hara et al., 2010). However, BMP4 treatment did not change the morphology or osteoclast presence of the metastases.

Taken together, transcriptional analysis and 3D in vitro data with MDA-MB-231 cells supports prior findings that in most breast cancer studies BMP4 induces migration (Ketolainen et al., 2010; Pal et al., 2012; Guo et al., 2012a; Owens et al., 2013; Cyr-Depauw et al., 2016). The effect of BMP4 on metastasis formation in vivo showed a non-significant trend of increased metastasis. Previously, BMP4 expression in breast cancer has been shown to be associated with increased frequency of tumor recurrence (Alarmo et al., 2013). However, besides migration and invasion capabilities, metastasis formation requires adaptation and growth of the cells in the destination sites (Valastyan and Weinberg, 2011), making research into metastasis more complicated. Thus more studies using in vivo models are needed to uncover the possible effect of BMP4 on metastasis.

6.3 BMP4 target genes and their regulation is context-dependent

BMP4 target genes have previously been studied in breast cancer cells that react to BMP4 mainly by decreased proliferation (Rodriguez-Martinez et al., 2011). In **Study III**, the differences in BMP4 target genes and their regulation were examined in a cell line that responds to BMP4 by increased migration (MDA-MB-231) and a cell line that responds by decreased proliferation (T-47D). RNA-seq and DNase-seq was performed on the BMP4 and vehicle-treated cells. RNA-seq revealed that the set of differentially expressed genes (DEGs) between the cell lines was very divergent. Out of 91 DEGs in MDA-MB-231 and 203 DEGs in T-47D, only 10 genes were shared, many of which were known to be related to the BMP pathway. Similarly, the number of shared genes compared to the study by Rodriguez-Martinez et al. (2011) was low, likely due to the different cell lines used. Moreover, Rodriguz-Martinez et al. (2011) also found that different breast cancer cell lines have divergent responses to BMP4, as seen here with MDA-MB-231 and T-47D. However, the 10 shared genes between MDA-MB-231 and T-47D were the most consistently BMP4-responsive genes also when additional breast cancer cell lines were used. In contrast to the shared genes, GO analysis of the unique DEGs from the two cell lines revealed that the enriched

categories reflected the response of the cells to BMP4. This was also corroborated by GREAT GO analysis of putative open chromatin regulatory regions.

Comparison of open regions of the chromatin (DHSs) after BMP4 and vehicle treatment showed that there was a shift to more intronic and intergenic DHSs in the BMP4-induced peaks, with a reduction in promoter and exon peaks. The opening of intergenic DHSs may be an indication of regulatory control through distal enhancers or silencers. It has been shown that distal DHSs are more divergent between cell lines compared to promoter DHSs (Thurman et al., 2012). Indeed, as described above, the GREAT analysis reflected the different responses of MDA-MB-231 and T-47D cells to BMP4. Based on the DNase-seq data, transcription start sites (TSSs) were mostly already open in BMP4-induced genes. It has been previously shown that TSS openness varies little even between cell lines of diverse origins (Natarajan et al., 2012), and thus a change in TSS openness is not necessarily expected.

The open chromatin regions of upregulated DEGs, as revealed by DNase-seq, were scanned for transcription factor binding sites (TFBSs), in order to further characterize BMP4 target gene regulation. From the top 15 lists of enriched TFs in BMP4-treated MDA-MB-231 and T-47D cells, five have previously been shown to regulate BMP target genes. E4F1 acted co-operatively with SMAD4 in C2C12 cells and E2F3 was recruited to the N-myc promoter in BMP6-treated keratinocytes (Chang et al., 2006; Nojima et al., 2010). In addition, XBP1, RELA and CREB1 were shown to influence BMP target gene expression, similarly in non-cancerous cells (Cao et al., 2006; Zhao et al., 2009; Hirata-Tsuchiya et al., 2014). Other TFs that bind to SMADs and influence BMP target gene regulation have been studied in various cell types (Table 1). However, as these studies are still mostly looking at single TFs, usually in non-cancerous cell lines, more data are needed to find out the extent of the action of TFs that regulate BMP target genes, both in normal and cancer cells.

In **Study III**, three TFs (CBFB, HIF1A and MBD2) were selected and experimentally studied using silencing of the TFs in MDA-MB-231 and T-47D cells to uncover their effect on BMP4 target gene expression. In addition, SMAD4, as a key component of BMP signaling, was used as a positive control. The silencing experiments showed that SMAD4 was needed for the expression of all the target genes tested, implying that they were regulated through the canonical pathway instead of the possible alternative pathways available for BMP signaling (Miyazono et al., 2010; Bragdon et al., 2011). The effects of the other TFs were more variable.

The transcription factor MBD2 is a methyl-CpG-binding transcription factor that plays a role in development (Klose and Bird, 2006; Menafra and Stunnenberg, 2014). It has previously been associated with both repressive and permissive chromatin

(Detich et al., 2002; Martinowich et al., 2003; Horike et al., 2005). In **Study III**, MBD2 was an activator of transcription in all the genes tested in MDA-MB-231 cells and in most of the genes in T-47D. Consistently with this, MBD2 had a large number of binding sites across DEGs and it was highly expressed in both cell lines. In addition, TFBSs for MBD2 were significantly associated with the SMAD GC-rich motifs, in contrast to the other TFs where SMAD motif association was not significant, likely due to having less TFBSs in the DEGs.

Hypoxia-inducible factor 1-α (HIF1A) is a key regulator of the hypoxia response and has been linked to breast cancer progression (Wang et al., 2014c). In **Study III** it was shown to repress target gene activation in MDA-MB-231 cells but to activate transcription or have no effect in T-47D cells. When considering all the DEGs, four hypoxia-related genes (*BDKRB2*, *PDGFB*, *ANGPTL4* and *UCN2*) were found to be upregulated in MDA-MB-231 cells, and three in T-47D cells (*CBFA2T3*, *EGLN3* and *FLT1*). Some of these genes have also been previously linked to cancer progression, for example HIF1A-dependent upregulation of *PDGFB* and *ANGPTL4* promotes metastasis of hypoxic breast cancer cells (Schito et al., 2012; Zhang et al., 2012a). Even though HIF1A in the target gene panel did not act as an activator in MDA-MB-231 cells, it is possible that HIF1A acts divergently on genes that are relevant in hypoxia. Interestingly, HIF1A has also been shown to activate BMP4 transcription in several tissues (Wu and Paulson, 2010; Wang et al., 2015; Pramono et al., 2016).

The core-binding factor subunit beta (CBFB) had varying effects on the expression of BMP4 target genes, but was generally an activator in T-47D cells. It is the beta subunit of a complex with RUNX1 or RUNX2 as alpha subunit. CBFB has been shown to be involved in hematopoiesis and skeletal development (Okuda et al., 2000; Yoshida et al., 2002) and RUNX2 has been shown in many studies to regulate BMP target gene expression (Table 1). Interestingly, CBFB promotes invasive properties in breast, prostate and ovarian cancer (Davis et al., 2010; Mendoza-Villanueva et al., 2010).

In summary, the different phenotypes induced by BMP4 in MDA-MB-231 and T-47D cells are reflected in the transcriptomic and chromatin levels, as shown by enrichment analysis of BMP4 target genes and open chromatin regions. In addition, different TFs appear to be recruited to the target genes depending on the cell line.

7 Conclusions

Breast cancer is the most common cancer in women worldwide and bone morphogenetic proteins (BMPs) have been suggested to play a role in the progression of the disease. BMP4 has previously been shown to inhibit proliferation and increase migration in breast cancer cell lines, and its expression in breast cancer has been associated with low proliferation index and increased frequency of tumor recurrence. The aim of this study was to decipher the effects of BMP4 on breast cancer cells in 3D cell culture and in an in vivo model, as well as to characterize BMP4 signaling in breast cancer cells at the chromatin and mRNA level.

BMP4 was found to inhibit breast cancer cell proliferation in 3D culture, both in the synthetic PEG gel as well as the basement membrane extract Matrigel. Growing normal breast epithelial cells in the two different materials revealed that Matrigel provided a more physiological environment. Notably, MDA-MB-231 cells, which were shown to respond to BMP4 by increased migration in 2D culture, reacted similarly in Matrigel but not in PEG gel. BMP4 induced in MDA-MB-231 cells in Matrigel a branching, stellate morphology, indicative of increased migration, and this phenotype was dependent on the action of matrix metalloproteinases (MMPs). In an in vivo metastatic model of MDA-MB-231 cells, BMP4 caused a trend of earlier metastasis and slightly more bone metastases. However, due to the limited number of metastases, statistical significance was not reached. The effects of BMP4 in 2D culture, both decreased growth and increased migration, were thus recapitulated in 3D culture. Still, more studies are needed to confirm the role of BMP4 on in vivo metastasis formation in breast cancer.

Analysis of BMP4 target genes revealed that the effects of BMP4 on proliferation and migration were reflected in the target genes that were induced. In MDA-MB-231 cells, which react to BMP4 mainly by increased migration, motility-related genes were enriched. In T-47D cells, which respond to BMP4 by inhibition of proliferation, developmental and signaling pathway genes were enriched. Similar results were obtained when enrichment of putative chromatin regulatory regions was analyzed. By examining open transcription factor binding sites, candidate TFs involved in BMP4 target gene regulation were found. Experimental validation of three TFs, MBD2, CBFB and HIF1A, showed that MBD2 was an activator of

transcription in both cell lines, whereas the effects of CBFB and HIF1A were more cell line-specific. HIF1A acted as a repressor in MDA-MB-231 cells and CBFB as an activator particularly in T-47D cells. Taken together, BMP4 induced a phenotype-specific gene expression pattern, which the experimentally validated TFs reflected. Further study regarding chromatin regulation and TFs in the BMP signaling pathway, including TFs not yet functionally characterized or uncovered in this study, will hopefully expand the results to an even wider context.

Acknowledgements

The research for this dissertation was carried out in the Laboratory of Cancer Genomics at the Institute of Biosciences and Medical Technology (BioMediTech), University of Tampere, during the years 2011-2017. I am grateful for the former Dean of BioMediTech, Doctor Hannu Hanhijärvi, and the current Dean of the new Faculty of Medicine and Life Sciences, Professor Tapio Visakorpi, for providing excellent research facilities and working environment for my research and studies. I would like to thank the Doctoral Programme in Biomedicine and Biotechnology (TGPBB), Alfred Kordelinin Foundation and Pirkanmaa Cancer Foundation (Pirkanmaan syöpäyhdistys) for funding my research. For additional financial support for my research I would like to thank Fimlab laboratories, Tampereen yliopiston tukisäätiö, The Finnish Concordia Fund, the Finnish Cancer Foundation and Tampereen tiederahasto.

My sincerest thanks go to my supervisors, Professor Anne Kallioniemi and Emma-Leena Alarmo, PhD. Anne, your guidance, ideas and insights have inspired me in my research. Thank you for giving me the chance to do my thesis in your group and for always showing such interest in my research and always being willing to help. Emma-Leena, thank you for sharing your experiences, helping with any problems and always being so positive and supportive of me. I've missed you at work!

I'd also like to thank the members of my thesis committee, Docent Susanna Miettinen and Hannu Turpeinen, PhD, for your input and questions concerning my thesis. Thank you also to pre-examiners Docent Erkki Hölttä and Docent Katri Koli, I'm grateful for your insights and feedback in finishing the writing of my thesis.

Thanks go to all my co-authors! Alejandra Rodriguez Martinez, PhD, thank you for all the help, laughs and conversation. Riikka Havunen, MSc, couldn't have wished for anyone better to work with when starting my PhD studies. Docent Kati Juuti-Uusitalo, thank you for your determination and focus and Maaria Palmroth, MSc, for your much-needed and well-timed help. Philip Owens, PhD, Agnes Gorska, MSc, and Professor Harold Moses, my short visit with you was full of good memories. Tommi Rantapero, MSc, and Professor Matti Nykter, thank you for your help, hard work and patience with someone not so well versed in bioinformatics!

I want to thank the members of our research group, Ms. Kati Rouhento for sharing your knowledge and helping in the lab, Elisa Vuorinen, MSc, and Nina Rajala, PhD, for your friendship all the way from the "other office" and Kati Porkka, PhD, for your positive attitude. Thank you also to the former members of the group, Hanna Rauhala, PhD, Johanna Ketolainen, MSc, Sanna Penkki, MSc, Eeva Laurila, PhD, Riina Kuuselo, PhD, Kimmo Savinainen, PhD, and all the summer and master's thesis workers. I also want to acknowledge all my other colleagues at the ever-expanding institute, you have all contributed to its wonderful atmosphere.

Thank you to friends from school (Minna B!) and dance classes, thank you to my relatives. My friends from university, Sina, Alexandra, Marja, Noora M and Noora N, I'll always be grateful for the happy coincidence that brought us together. Your humor lights up the day!

Finally, thank you to my family. Thank you to my wonderful brothers Henrik and Roni, I'm proud of you both. Senni, I'm glad that you and Henrik found each other. Thank you for your kindness and positivity. Dear Mother and Father, thank you for always being there. I couldn't have done any of this without you.

Tampere, January 2017

Minna Ampuja

References

Achilli TM, Meyer J, Morgan JR. Advances in the formation, use and understanding of multi-cellular spheroids. Expert Opin Biol Ther 2012;12:1347-60.

Adams LM, Warburton MJ, Hayman AR. Human breast cancer cell lines and tissues express tartrate-resistant acid phosphatase (TRAP). Cell Biol Int 2007;31:191-5.

Afzal F, Pratap J, Ito K, Ito Y, Stein JL, van Wijnen AJ, et al. Smad function and intranuclear targeting share a Runx2 motif required for osteogenic lineage induction and BMP2 responsive transcription. J Cell Physiol 2005;204:63-72.

Alarmo EL, Huhtala H, Korhonen T, Pylkkanen L, Holli K, Kuukasjarvi T, et al. Bone morphogenetic protein 4 expression in multiple normal and tumor tissues reveals its importance beyond development. Mod Pathol 2013;26:10-21.

Alarmo EL, Kallioniemi A. Bone morphogenetic proteins in breast cancer: dual role in tumourigenesis? Endocr Relat Cancer 2010;17:R123-39.

Alarmo EL, Kuukasjärvi T, Karhu R, Kallioniemi A. A comprehensive expression survey of bone morphogenetic proteins in breast cancer highlights the importance of BMP4 and BMP7. Breast Cancer Res Treat 2007;103:239-46.

Antoni D, Burckel H, Josset E, Noel G. Three-dimensional cell culture: a breakthrough in vivo. Int J Mol Sci 2015;16:5517-27.

Bae SC, Lee KS, Zhang YW, Ito Y. Intimate relationship between TGF-beta/BMP signaling and runt domain transcription factor, PEBP2/CBF. J Bone Joint Surg Am 2001;83-A Suppl 1:S48-55.

Bai RY, Koester C, Ouyang T, Hahn SA, Hammerschmidt M, Peschel C, et al. SMIF, a Smad4-interacting protein that functions as a co-activator in TGFbeta signalling. Nat Cell Biol 2002;4:181-90.

Bai S, Shi X, Yang X, Cao X. Smad6 as a transcriptional corepressor. J Biol Chem 2000;275:8267-70.

Balboni AL, Cherukuri P, Ung M, DeCastro AJ, Cheng C, DiRenzo J. p53 and DeltaNp63alpha Coregulate the Transcriptional and Cellular Response to TGFbeta and BMP Signals. Mol Cancer Res 2015;13:732-42.

Benien P, Swami A. 3D tumor models: history, advances and future perspectives. Future Oncol 2014;10:1311-27.

Bianchini G, Balko JM, Mayer IA, Sanders ME, Gianni L. Triple-negative breast cancer: challenges and opportunities of a heterogeneous disease. Nat Rev Clin Oncol 2016;13:674-90.

Blitz IL, Cho KW. Finding partners: how BMPs select their targets. Dev Dyn 2009;238:1321-31.

Bowers RR, Lane MD. A role for bone morphogenetic protein-4 in adipocyte development. Cell Cycle 2007;6:385-9.

Bragdon B, Moseychuk O, Saldanha S, King D, Julian J, Nohe A. Bone morphogenetic proteins: a critical review. Cell Signal 2011;23:609-20.

Brazil DP, Church RH, Surae S, Godson C, Martin F. BMP signalling: agony and antagony in the family. Trends Cell Biol 2015;25:249-64.

Brown CO,3rd, Chi X, Garcia-Gras E, Shirai M, Feng XH, Schwartz RJ. The cardiac determination factor, Nkx2-5, is activated by mutual cofactors GATA-4 and Smad1/4 via a novel upstream enhancer. J Biol Chem 2004;279:10659-69.

Brubaker KD, Corey E, Brown LG, Vessella RL. Bone morphogenetic protein signaling in prostate cancer cell lines. J Cell Biochem 2004;91:151-60.

Buchsbaum RJ, Oh SY. Breast Cancer-Associated Fibroblasts: Where We Are and Where We Need to Go. Cancers (Basel) 2016;8:10.3390.

Buckley S, Shi W, Driscoll B, Ferrario A, Anderson K, Warburton D. BMP4 signaling induces senescence and modulates the oncogenic phenotype of A549 lung adenocarcinoma cells. Am J Physiol Lung Cell Mol Physiol 2004;286:L81-6.

Buijs JT, Rentsch CA, van der Horst G, van Overveld PG, Wetterwald A, Schwaninger R, et al. BMP7, a putative regulator of epithelial homeostasis in the human prostate, is a potent inhibitor of prostate cancer bone metastasis in vivo. Am J Pathol 2007;171:1047-57.

Cao Y, Knochel S, Oswald F, Donow C, Zhao H, Knochel W. XBP1 forms a regulatory loop with BMP-4 and suppresses mesodermal and neural differentiation in Xenopus embryos. Mech Dev 2006;123:84-96.

Cao Y, Slaney CY, Bidwell BN, Parker BS, Johnstone CN, Rautela J, et al. BMP4 inhibits breast cancer metastasis by blocking myeloid-derived suppressor cell activity. Cancer Res 2014;74:5091-102.

Carletti E, Motta A, Migliaresi C. Scaffolds for tissue engineering and 3D cell culture. Methods Mol Biol 2011;695:17-39.

Carreira AC, Zambuzzi WF, Rossi MC, Astorino Filho R, Sogayar MC, Granjeiro JM. Bone Morphogenetic Proteins: Promising Molecules for Bone Healing, Bioengineering, and Regenerative Medicine. Vitam Horm 2015;99:293-322.

Cekanova M, Rathore K. Animal models and therapeutic molecular targets of cancer: utility and limitations. Drug Des Devel Ther 2014;8:1911-21.

Chang SF, Chang TK, Peng HH, Yeh YT, Lee DY, Yeh CR, et al. BMP-4 induction of arrest and differentiation of osteoblast-like cells via p21 CIP1 and p27 KIP1 regulation. Mol Endocrinol 2009;23:1827-38.

Chang WY, Andrews J, Carter DE, Dagnino L. Differentiation and injury-repair signals modulate the interaction of E2F and pRB proteins with novel target genes in keratinocytes. Cell Cycle 2006;5:1872-9.

Chen A, Wang D, Liu X, He S, Yu Z, Wang J. Inhibitory effect of BMP-2 on the proliferation of breast cancer cells. Mol Med Rep 2012;6:615-20.

Chen QK, Lee K, Radisky DC, Nelson CM. Extracellular matrix proteins regulate epithelial-mesenchymal transition in mammary epithelial cells. Differentiation 2013;86:126-32.

Chiu CY, Kuo KK, Kuo TL, Lee KT, Cheng KH. The activation of MEK/ERK signaling pathway by bone morphogenetic protein 4 to increase hepatocellular carcinoma cell proliferation and migration. Mol Cancer Res 2012;10:415-27.

Claus EB, Schildkraut JM, Thompson WD, Risch NJ. The genetic attributable risk of breast and ovarian cancer. Cancer 1996;77:2318-24.

Conesa A, Madrigal P, Tarazona S, Gomez-Cabrero D, Cervera A, McPherson A, et al. A survey of best practices for RNA-seq data analysis. Genome Biol 2016;17:13,016-0881-8.

Conidi A, van den Berghe V, Leslie K, Stryjewska A, Xue H, Chen YG, et al. Four amino acids within a tandem QxVx repeat in a predicted extended alpha-helix of the Smad-binding domain of Sip1 are necessary for binding to activated Smad proteins. PLoS One 2013;8:e76733.

Croce CM. Oncogenes and cancer. N Engl J Med 2008;358:502-11.

Cyr-Depauw C, Northey JJ, Tabaries S, Annis MG, Dong Z, Cory S, et al. Chordin-Like 1 Suppresses Bone Morphogenetic Protein 4-Induced Breast Cancer Cell Migration and Invasion. Mol Cell Biol 2016;36:1509-25.

Dai J, Keller J, Zhang J, Lu Y, Yao Z, Keller ET. Bone morphogenetic protein-6 promotes osteoblastic prostate cancer bone metastases through a dual mechanism. Cancer Res 2005;65:8274-85.

Davis JN, Rogers D, Adams L, Yong T, Jung JS, Cheng B, et al. Association of core-binding factor beta with the malignant phenotype of prostate and ovarian cancer cells. J Cell Physiol 2010;225:875-87.

de Jong DS, Vaes BL, Dechering KJ, Feijen A, Hendriks JM, Wehrens R, et al. Identification of novel regulators associated with early-phase osteoblast differentiation. J Bone Miner Res 2004;19:947-58.

Debnath J, Muthuswamy SK, Brugge JS. Morphogenesis and oncogenesis of MCF-10A mammary epithelial acini grown in three-dimensional basement membrane cultures. Methods 2003;30:256-68.

Deng H, Makizumi R, Ravikumar TS, Dong H, Yang W, Yang WL. Bone morphogenetic protein-4 is overexpressed in colonic adenocarcinomas and promotes migration and invasion of HCT116 cells. Exp Cell Res 2007a;313:1033-44.

Deng H, Ravikumar TS, Yang WL. Overexpression of bone morphogenetic protein 4 enhances the invasiveness of Smad4-deficient human colorectal cancer cells. Cancer Lett 2009;281:220-31.

Deng H, Ravikumar TS, Yang WL. Bone morphogenetic protein-4 inhibits heat-induced apoptosis by modulating MAPK pathways in human colon cancer HCT116 cells. Cancer Lett 2007b;256:207-17.

Detich N, Theberge J, Szyf M. Promoter-specific activation and demethylation by MBD2/demethylase. J Biol Chem 2002;277:35791-4.

Devy L, Huang L, Naa L, Yanamandra N, Pieters H, Frans N, et al. Selective inhibition of matrix metalloproteinase-14 blocks tumor growth, invasion, and angiogenesis. Cancer Res 2009;69:1517-26.

Dunn NR, Winnier GE, Hargett LK, Schrick JJ, Fogo AB, Hogan BL. Haploinsufficient phenotypes in Bmp4 heterozygous null mice and modification by mutations in Gli3 and Alx4. Dev Biol 1997;188:235-47.

Egeblad M, Werb Z. New functions for the matrix metalloproteinases in cancer progression. Nat Rev Cancer 2002;2:161-74.

Ehata S, Yokoyama Y, Takahashi K, Miyazono K. Bi-directional roles of bone morphogenetic proteins in cancer: another molecular Jekyll and Hyde? Pathol Int 2013;63:287-96.

ENCODE Project Consortium. An integrated encyclopedia of DNA elements in the human genome. Nature 2012;489:57-74.

Esch EW, Bahinski A, Huh D. Organs-on-chips at the frontiers of drug discovery. Nat Rev Drug Discov 2015;14:248-60.

Fang WT, Fan CC, Li SM, Jang TH, Lin HP, Shih NY, et al. Downregulation of a putative tumor suppressor BMP4 by SOX2 promotes growth of lung squamous cell carcinoma. Int J Cancer 2014;135:809-19.

Farnsworth RH, Karnezis T, Shayan R, Matsumoto M, Nowell CJ, Achen MG, et al. A role for bone morphogenetic protein-4 in lymph node vascular remodeling and primary tumor growth. Cancer Res 2011;71:6547-57.

Feeley BT, Gamradt SC, Hsu WK, Liu N, Krenek L, Robbins P, et al. Influence of BMPs on the formation of osteoblastic lesions in metastatic prostate cancer. J Bone Miner Res 2005;20:2189-99.

Fei T, Xia K, Li Z, Zhou B, Zhu S, Chen H, et al. Genome-wide mapping of SMAD target genes reveals the role of BMP signaling in embryonic stem cell fate determination. Genome Res 2010;20:36-44.

Ferdowsian HR, Beck N. Ethical and scientific considerations regarding animal testing and research. PLoS One 2011;6:e24059.

Ferlay J, Soerjomataram I, Dikshit R, Eser S, Mathers C, Rebelo M, et al. Cancer incidence and mortality worldwide: sources, methods and major patterns in GLOBOCAN 2012. Int J Cancer 2015;136:E359-86.

Finotello F, Di Camillo B. Measuring differential gene expression with RNA-seq: challenges and strategies for data analysis. Brief Funct Genomics 2015;14:130-42.

Frese KK, Tuveson DA. Maximizing mouse cancer models. Nat Rev Cancer 2007;7:645-58.

Garcia de Vinuesa A, Abdelilah-Seyfried S, Knaus P, Zwijsen A, Bailly S. BMP signaling in vascular biology and dysfunction. Cytokine Growth Factor Rev 2016;27:65-79.

Gazzerro E, Gangji V, Canalis E. Bone morphogenetic proteins induce the expression of noggin, which limits their activity in cultured rat osteoblasts. J Clin Invest 1998;102:2106-14.

Genander M, Cook PJ, Ramskold D, Keyes BE, Mertz AF, Sandberg R, et al. BMP signaling and its pSMAD1/5 target genes differentially regulate hair follicle stem cell lineages. Cell Stem Cell 2014;15:619-33.

Ghosh-Choudhury N, Ghosh-Choudhury G, Celeste A, Ghosh PM, Moyer M, Abboud SL, et al. Bone morphogenetic protein-2 induces cyclin kinase inhibitor p21 and hypophosphorylation of retinoblastoma protein in estradiol-treated MCF-7 human breast cancer cells. Biochim Biophys Acta 2000a;1497:186-96.

Ghosh-Choudhury N, Singha PK, Woodruff K, St Clair P, Bsoul S, Werner SL, et al. Concerted action of Smad and CREB-binding protein regulates bone morphogenetic protein-2-stimulated osteoblastic colony-stimulating factor-1 expression. J Biol Chem 2006;281:20160-70.

Ghosh-Choudhury N, Woodruff K, Qi W, Celeste A, Abboud SL, Ghosh Choudhury G. Bone morphogenetic protein-2 blocks MDA MB 231 human breast cancer cell proliferation by inhibiting cyclin-dependent kinase-mediated retinoblastoma protein phosphorylation. Biochem Biophys Res Commun 2000b;272:705-11.

Giacomini D, Paez-Pereda M, Theodoropoulou M, Labeur M, Refojo D, Gerez J, et al. Bone morphogenetic protein-4 inhibits corticotroph tumor cells: involvement in the retinoic acid inhibitory action. Endocrinology 2006;147:247-56.

Gialeli C, Theocharis AD, Karamanos NK. Roles of matrix metalloproteinases in cancer progression and their pharmacological targeting. FEBS J 2011;278:16-27.

Giancotti FG. Deregulation of cell signaling in cancer. FEBS Lett 2014;588:2558-70.

Global Burden of Disease Cancer Collaboration, Fitzmaurice C, Dicker D, Pain A, Hamavid H, Moradi-Lakeh M, et al. The Global Burden of Cancer 2013. JAMA Oncol 2015;1:505-27.

Gordon KJ, Kirkbride KC, How T, Blobe GC. Bone morphogenetic proteins induce pancreatic cancer cell invasiveness through a Smad1-dependent mechanism that involves matrix metalloproteinase-2. Carcinogenesis 2009;30:238-48.

Gordon LA, Mulligan KT, Maxwell-Jones H, Adams M, Walker RA, Jones JL. Breast cell invasive potential relates to the myoepithelial phenotype. Int J Cancer 2003;106:8-16.

Goulley J, Dahl U, Baeza N, Mishina Y, Edlund H. BMP4-BMPR1A signaling in beta cells is required for and augments glucose-stimulated insulin secretion. Cell Metab 2007;5:207-19.

Gudjonsson T, Ronnov-Jessen L, Villadsen R, Rank F, Bissell MJ, Petersen OW. Normal and tumor-derived myoepithelial cells differ in their ability to interact with luminal breast epithelial cells for polarity and basement membrane deposition. J Cell Sci 2002;115:39-50.

Guo D, Huang J, Gong J. Bone morphogenetic protein 4 (BMP4) is required for migration and invasion of breast cancer. Mol Cell Biochem 2012a;363:179-90.

Guo X, Xiong L, Zou L, Zhao J. Upregulation of bone morphogenetic protein 4 is associated with poor prognosis in patients with hepatocellular carcinoma. Pathol Oncol Res 2012b;18:635-40.

Hamada S, Satoh K, Hirota M, Kimura K, Kanno A, Masamune A, et al. Bone morphogenetic protein 4 induces epithelial-mesenchymal transition through MSX2 induction on pancreatic cancer cell line. J Cell Physiol 2007;213:768-74.

Hanai J, Chen LF, Kanno T, Ohtani-Fujita N, Kim WY, Guo WH, et al. Interaction and functional cooperation of PEBP2/CBF with Smads. Synergistic induction of the immunoglobulin germline Calpha promoter. J Biol Chem 1999;274:31577-82.

Harada J, Kokura K, Kanei-Ishii C, Nomura T, Khan MM, Kim Y, et al. Requirement of the co-repressor homeodomain-interacting protein kinase 2 for ski-mediated inhibition of bone morphogenetic protein-induced transcriptional activation. J Biol Chem 2003;278:38998-9005.

Hartung T. 3D - a new dimension of in vitro research. Adv Drug Deliv Rev 2014;69-70:vi.

Hata A, Seoane J, Lagna G, Montalvo E, Hemmati-Brivanlou A, Massague J. OAZ uses distinct DNA- and protein-binding zinc fingers in separate BMP-Smad and Olf signaling pathways. Cell 2000;100:229-40.

Haubold M, Weise A, Stephan H, Dunker N. Bone morphogenetic protein 4 (BMP4) signaling in retinoblastoma cells. Int J Biol Sci 2010;6:700-15.

Haycock JW. 3D cell culture: a review of current approaches and techniques. Methods Mol Biol 2011;695:1-15.

He HH, Meyer CA, Chen MW, Jordan VC, Brown M, Liu XS. Differential DNase I hypersensitivity reveals factor-dependent chromatin dynamics. Genome Res 2012;22:1015-25.

Hennighausen L. Mouse models for breast cancer. Breast Cancer Res. 2000;2:2-7.

Hirata-Tsuchiya S, Fukushima H, Katagiri T, Ohte S, Shin M, Nagano K, et al. Inhibition of BMP2-induced bone formation by the p65 subunit of NF-kappaB via an interaction with Smad4. Mol Endocrinol 2014;28:1460-70.

Hjertner O, Hjorth-Hansen H, Borset M, Seidel C, Waage A, Sundan A. Bone morphogenetic protein-4 inhibits proliferation and induces apoptosis of multiple myeloma cells. Blood 2001;97:516-22.

Holien T, Våtsveen TK, Hella H, Rampa C, Brede G, Grøseth LA, et al. Bone morphogenetic proteins induce apoptosis in multiple myeloma cells by Smad-dependent repression of MYC. Leukemia 2012;26:1073-80.

Hollnagel A, Oehlmann V, Heymer J, Ruther U, Nordheim A. Id genes are direct targets of bone morphogenetic protein induction in embryonic stem cells. J Biol Chem 1999;274:19838-45.

Horike S, Cai S, Miyano M, Cheng JF, Kohwi-Shigematsu T. Loss of silent-chromatin looping and impaired imprinting of DLX5 in Rett syndrome. Nat Genet 2005;37:31-40.

Hu F, Meng X, Tong Q, Liang L, Xiang R, Zhu T, et al. BMP-6 inhibits cell proliferation by targeting microRNA-192 in breast cancer. Biochim Biophys Acta 2013;1832:2379-90.

Hu MC, Rosenblum ND. Smad1, beta-catenin and Tcf4 associate in a molecular complex with the Myc promoter in dysplastic renal tissue and cooperate to control Myc transcription. Development 2005;132:215-25.

Huang da W, Sherman BT, Lempicki RA. Bioinformatics enrichment tools: paths toward the comprehensive functional analysis of large gene lists. Nucleic Acids Res 2009a;37:1-13.

Huang da W, Sherman BT, Lempicki RA. Systematic and integrative analysis of large gene lists using DAVID bioinformatics resources. Nat Protoc 2009b;4:44-57.

Hughes CS, Postovit LM, Lajoie GA. Matrigel: a complex protein mixture required for optimal growth of cell culture. Proteomics 2010;10:1886-90.

Iantosca MR, McPherson CE, Ho SY, Maxwell GD. Bone morphogenetic proteins-2 and -4 attenuate apoptosis in a cerebellar primitive neuroectodermal tumor cell line. J Neurosci Res 1999;56:248-58.

Iorns E, Drews-Elger K, Ward TM, Dean S, Clarke J, Berry D, et al. A new mouse model for the study of human breast cancer metastasis. PLoS One 2012;7:e47995.

Ito Y, Bae SC, Chuang LS. The RUNX family: developmental regulators in cancer. Nat Rev Cancer 2015;15:81-95.

Ivanova T, Zouridis H, Wu Y, Cheng LL, Tan IB, Gopalakrishnan V, et al. Integrated epigenomics identifies BMP4 as a modulator of cisplatin sensitivity in gastric cancer. Gut 2013;62:22-33.

Javed A, Bae JS, Afzal F, Gutierrez S, Pratap J, Zaidi SK, et al. Structural coupling of Smad and Runx2 for execution of the BMP2 osteogenic signal. J Biol Chem 2008;283:8412-22.

Jia S, Zhou J, Gao Y, Baek JA, Martin JF, Lan Y, et al. Roles of Bmp4 during tooth morphogenesis and sequential tooth formation. Development 2013;140:423-32.

Jiao K, Zhou Y, Hogan BL. Identification of mZnf8, a mouse Kruppel-like transcriptional repressor, as a novel nuclear interaction partner of Smad1. Mol Cell Biol 2002;22:7633-44.

Johnson MD, O'Connell MJ, Vito F, Pilcher W. Bone morphogenetic protein 4 and its receptors are expressed in the leptomeninges and meningiomas and signal via the Smad pathway. J Neuropathol Exp Neurol 2009;68:1177-83.

Jonk LJ, Itoh S, Heldin CH, ten Dijke P, Kruijer W. Identification and functional characterization of a Smad binding element (SBE) in the JunB promoter that acts as a transforming growth factor-beta, activin, and bone morphogenetic protein-inducible enhancer. J Biol Chem 1998;273:21145-52.

Jung J. Human tumor xenograft models for preclinical assessment of anticancer drug development. Toxicol Res 2014;30:1-5.

Kahata K, Hayashi M, Asaka M, Hellman U, Kitagawa H, Yanagisawa J, et al. Regulation of transforming growth factor-beta and bone morphogenetic protein signalling by transcriptional coactivator GCN5. Genes Cells 2004;9:143-51.

Kallioniemi A. Bone morphogenetic protein 4-a fascinating regulator of cancer cell behavior. Cancer Genet 2012;205:267-77.

Katagiri T, Watabe T. Bone Morphogenetic Proteins. Cold Spring Harb Perspect Biol 2016;8:10.1101.

Katt ME, Placone AL, Wong AD, Xu ZS, Searson PC. In Vitro Tumor Models: Advantages, Disadvantages, Variables, and Selecting the Right Platform. Front Bioeng Biotechnol 2016;4:12.

Kenny PA, Lee GY, Myers CA, Neve RM, Semeiks JR, Spellman PT, et al. The morphologies of breast cancer cell lines in three-dimensional assays correlate with their profiles of gene expression. Mol Oncol 2007;1:84-96.

Ketolainen JM, Alarmo EL, Tuominen VJ, Kallioniemi A. Parallel inhibition of cell growth and induction of cell migration and invasion in breast cancer cells by bone morphogenetic protein 4. Breast Cancer Res Treat 2010;124:377-86.

Khan MP, Khan K, Yadav PS, Singh AK, Nag A, Prasahar P, et al. BMP signaling is required for adult skeletal homeostasis and mediates bone anabolic action of parathyroid hormone. Bone 2016;92:132-44.

Khanna C, Hunter K. Modeling metastasis in vivo. Carcinogenesis 2005;26:513-23.

Khurana S, Buckley S, Schouteden S, Ekker S, Petryk A, Delforge M, et al. A novel role of BMP4 in adult hematopoietic stem and progenitor cell homing via Smad independent regulation of integrin-alpha4 expression. Blood 2013;121:781-90.

Kida Y, Maeda Y, Shiraishi T, Suzuki T, Ogura T. Chick Dach1 interacts with the Smad complex and Sin3a to control AER formation and limb development along the proximodistal axis. Development 2004;131:4179-87.

Kim D, Pertea G, Trapnell C, Pimentel H, Kelley R, Salzberg SL. TopHat2: accurate alignment of transcriptomes in the presence of insertions, deletions and gene fusions. Genome Biol 2013;14:R36.

Kim DW, Lassar AB. Smad-dependent recruitment of a histone deacetylase/Sin3A complex modulates the bone morphogenetic protein-dependent transcriptional repressor activity of Nkx3.2. Mol Cell Biol 2003;23:8704-17.

Kim IY, Lee DH, Lee DK, Kim WJ, Kim MM, Morton RA, et al. Restoration of bone morphogenetic protein receptor type II expression leads to a decreased rate of tumor growth in bladder transitional cell carcinoma cell line TSU-Pr1. Cancer Res 2004;64:7355-60.

Kim J, Johnson K, Chen HJ, Carroll S, Laughon A. Drosophila Mad binds to DNA and directly mediates activation of vestigial by Decapentaplegic. Nature 1997;388:304-8.

Kim JS, Kurie JM, Ahn YH. BMP4 depletion by miR-200 inhibits tumorigenesis and metastasis of lung adenocarcinoma cells. Mol Cancer 2015;14:173.

Kleinman HK, Martin GR. Matrigel: basement membrane matrix with biological activity. Semin Cancer Biol 2005;15:378-86.

Klose A, Waerzeggers Y, Monfared P, Vukicevic S, Kaijzel EL, Winkeler A, et al. Imaging bone morphogenetic protein 7 induced cell cycle arrest in experimental gliomas. Neoplasia 2011;13:276-85.

Klose RJ, Bird AP. Genomic DNA methylation: the mark and its mediators. Trends Biochem Sci 2006;31:89-97.

Knight E, Przyborski S. Advances in 3D cell culture technologies enabling tissue-like structures to be created in vitro. J Anat 2015;227:746-56.

Kulakovskiy IV, Medvedeva YA, Schaefer U, Kasianov AS, Vorontsov IE, Bajic VB, et al. HOCOMOCO: a comprehensive collection of human transcription factor binding sites models. Nucleic Acids Res 2013;41:D195-202.

Kumar S, Vo AD, Qin F, Li H. Comparative assessment of methods for the fusion transcripts detection from RNA-Seq data. Sci Rep 2016;6:21597.

Kumar V, Muratani M, Rayan NA, Kraus P, Lufkin T, Ng HH, et al. Uniform, optimal signal processing of mapped deep-sequencing data. Nat Biotechnol 2013;31:615-22.

Kuperwasser C, Dessain S, Bierbaum BE, Garnet D, Sperandio K, Gauvin GP, et al. A mouse model of human breast cancer metastasis to human bone. Cancer Res 2005;65:6130-8.

Kurisaki K, Kurisaki A, Valcourt U, Terentiev AA, Pardali K, Ten Dijke P, et al. Nuclear factor YY1 inhibits transforming growth factor beta- and bone morphogenetic protein-induced cell differentiation. Mol Cell Biol 2003;23:4494-510.

Laatio L, Myllynen P, Serpi R, Rysa J, Ilves M, Lappi-Blanco E, et al. BMP-4 expression has prognostic significance in advanced serous ovarian carcinoma and is affected by cisplatin in OVCAR-3 cells. Tumour Biol 2011;32:985-95.

Lai CF, Cheng SL. Signal transductions induced by bone morphogenetic protein-2 and transforming growth factor-beta in normal human osteoblastic cells. J Biol Chem 2002;277:15514-22.

Langmead B, Salzberg SL. Fast gapped-read alignment with Bowtie 2. Nat Methods 2012;9:357-9.

Lasorella A, Benezra R, Iavarone A. The ID proteins: master regulators of cancer stem cells and tumour aggressiveness. Nat Rev Cancer 2014;14:77-91.

Leboy P, Grasso-Knight G, D'Angelo M, Volk SW, Lian JV, Drissi H, et al. Smad-Runx interactions during chondrocyte maturation. J Bone Joint Surg Am 2001;83-A Suppl 1:S15-22.

Lee EY, Muller WJ. Oncogenes and tumor suppressor genes. Cold Spring Harb Perspect Biol 2010;2:a003236.

Lee JH, Lee GT, Kwon SJ, Jeong J, Ha YS, Kim WJ, et al. CREBZF, a novel Smad8-binding protein. Mol Cell Biochem 2012;368:147-53.

Lee KH, Evans S, Ruan TY, Lassar AB. SMAD-mediated modulation of YY1 activity regulates the BMP response and cardiac-specific expression of a GATA4/5/6-dependent chick Nkx2.5 enhancer. Development 2004;131:4709-23.

Lee KS, Kim HJ, Li QL, Chi XZ, Ueta C, Komori T, et al. Runx2 is a common target of transforming growth factor beta1 and bone morphogenetic protein 2, and cooperation between Runx2 and Smad5 induces osteoblast-specific gene expression in the pluripotent mesenchymal precursor cell line C2C12. Mol Cell Biol 2000;20:8783-92.

Lee YC, Cheng CJ, Bilen MA, Lu JF, Satcher RL, Yu-Lee LY, et al. BMP4 promotes prostate tumor growth in bone through osteogenesis. Cancer Res 2011;71:5194-203.

Li J, Sun C, Yuan Y, Liu L, Xiong G, Wu J. Bone morphogenetic protein-4 polymorphism and colorectal cancer risk: a meta analysis. Mol Biol Rep 2012;39:5239-51.

Lian WJ, Liu G, Liu YJ, Zhao ZW, Yi T, Zhou HY. Downregulation of BMP6 enhances cell proliferation and chemoresistance via activation of the ERK signaling pathway in breast cancer. Oncol Rep 2013;30:193-200.

Lim E, Metzger-Filho O, Winer EP. The natural history of hormone receptor-positive breast cancer. Oncology (Williston Park) 2012;26:688.

Ling G, Waxman DJ. DNase I digestion of isolated nulcei for genome-wide mapping of DNase hypersensitivity sites in chromatin. Methods Mol Biol 2013;977:21-33.

Liu B, Chen Q, Tian D, Wu L, Dong H, Wang J, et al. BMP4 reverses multidrug resistance through modulation of BCL-2 and GDNF in glioblastoma. Brain Res 2013;1507:115-24.

Liu F, Massague J, Ruiz i Altaba A. Carboxy-terminally truncated Gli3 proteins associate with Smads. Nat Genet 1998;20:325-6.

Lombardo Y, Scopelliti A, Cammareri P, Todaro M, Iovino F, Ricci-Vitiani L, et al. Bone morphogenetic protein 4 induces differentiation of colorectal cancer stem cells and increases their response to chemotherapy in mice. Gastroenterology 2011;140:297-309.

Love MI, Huber W, Anders S. Moderated estimation of fold change and dispersion for RNA-seq data with DESeq2. Genome Biol 2014;15:550.

Lu P, Takai K, Weaver VM, Werb Z. Extracellular matrix degradation and remodeling in development and disease. Cold Spring Harb Perspect Biol 2011;3:10.1101.

Lu P, Weaver VM, Werb Z. The extracellular matrix: a dynamic niche in cancer progression. J Cell Biol 2012;196:395-406.

Maegdefrau U, Amann T, Winklmeier A, Braig S, Schubert T, Weiss TS, et al. Bone morphogenetic protein 4 is induced in hepatocellular carcinoma by hypoxia and promotes tumour progression. J Pathol 2009;218:520-9.

Mak IW, Evaniew N, Ghert M. Lost in translation: animal models and clinical trials in cancer treatment. Am J Transl Res 2014;6:114-8.

Makeev VJ, Lifanov AP, Nazina AG, Papatsenko DA. Distance preferences in the arrangement of binding motifs and hierarchical levels in organization of transcription regulatory information. Nucleic Acids Res 2003;31:6016-26.

Mangraviti A, Tzeng SY, Gullotti D, Kozielski KL, Kim JE, Seng M, et al. Non-virally engineered human adipose mesenchymal stem cells produce BMP4, target brain tumors, and extend survival. Biomaterials 2016;100:53-66.

Markossian S, Flamant F. CRISPR/Cas9: a breakthrough in generating mouse models for endocrinologists. J Mol Endocrinol 2016;57:R81-92.

Martin AM, Weber BL. Genetic and hormonal risk factors in breast cancer. J Natl Cancer Inst 2000;92:1126-35.

Martinowich K, Hattori D, Wu H, Fouse S, He F, Hu Y, et al. DNA methylation-related chromatin remodeling in activity-dependent BDNF gene regulation. Science 2003;302:890-3.

Massague J. TGFbeta signalling in context. Nat Rev Mol Cell Biol 2012;13:616-30.

Massague J, Seoane J, Wotton D. Smad transcription factors. Genes Dev 2005;19:2783-810.

McCleary-Wheeler AL, McWilliams R, Fernandez-Zapico ME. Aberrant signaling pathways in pancreatic cancer: a two compartment view. Mol Carcinog 2012;51:25-39.

McLean CY, Bristor D, Hiller M, Clarke SL, Schaar BT, Lowe CB, et al. GREAT improves functional interpretation of cis-regulatory regions. Nat Biotechnol 2010;28:495-501.

Menafra R, Stunnenberg HG. MBD2 and MBD3: elusive functions and mechanisms. Front Genet 2014;5:428.

Mendoza-Villanueva D, Deng W, Lopez-Camacho C, Shore P. The Runx transcriptional co-activator, CBFbeta, is essential for invasion of breast cancer cells. Mol Cancer 2010;9:171.

Miyazono K, Kamiya Y, Morikawa M. Bone morphogenetic protein receptors and signal transduction. J Biochem 2010;147:35-51.

Miyazono K, Maeda S, Imamura T. BMP receptor signaling: transcriptional targets, regulation of signals, and signaling cross-talk. Cytokine Growth Factor Rev 2005;16:251-63.

Monzen K, Hiroi Y, Kudoh S, Akazawa H, Oka T, Takimoto E, et al. Smads, TAK1, and their common target ATF-2 play a critical role in cardiomyocyte differentiation. J Cell Biol 2001;153:687-98.

Morikawa M, Koinuma D, Miyazono K, Heldin CH. Genome-wide mechanisms of Smad binding. Oncogene 2013;32:1609-15.

Morikawa M, Koinuma D, Tsutsumi S, Vasilaki E, Kanki Y, Heldin CH, et al. ChIP-seq reveals cell type-specific binding patterns of BMP-specific Smads and a novel binding motif. Nucleic Acids Res 2011;39:8712-27.

Mu D, Cambier S, Fjellbirkeland L, Baron JL, Munger JS, Kawakatsu H, et al. The integrin alpha(v)beta8 mediates epithelial homeostasis through MT1-MMP-dependent activation of TGF-beta1. J Cell Biol 2002;157:493-507.

Mulloy B, Rider CC. The Bone Morphogenetic Proteins and Their Antagonists. Vitam Horm 2015;99:63-90.

Nakahiro T, Kurooka H, Mori K, Sano K, Yokota Y. Identification of BMP-responsive elements in the mouse Id2 gene. Biochem Biophys Res Commun 2010;399:416-21.

Nakase T, Yoshikawa H. Potential roles of bone morphogenetic proteins (BMPs) in skeletal repair and regeneration. J Bone Miner Metab 2006;24:425-33.

Natarajan A, Yardimci GG, Sheffield NC, Crawford GE, Ohler U. Predicting cell-type-specific gene expression from regions of open chromatin. Genome Res 2012;22:1711-22.

Neph S, Vierstra J, Stergachis AB, Reynolds AP, Haugen E, Vernot B, et al. An expansive human regulatory lexicon encoded in transcription factor footprints. Nature 2012;489:83-90.

Nguyen DX, Bos PD, Massague J. Metastasis: from dissemination to organ-specific colonization. Nat Rev Cancer 2009;9:274-84.

Niehrs C. On growth and form: a Cartesian coordinate system of Wnt and BMP signaling specifies bilaterian body axes. Development 2010;137:845-57.

Nishanian TG, Kim JS, Foxworth A, Waldman T. Suppression of tumorigenesis and activation of Wnt signaling by bone morphogenetic protein 4 in human cancer cells. Cancer Biol Ther 2004;3:667-75.

Nojima J, Kanomata K, Takada Y, Fukuda T, Kokabu S, Ohte S, et al. Dual roles of smad proteins in the conversion from myoblasts to osteoblastic cells by bone morphogenetic proteins. J Biol Chem 2010;285:15577-86.

Nordin K, LaBonne C. Sox5 Is a DNA-binding cofactor for BMP R-Smads that directs target specificity during patterning of the early ectoderm. Dev Cell 2014;31:374-82.

Okuda T, Takeda K, Fujita Y, Nishimura M, Yagyu S, Yoshida M, et al. Biological characteristics of the leukemia-associated transcriptional factor AML1 disclosed by hematopoietic rescue of AML1-deficient embryonic stem cells by using a knock-in strategy. Mol Cell Biol 2000;20:319-28.

Oliveira AM, Ross JS, Fletcher JA. Tumor suppressor genes in breast cancer: the gatekeepers and the caretakers. Am J Clin Pathol 2005;124 Suppl:S16-28.

Onichtchouk D, Chen YG, Dosch R, Gawantka V, Delius H, Massague J, et al. Silencing of TGF-beta signalling by the pseudoreceptor BAMBI. Nature 1999;401:480-5.

Oshlack A, Robinson MD, Young MD. From RNA-seq reads to differential expression results. Genome Biol 2010;11:220.

Otsuka F. Multiple endocrine regulation by bone morphogenetic protein system. Endocr J 2010;57:3-14.

Owens P, Polikowsky H, Pickup MW, Gorska AE, Jovanovic B, Shaw AK, et al. Bone morphogenetic proteins stimulate mammary fibroblasts to promote mammary carcinoma cell invasion. PLoS One 2013;8:e67533.

Paez-Pereda M, Giacomini D, Refojo D, Nagashima AC, Hopfner U, Grubler Y, et al. Involvement of bone morphogenetic protein 4 (BMP-4) in pituitary prolactinoma pathogenesis through a Smad/estrogen receptor crosstalk. Proc Natl Acad Sci U S A 2003;100:1034-9.

Pal A, Huang W, Li X, Toy KA, Nikolovska-Coleska Z, Kleer CG. CCN6 Modulates BMP Signaling via the Smad-Independent TAK1/p38 Pathway, Acting to Suppress Metastasis of Breast Cancer. Cancer Res 2012.

Parssinen J, Alarmo EL, Karhu R, Kallioniemi A. PPM1D silencing by RNA interference inhibits proliferation and induces apoptosis in breast cancer cell lines with wild-type p53. Cancer Genet Cytogenet 2008;182:33-9.

Paulsen M, Legewie S, Eils R, Karaulanov E, Niehrs C. Negative feedback in the bone morphogenetic protein 4 (BMP4) synexpression group governs its dynamic signaling range and canalizes development. Proc Natl Acad Sci U S A 2011;108:10202-7.

Payne SJ, Bowen RL, Jones JL, Wells CA. Predictive markers in breast cancer--the present. Histopathology 2008;52:82-90.

Peng Y, Zhao S, Song L, Wang M, Jiao K. Sertad1 encodes a novel transcriptional co-activator of SMAD1 in mouse embryonic hearts. Biochem Biophys Res Commun 2013;441:751-6.

Petersen OW, Ronnov-Jessen L, Howlett AR, Bissell MJ. Interaction with basement membrane serves to rapidly distinguish growth and differentiation pattern of normal and malignant human breast epithelial cells. Proc Natl Acad Sci U S A 1992;89:9064-8.

Phimphilai M, Zhao Z, Boules H, Roca H, Franceschi RT. BMP signaling is required for RUNX2-dependent induction of the osteoblast phenotype. J Bone Miner Res 2006;21:637-46.

Piccirillo SG, Reynolds BA, Zanetti N, Lamorte G, Binda E, Broggi G, et al. Bone morphogenetic proteins inhibit the tumorigenic potential of human brain tumour-initiating cells. Nature 2006;444:761-5.

Postigo AA. Opposing functions of ZEB proteins in the regulation of the TGFbeta/BMP signaling pathway. EMBO J 2003;22:2443-52.

Pouponnot C, Jayaraman L, Massague J. Physical and functional interaction of SMADs and p300/CBP. J Biol Chem 1998;273:22865-8.

Pramono A, Zahabi A, Morishima T, Lan D, Welte K, Skokowa J. Thrombopoietin induces hematopoiesis from mouse ES cells via HIF-1alpha-dependent activation of a BMP4 autoregulatory loop. Ann N Y Acad Sci 2016;1375:38-51.

Prashar P, Yadav PS, Samarjeet F, Bandyopadhyay A. Microarray meta-analysis identifies evolutionarily conserved BMP signaling targets in developing long bones. Dev Biol 2014;389:192-207.

Quinlan AR, Hall IM. BEDTools: a flexible suite of utilities for comparing genomic features. Bioinformatics 2010;26:841-2.

Rahman MS, Akhtar N, Jamil HM, Banik RS, Asaduzzaman SM. TGF-beta/BMP signaling and other molecular events: regulation of osteoblastogenesis and bone formation. Bone Res 2015;3:15005.

Raju GP, Dimova N, Klein PS, Huang HC. SANE, a novel LEM domain protein, regulates bone morphogenetic protein signaling through interaction with Smad1. J Biol Chem 2003;278:428-37.

Rakha EA, Reis-Filho JS, Baehner F, Dabbs DJ, Decker T, Eusebi V, et al. Breast cancer prognostic classification in the molecular era: the role of histological grade. Breast Cancer Res 2010;12:207.

Redig AJ, McAllister SS. Breast cancer as a systemic disease: a view of metastasis. J Intern Med 2013;274:113-26.

Ren W, Sun X, Wang K, Feng H, Liu Y, Fei C, et al. BMP9 inhibits the bone metastasis of breast cancer cells by downregulating CCN2 (connective tissue growth factor, CTGF) expression. Mol Biol Rep 2014;41:1373-83.

Reymond N, d'Agua BB, Ridley AJ. Crossing the endothelial barrier during metastasis. Nat Rev Cancer 2013;13:858-70.

Richmond A, Su Y. Mouse xenograft models vs GEM models for human cancer therapeutics. Dis Model Mech 2008;1:78-82.

Rider CC, Mulloy B. Bone morphogenetic protein and growth differentiation factor cytokine families and their protein antagonists. Biochem J 2010;429:1-12.

Rodriguez-Martinez A, Alarmo EL, Saarinen L, Ketolainen J, Nousiainen K, Hautaniemi S, et al. Analysis of BMP4 and BMP7 signaling in breast cancer cells unveils time-dependent transcription patterns and highlights a common synexpression group of genes. BMC Med Genomics 2011;4:80.

Rothhammer T, Poser I, Soncin F, Bataille F, Moser M, Bosserhoff AK. Bone morphogenic proteins are overexpressed in malignant melanoma and promote cell invasion and migration. Cancer Res 2005;65:448-56.

Ruedinger F, Lavrentieva A, Blume C, Pepelanova I, Scheper T. Hydrogels for 3D mammalian cell culture: a starting guide for laboratory practice. Appl Microbiol Biotechnol 2015;99:623-36.

Saxena M, Christofori G. Rebuilding cancer metastasis in the mouse. Mol Oncol 2013;7:283-96.

Scheufler C, Sebald W, Hulsmeyer M. Crystal structure of human bone morphogenetic protein-2 at 2.7 A resolution. J Mol Biol 1999;287:103-15.

Schito L, Rey S, Tafani M, Zhang H, Wong CC, Russo A, et al. Hypoxia-inducible factor 1-dependent expression of platelet-derived growth factor B promotes lymphatic metastasis of hypoxic breast cancer cells. Proc Natl Acad Sci U S A 2012;109:E2707-16.

Selever J, Liu W, Lu MF, Behringer RR, Martin JF. Bmp4 in limb bud mesoderm regulates digit pattern by controlling AER development. Dev Biol 2004;276:268-79.

Sengle G, Ono RN, Sasaki T, Sakai LY. Prodomains of transforming growth factor beta (TGFbeta) superfamily members specify different functions: extracellular matrix interactions and growth factor bioavailability. J Biol Chem 2011;286:5087-99.

Shaw A, Gipp J, Bushman W. Exploration of Shh and BMP paracrine signaling in a prostate cancer xenograft. Differentiation 2010;79:41-7.

Shen ZJ, Nakamoto T, Tsuji K, Nifuji A, Miyazono K, Komori T, et al. Negative regulation of bone morphogenetic protein/Smad signaling by Cas-interacting zinc finger protein in osteoblasts. J Biol Chem 2002;277:29840-6.

Shepherd TG, Nachtigal MW. Identification of a putative autocrine bone morphogenetic protein-signaling pathway in human ovarian surface epithelium and ovarian cancer cells. Endocrinology 2003;144:3306-14.

Shi X, Yang X, Chen D, Chang Z, Cao X. Smad1 interacts with homeobox DNA-binding proteins in bone morphogenetic protein signaling. J Biol Chem 1999;274:13711-7.

Shirai YT, Ehata S, Yashiro M, Yanagihara K, Hirakawa K, Miyazono K. Bone morphogenetic protein-2 and -4 play tumor suppressive roles in human diffuse-type gastric carcinoma. Am J Pathol 2011;179:2920-30.

Shishido-Hara Y, Kurata A, Fujiwara M, Itoh H, Imoto S, Kamma H. Two cases of breast carcinoma with osteoclastic giant cells: are the osteoclastic giant cells pro-tumoural differentiation of macrophages? Diagn Pathol 2010;5:55..

Shola DT, Wang H, Wahdan-Alaswad R, Danielpour D. Hic-5 controls BMP4 responses in prostate cancer cells through interacting with Smads 1, 5 and 8. Oncogene 2012;31:2480-90.

Shon SK, Kim A, Kim JY, Kim KI, Yang Y, Lim JS. Bone morphogenetic protein-4 induced by NDRG2 expression inhibits MMP-9 activity in breast cancer cells. Biochem Biophys Res Commun 2009;385:198-203.

Singh A, Morris RJ. The Yin and Yang of bone morphogenetic proteins in cancer. Cytokine Growth Factor Rev 2010;21:299-313.

Singletary SE. Rating the risk factors for breast cancer. Ann Surg 2003;237:474-82.

Skardal A, Shupe T, Atala A. Organoid-on-a-chip and body-on-a-chip systems for drug screening and disease modeling. Drug Discov Today 2016;21:1399-411.

Smalley KS, Lioni M, Herlyn M. Life isn't flat: taking cancer biology to the next dimension. In Vitro Cell Dev Biol Anim 2006;42:242-7.

Sneddon JB, Zhen HH, Montgomery K, van de Rijn M, Tward AD, West R, et al. Bone morphogenetic protein antagonist gremlin 1 is widely expressed by cancer-associated stromal cells and can promote tumor cell proliferation. Proc Natl Acad Sci U S A 2006;103:14842-7.

Song HH, Park KM, Gerecht S. Hydrogels to model 3D in vitro microenvironment of tumor vascularization. Adv Drug Deliv Rev 2014;79-80:19-29.

Song L, Crawford GE. DNase-seq: a high-resolution technique for mapping active gene regulatory elements across the genome from mammalian cells. Cold Spring Harb Protoc 2010;2010:pdb.prot5384.

Sorlie T, Tibshirani R, Parker J, Hastie T, Marron JS, Nobel A, Deng S, Johnsen H, Pesich R, Geisler S, Demeter J, Perou CM, Lønning PE, Brown PO, Børresen-Dale AL, Botstein D. Proc Natl Acad Sci U S A 2003;100:8418-23.

Sosnoski DM, Krishnan V, Kraemer WJ, Dunn-Lewis C, Mastro AM. Changes in Cytokines of the Bone Microenvironment during Breast Cancer Metastasis. Int J Breast Cancer 2012;2012:160265.

Stewart RL, O'Connor KL. Clinical significance of the integrin α6β4 in human malignancies. Lab Invest 2015;95:976-86.

Stock K, Estrada MF, Vidic S, Gjerde K, Rudisch A, Santo VE, et al. Capturing tumor complexity in vitro: Comparative analysis of 2D and 3D tumor models for drug discovery. Sci Rep 2016;6:28951.

Stratton MR, Campbell PJ, Futreal PA. The cancer genome. Nature 2009;458:719-24.

Strino F, Lappe M. Identifying peaks in *-seq data using shape information. BMC Bioinformatics 2016;17 Suppl 5:206.

Su D, Zhu S, Han X, Feng Y, Huang H, Ren G, et al. BMP4-Smad signaling pathway mediates adriamycin-induced premature senescence in lung cancer cells. J Biol Chem 2009;284:12153-64.

Sun P, Wang J, Zheng Y, Fan Y, Gu Z. BMP2/7 heterodimer is a stronger inducer of bone regeneration in peri-implant bone defects model than BMP2 or BMP7 homodimer. Dent Mater J 2012;31:239-48.

Suzuki M, Raab G, Moses MA, Fernandez CA, Klagsbrun M. Matrix metalloproteinase-3 releases active heparin-binding EGF-like growth factor by cleavage at a specific juxtamembrane site. J Biol Chem 1997;272:31730-7.

Takahashi Y, Ishigaki T, Okuhashi Y, Ono A, Itoh M, Nara N, et al. Effect of BMP4 on the growth and clonogenicity of human leukemia and lymphoma cells. Anticancer Res 2012;32:2813-7.

Teicher BA. Tumor models for efficacy determination. Mol Cancer Ther 2006;5:2435-43.

ten Dijke P, Yamashita H, Sampath TK, Reddi AH, Estevez M, Riddle DL, et al. Identification of type I receptors for osteogenic protein-1 and bone morphogenetic protein-4. J Biol Chem 1994;269:16985-8.

Theriault BL, Nachtigal MW. Human ovarian cancer cell morphology, motility, and proliferation are differentially influenced by autocrine TGFbeta superfamily signalling. Cancer Lett 2011;313:108-21.

Theriault BL, Shepherd TG, Mujoomdar ML, Nachtigal MW. BMP4 induces EMT and Rho GTPase activation in human ovarian cancer cells. Carcinogenesis 2007;28:1153-62.

Thurman RE, Rynes E, Humbert R, Vierstra J, Maurano MT, Haugen E, et al. The accessible chromatin landscape of the human genome. Nature 2012;489:75-82.

Tomayko MM, Reynolds CP. Determination of subcutaneous tumor size in athymic (nude) mice. Cancer Chemother Pharmacol 1989;24:148-54.

Tsompana M, Buck MJ. Chromatin accessibility: a window into the genome. Epigenetics Chromatin 2014;7:33.

Tsuchida R, Osawa T, Wang F, Nishii R, Das B, Tsuchida S, et al. BMP4/Thrombospondin-1 loop paracrinically inhibits tumor angiogenesis and suppresses the growth of solid tumors. Oncogene 2014;33:3803-11.

Tung YC, Hsiao AY, Allen SG, Torisawa YS, Ho M, Takayama S. High-throughput 3D spheroid culture and drug testing using a 384 hanging drop array. Analyst 2011;136:473-8.

Tylzanowski P, Verschueren K, Huylebroeck D, Luyten FP. Smad-interacting protein 1 is a repressor of liver/bone/kidney alkaline phosphatase transcription in bone morphogenetic protein-induced osteogenic differentiation of C2C12 cells. J Biol Chem 2001;276:40001-7.

Urist MR. Bone: formation by autoinduction. Science 1965;150:893-9.

Urist MR, Strates BS. Bone morphogenetic protein. J Dent Res 1971;50:1392-406.

Vainio S, Karavanova I, Jowett A, Thesleff I. Identification of BMP-4 as a signal mediating secondary induction between epithelial and mesenchymal tissues during early tooth development. Cell 1993;75:45-58.

Valastyan S, Weinberg RA. Tumor metastasis: molecular insights and evolving paradigms. Cell 2011;147:275-92.

Valera E, Isaacs MJ, Kawakami Y, Izpisua Belmonte JC, Choe S. BMP-2/6 heterodimer is more effective than BMP-2 or BMP-6 homodimers as inductor of differentiation of human embryonic stem cells. PLoS One 2010;5:e11167.

Verschueren K, Remacle JE, Collart C, Kraft H, Baker BS, Tylzanowski P, et al. SIP1, a novel zinc finger/homeodomain repressor, interacts with Smad proteins and binds to 5'-CACCT sequences in candidate target genes. J Biol Chem 1999;274:20489-98.

Vigier, S , Fülöp, T. Exploring the Extracellular Matrix to Create Biomaterials, Composition and Function of the Extracellular Matrix in the Human Body, Dr. Francesco Travascio (Ed.), InTech, (2016). DOI: 10.5772/62979.

Virtanen S, Alarmo EL, Sandstrom S, Ampuja M, Kallioniemi A. Bone morphogenetic protein -4 and -5 in pancreatic cancer--novel bidirectional players. Exp Cell Res 2011;317:2136-46.

Wang C, Hu F, Guo S, Mi D, Shen W, Zhang J, et al. BMP-6 inhibits MMP-9 expression by regulating heme oxygenase-1 in MCF-7 breast cancer cells. J Cancer Res Clin Oncol 2011;137:985-95.

Wang C, Tang Z, Zhao Y, Yao R, Li L, Sun W. Three-dimensional in vitro cancer models: a short review. Biofabrication 2014a;6:022001.

Wang J, Fu X, Yang K, Jiang Q, Chen Y, Jia J, et al. Hypoxia inducible factor-1-dependent up-regulation of BMP4 mediates hypoxia-induced increase of TRPC expression in PASMCs. Cardiovasc Res 2015;107:108-18.

Wang RN, Green J, Wang Z, Deng Y, Qiao M, Peabody M, et al. Bone Morphogenetic Protein (BMP) signaling in development and human diseases. Genes Dis 2014b;1:87-105.

Wang W, He YF, Sun QK, Wang Y, Han XH, Peng DF, et al. Hypoxia-inducible factor 1alpha in breast cancer prognosis. Clin Chim Acta 2014c;428:32-7.

Wang W, Mariani FV, Harland RM, Luo K. Ski represses bone morphogenic protein signaling in Xenopus and mammalian cells. Proc Natl Acad Sci U S A 2000;97:14394-9.

Wang Z, Gerstein M, Snyder M. RNA-Seq: a revolutionary tool for transcriptomics. Nat Rev Genet 2009;10:57-63.

Weigelt B, Geyer FC, Reis-Filho JS. Histological types of breast cancer: how special are they? Mol Oncol 2010;4:192-208.

Weigelt B, Peterse JL, van 't Veer LJ. Breast cancer metastasis: markers and models. Nat Rev Cancer 2005;5:591-602.

Weigelt B, Reis-Filho JS. Histological and molecular types of breast cancer: is there a unifying taxonomy? Nat Rev Clin Oncol 2009;6:718-30.

Whissell G, Montagni E, Martinelli P, Hernando-Momblona X, Sevillano M, Jung P, et al. The transcription factor GATA6 enables self-renewal of colon adenoma stem cells by repressing BMP gene expression. Nat Cell Biol 2014;16:695-707.

Winnier G, Blessing M, Labosky PA, Hogan BL. Bone morphogenetic protein-4 is required for mesoderm formation and patterning in the mouse. Genes Dev 1995;9:2105-16.

Wozney JM. Bone morphogenetic proteins. Prog Growth Factor Res 1989;1:267-80.

Wu DC, Paulson RF. Hypoxia regulates BMP4 expression in the murine spleen during the recovery from acute anemia. PLoS One 2010;5:e11303.

Wu Q, Yao J. BMP4, a new prognostic factor for glioma. World J Surg Oncol 2013;11:264.

Xu H, Huang W, Wang Y, Sun W, Tang J, Li D, et al. The function of BMP4 during neurogenesis in the adult hippocampus in Alzheimer's disease. Ageing Res Rev 2013;12:157-64.

Xu J, Zhu D, Sonoda S, He S, Spee C, Ryan SJ, et al. Over-expression of BMP4 inhibits experimental choroidal neovascularization by modulating VEGF and MMP-9. Angiogenesis 2012;15:213-27.

Yadin D, Knaus P, Mueller TD. Structural insights into BMP receptors: Specificity, activation and inhibition. Cytokine Growth Factor Rev 2016;27:13-34.

Yan T, Lin Z, Jiang J, Lu S, Chen M, Que H, et al. MMP14 regulates cell migration and invasion through epithelial-mesenchymal transition in nasopharyngeal carcinoma. Am J Transl Res 2015;7:950-8.

Yang WH, Lan HY, Tai SK, Yang MH. Repression of bone morphogenetic protein 4 by let-7i attenuates mesenchymal migration of head and neck cancer cells. Biochem Biophys Res Commun 2013;433:24-30.

Yao LC, Blitz IL, Peiffer DA, Phin S, Wang Y, Ogata S, et al. Schnurri transcription factors from Drosophila and vertebrates can mediate Bmp signaling through a phylogenetically conserved mechanism. Development 2006;133:4025-34.

Ye L, Bokobza S, Li J, Moazzam M, Chen J, Mansel RE, et al. Bone morphogenetic protein-10 (BMP-10) inhibits aggressiveness of breast cancer cells and correlates with poor prognosis in breast cancer. Cancer Sci 2010;101:2137-44.

Yoshida CA, Furuichi T, Fujita T, Fukuyama R, Kanatani N, Kobayashi S, et al. Core-binding factor beta interacts with Runx2 and is required for skeletal development. Nat Genet 2002;32:633-8.

Yoshida Y, Tanaka S, Umemori H, Minowa O, Usui M, Ikematsu N, et al. Negative regulation of BMP/Smad signaling by Tob in osteoblasts. Cell 2000;103:1085-97.

Zawel L, Dai JL, Buckhaults P, Zhou S, Kinzler KW, Vogelstein B, et al. Human Smad3 and Smad4 are sequence-specific transcription activators. Mol Cell 1998;1:611-7.

Zhang H, Wong CC, Wei H, Gilkes DM, Korangath P, Chaturvedi P, et al. HIF-1-dependent expression of angiopoietin-like 4 and L1CAM mediates vascular metastasis of hypoxic breast cancer cells to the lungs. Oncogene 2012a;31:1757-70.

Zhang L, Sun H, Zhao F, Lu P, Ge C, Li H, et al. BMP4 administration induces differentiation of CD133+ hepatic cancer stem cells, blocking their contributions to hepatocellular carcinoma. Cancer Res 2012b;72:4276-85.

Zhang N, Ye L, Wu L, Deng X, Yang Y, Jiang WG. Expression of bone morphogenetic protein-10 (BMP10) in human urothelial cancer of the bladder and its effects on the aggressiveness of bladder cancer cells in vitro. Anticancer Res 2013;33:1917-25.

Zhao H, Ayrault O, Zindy F, Kim JH, Roussel MF. Post-transcriptional down-regulation of Atoh1/Math1 by bone morphogenic proteins suppresses medulloblastoma development. Genes Dev 2008;22:722-7.

Zhao L, Li G, Zhou GQ. SOX9 directly binds CREB as a novel synergism with the PKA pathway in BMP-2-induced osteochondrogenic differentiation. J Bone Miner Res 2009;24:826-36.

Zhao X, Liu J, Peng M, Liu J, Chen F. BMP4 is involved in the chemoresistance of myeloid leukemia cells through regulating autophagy-apoptosis balance. Cancer Invest 2013;31:555-62.

Zhou Z, Sun L, Wang Y, Wu Z, Geng J, Miu W, et al. Bone morphogenetic protein 4 inhibits cell proliferation and induces apoptosis in glioma stem cells. Cancer Biother Radiopharm 2011;26:77-83.

Zhu H, Kavsak P, Abdollah S, Wrana JL, Thomsen GH. A SMAD ubiquitin ligase targets the BMP pathway and affects embryonic pattern formation. Nature 1999;400:687-93.

Zhu J. Bioactive modification of poly(ethylene glycol) hydrogels for tissue engineering. Biomaterials 2010;31:4639-56.

Zinn KR, Chaudhuri TR, Szafran AA, O'Quinn D, Weaver C, Dugger K, et al. Noninvasive bioluminescence imaging in small animals. ILAR J 2008;49:103-15.

Original communications

BMC Cancer

RESEARCH ARTICLE Open Access

BMP4 inhibits the proliferation of breast cancer cells and induces an MMP-dependent migratory phenotype in MDA-MB-231 cells in 3D environment

Minna Ampuja[1,2], Riikka Jokimäki[1,2], Kati Juuti-Uusitalo[1], Alejandra Rodriguez-Martinez[1,2], Emma-Leena Alarmo[1,2] and Anne Kallioniemi[1,2*]

Abstract

Background: Bone morphogenetic protein 4 (BMP4) belongs to the transforming growth factor β (TGF-β) family of proteins. BMPs regulate cell proliferation, differentiation and motility, and have also been reported to be involved in cancer pathogenesis. We have previously shown that BMP4 reduces breast cancer cell proliferation through G1 cell cycle arrest and simultaneously induces migration in a subset of these cell lines. Here we examined the effects of BMP4 in a more physiological environment, in a 3D culture system.

Methods: We used two different 3D culture systems; Matrigel, a basement membrane extract from mouse sarcoma cells, and a synthetic polyethylene glycol (PEG) gel. AlamarBlue reagent was used for cell proliferation measurements and immunofluorescence was used to determine cell polarity. Expression of cell cycle regulators was examined by Western blot and matrix metalloproteinase (MMP) expression by qRT-PCR.

Results: The MCF-10A normal breast epithelial cells formed round acini with correct apicobasal localization of α6 integrin in Matrigel whereas irregular structures were seen in PEG gel. The two 3D matrices also supported dissimilar morphology for the breast cancer cells. In PEG gel, BMP4 inhibited the growth of MCF-10A and the three breast cancer cell lines examined, thus closely resembling the 2D culture conditions, but in Matrigel, no growth inhibition was observed in MDA-MB-231 and MDA-MB-361 cells. Furthermore, BMP4 induced the expression of the cell cycle inhibitor p21 both in 2D and 3D culture, thereby partly explaining the growth arrest. Interestingly, MDA-MB-231 cells formed large branching, stellate structures in response to BMP4 treatment in Matrigel, suggestive of increased cell migration or invasion. This effect was reversed by Batimastat, a broad-spectrum MMP inhibitor, and subsequent analyses showed BMP4 to induce the expression of *MMP3* and *MMP14*, that are thus likely to be responsible for the stellate phenotype.

Conclusions: Taken together, our results show that Matrigel provides a more physiological environment for breast epithelial cells than PEG gel. Moreover, BMP4 partly recapitulates in 3D culture the growth suppressive abilities previously seen in 2D culture and induces an MMP-dependent migratory phenotype in MDA-MB-231 cells.

Keywords: 3D culture, Matrigel, Breast cancer, BMP4, Proliferation, Migration

* Correspondence: anne.kallioniemi@uta.fi
[1]Institute of Biomedical Technology, University of Tampere and BioMediTech, Tampere, Finland
[2]Fimlab Laboratories, Tampere, Finland

Background

Bone morphogenetic protein 4 (BMP4) is a growth factor that belongs to the bone morphogenetic protein (BMP) family, which comprises the majority of the transforming growth factor β (TGF-β) –superfamily [1]. BMPs are extracellular ligands that bind serine/threonine receptors on the cell membrane and signal through intracellular SMAD mediators as well as through other pathways such as the MAP kinase pathway. BMPs were first found due to their bone-inducing effects and later studies showed them to be also powerful developmental regulators. For example, BMP4 is involved in gastrulation, mesoderm formation, hematopoiesis and the development of several organs and tissues including mammary gland [2-4].

Due to their multifunctionality, BMPs have been increasingly studied as potential players in cancer. BMP4 expression in cancer varies and both increased and decreased expression has been reported depending on the tissue of origin [5]. In breast cancer, strong *BMP4* expression has been found in both cell lines and tissues [6-8] and immunohistochemical data indicate that BMP4 protein is expressed in one fourth to half of primary tumors [9]. Functional studies in multiple malignancies suggest that BMP4 typically causes reduced growth and increased migration of cancer cells [5]. We have previously shown, using a large set of breast cancer cell lines, that BMP4 treatment systematically inhibits proliferation in all cell lines and simultaneously increases migration of MDA-MB-231, MDA-MB-361 and HCC1954 cells, but reduces migrativeness of T-47D cells [10]. Similarly, Guo and colleagues [6] demonstrated increased migration and decreased proliferation upon BMP4 overexpression in MDA-MB-231 and MCF-7 breast cancer cells. These data were corroborated by an *in vivo* study where inhibition of BMP4 signaling decreased metastasis of MDA-MB-231 breast cancer cells [11]. Yet there is one study where BMP4 reduced migration of MDA-MB-231 cells [12]. Nevertheless, the majority of the data implies that BMP4 has a dualist effect on breast cancer cells, with inhibition of cell proliferation and induction of a migratory phenotype.

The aforementioned *in vitro* functional studies were done using cells growing as two-dimensional (2D) monolayer. However, there is an increasing interest in culturing cells in a more biologically relevant three-dimensional (3D) environment [13]. This has been generally achieved by growing cells in synthetic scaffolds or gels of biological or synthetic origin [14]. Matrigel, basement membrane extract from mouse sarcoma, is the most commonly used biological scaffold and consists mainly of laminin, collagen IV and various growth factors [15]. Other biological materials that are often used include collagen, alginate and hyaluronic acid [14]. Synthetic gels have been developed as alternatives to the biological gels due to the difficulties in defining the exact composition of the biological materials and the fact that they may suffer from batch-to-batch variability [14]. Synthetic gels, mainly different polymers, such as polyethylene glycol and polyvinyl alcohol, have a constant composition and are easy to manipulate. However, they may not adequately represent the complicated extracellular matrix (ECM) that surrounds cells in tissues [14,16].

Various cell types, including epithelial, neural and endothelial cells, have been successfully grown in 3D and are capable of forming structures that resemble the normal tissue organization [15]. For example, normal immortalized mammary epithelial cells, such as the MCF-10A cells, form polarized acini structures in Matrigel, reminiscent of the normal breast architecture [17], whereas breast cancer cells generate more variable structures [18]. Similarly, biologically appropriate cellular organization has been observed e.g. for epithelial and neural cells in different synthetic gels [19-21]. More importantly, the shift from 2D to 3D culture also results in changes in gene expression in multiple tissue types [13,22-25]. For example, breast epithelial cells begin to produce milk proteins when grown in Matrigel [25].

Previous data from us and others showed that BMP4 is able to reduce the growth of breast cancer cells whilst inducing cell migration and invasion [6,10,11]. Here we utilized two different 3D culture systems to evaluate whether these phenotypes persist under more physiological culture conditions and further explored the mechanisms of BMP4-induced changes in cell proliferation and mobility.

Methods

Cell lines

The MCF-10A, MDA-MB-231, MDA-MB-361, BT-474 and T-47D cell lines were purchased from ATCC (Manassas, VA, USA) and cultured according to ATCC instructions, except for MCF-10A, which was maintained as previously described [17]. In 3D experiments, MDA-MB-231 and MDA-MB-361 cells were cultured in DMEM (Sigma-Aldrich, St. Louis, MO, USA). For MCF-10A cells a reduced concentration of EGF (5 ng/ml) was used in Matrigel [17].

BMP4 and inhibitor treatments

rhBMP4 (100 ng/ml, R&D Systems, Minneapolis, MN, USA), BMP antagonist Gremlin (1 μg/ml, R&D Systems), MMP inhibitor Batimastat (10 μM, Millipore, Billerica, MA, USA) or a combination of these was added to the medium at the start of the experiments and replenished every two to three days as the medium was exchanged. Vehicle-treated cells received BMP4 dilution buffer (4 mM HCl with 0.1% BSA), Gremlin dilution buffer (0.1% BSA in PBS), Batimastat dilution buffer (DMSO),

or a combination of these. All experiments were done in two to six replicates and were repeated at least twice.

Cell proliferation assay

Medium with 10% alamarBlue (Invitrogen) was added to the cells and incubated for 1 hour (2D culture) or 4 hours (Matrigel and PEG gel). Medium was collected and fluorescence (excitation wavelength 560 nm, emission wavelength 590 nm) measured using Tecan infinite F200 Pro plate reader (Tecan, Männedorf, Switzerland). Additionally, the number of cells in 2D culture was counted using the Z1 Coulter Counter (Beckman Coulter, Fullerton, CA) at indicated time points. The experiments were done in four to six replicates and repeated at least twice.

Cell cycle

MCF-10A cells were cultured on 24-well plates and analyzed 3 and 5 days after first addition of BMP4. The cells were stained with PI as described [26]. The cell cycle distribution was determined using the Accuri C6 flow cytometer (Accuri, Ann Arbor, MI, USA) and ModFit LT 3.0 (Verity software house, USA). The experiment was performed twice with six replicates.

3D Matrigel assay

Cells were cultured on growth factor-reduced Matrigel (BD Biosciences, Franklin Lakes, NJ, USA) using the overlay method [17]. Briefly, 4-chambered Lab-Tek chamber slides (Nalge Nunc International, Rochester, NY, USA) or 24-well plates were coated with Matrigel. Cells (2.0×10^4 cells/ml for MDA-MB-231 and T-47D, 2.4×10^4 cells/ml for MCF-10A, 6.0×10^4 cells/ml for BT-474 and 1.2×10^5 cells/ml for MDA-MB-361) suspended in 2.5% Matrigel solution were added on coated chamber slides and allowed to grow up to 17 days.

3D PEG gel assay

MMP-degradable polyethylene glycol (PEG) gel with RGD peptides was purchased from QGel (Lausanne, Switzerland). Briefly, 400 μl of Buffer A was mixed with QGelTM MT 3D Matrix powder, before addition of 100 μl of cell suspension (given a final concentration of 1.4×10^5 cells/ml for MCF-10A, 1.0×10^5 cells/ml for MDA-MB-231, 8.0×10^4 cells/ml for T-47D, and 4.0×10^5 cells/ml for MDA-MB-361). Drops of 40 μl were applied into a disc caster and after 30 min incubation at 37°C the gelled discs were removed and placed on 24-well plates with 1 ml of medium per well. The cells were allowed to grow up to 18 days.

Immunofluorescence

The MCF-10A cells in Matrigel and PEG gel were fixed in 4% paraformaldehyde for 1 hour at 37°C followed by permeabilization with 0.1% Triton-X100 for 45 min at room temperature and blocking with 3% BSA for 1.5 hours at 37°C. The fixed cells were incubated with mouse monoclonal anti-α6 integrin antibody (1:300, Abcam, Cambridge, UK) for 1.5 hours at 37°C. The secondary goat anti-mouse Alexa Fluor 488 (1:200, Invitrogen) was used similarly. The cells were stained with DAPI (Invitrogen) and mounted with Vectashield (Vector Laboratories, Burlingame, CA, USA). Images were taken with Zeiss Axio Imager. M2 microscope (Carl Zeiss, Oberkochen, Germany) connected to an ApoTome slider module (Carl Zeiss).

Image analysis

Images were taken from the cells in Matrigel and PEG gel using Olympus IX71 microscope (Olympus, Tokyo, Japan) and processed with ImageJ (U.S. National Institutes of Health, Bethesda, MD, USA). Four images from each experiment at designated time points were analyzed and the average area covered by the cells was calculated.

Protein extraction

The cells were collected 24 hours or 5 days (2D culture) and 4 or 7 days (Matrigel) after first addition of BMP4. Matrigel was first dissolved by adding cold PBS with 5 mM EDTA and the cells were kept on ice for 15 min. The cell-Matrigel solution was then collected, kept on ice for 30 min and centrifuged for 15 min at 3300 × g, at 4°C. Cells were lysed and protein concentration measured as previously described [10].

Western blot

Fifty μg of protein was loaded onto SDS-PAGE gels. After gel electrophoresis, the proteins were transferred to a PVDF membrane. The following primary antibodies (Santa Cruz Biotechnology, CA, USA) and dilutions were used: p21 (1:100), Cdk4 (1:1000), Cdc2 (1:1000), p-Cdc2 (Thr14/Tyr15, 1:200), p27 (1:500), p16 (1:100), p15 (1:200), Cyclin B1 (1:200), Cyclin B2 (1:100) and Cyclin D1 (1:200). All antibodies were rabbit polyclonal, with the exception of p16 (mouse monoclonal) and Cyclin B2 (goat polyclonal). In addition, a mouse monoclonal anti-GTF2H1 antibody (1:1000, Abcam) was used. Proteins were detected using the BM Chemiluminescence Western Blotting kit (Roche, Mannheim, Germany) according to manufacturer's instructions. Anti-mouse/rabbit secondary antibody (1:5000, Roche) was used for all antibodies, except for Cyclin B2, which was detected with anti-goat secondary antibody (1:5000, Santa-Cruz Biotechnology). The membranes were stripped and probed with β-tubulin (Sigma-Aldrich) as a loading control.

Quantitative RT-PCR

The expression of *MMP-1*, *-2*, *-3*, *-7*, *-9*, *-14* and *ADAM17* was examined in BMP4- and vehicle-treated MDA-MB-231 and BT-474 (*MMP3* and *MMP14* only) cells grown for 14 days in Matrigel. The cells were harvested as described above for protein extraction. Total RNA was extracted using RNeasy Mini kit (Qiagen, Valencia, CA) and was reverse transcribed using SuperScriptTM III First-Strand Synthesis System for RT-PCR (Invitrogen) as described [7]. qRT-PCR was performed using gene specific primers and UPL probes (Roche, Additional file 1: Table S1) and the LightCycler equipment (Roche) as described [27] with 1.2 μM concentration of primers and probes and the following program: 10 min denaturation at 95°C followed by 45 cycles of 10 s denaturation at 95°C, 10 s annealing at 55°C and 15 s elongation at 72°C. The experiments were done in three replicates and the expression levels were normalized using Phosphoglycerate kinase 1 (*PGK1*) housekeeping gene.

Statistical analyses

The difference between BMP4- and vehicle-treated samples in cell proliferation and area analysis was evaluated using the Mann–Whitney test with GraphPad Prism 4 (GraphPad Software, La Jolla, CA, USA). A P-value of less than 0.05 was considered significant.

Results

BMP4 inhibits the growth of MCF-10A cells in both 2D and 3D cell culture

We began the study using an immortalized breast epithelial cell line MCF-10A, which is widely used in 3D cultures. However, since no previous data existed, we first tested the effects of BMP4 on these cells in standard 2D culture. Similar to breast cancer cell lines [10], BMP4 decreased the proliferation of the MCF-10A cells as determined by cell counting and alamarBlue (Figure 1A). A highly significant decrease in cell number was evident at day 3 and day 6 (42% and 50%, respectively, as compared to vehicle; $P < 0.01$).

In 3D assays, both biological (Matrigel) and synthetic (polyethylene glycol, PEG gel) materials were used. In Matrigel, MCF-10A cells formed round acini-like structures with correct apicobasal polarity of the acini, as illustrated by the basal localization of α6-integrin (Figure 1B, left panel). In contrast, MCF-10A cells grown in PEG gel demonstrated a disordered structure with no obvious lumen formation and no basal localization of α6-integrin (Figure 1B, right panel).

When MCF-10A cells in Matrigel were treated with BMP4 (100 ng/ml), there was no change in the acinar morphology but proliferation of the cells was reduced (Figure 2A-C). The proliferation rate (as measured by alamarBlue) was decreased by 41% at day 14 in BMP4-treated cells as compared to vehicle-treated cells ($P < 0.05$, Figure 2B). Accordingly, BMP4 also significantly decreased the size of the acini structures as evidenced by a 40% reduction in the total area covered by the cell clusters at day 14 ($P < 0.05$, Figure 2C).

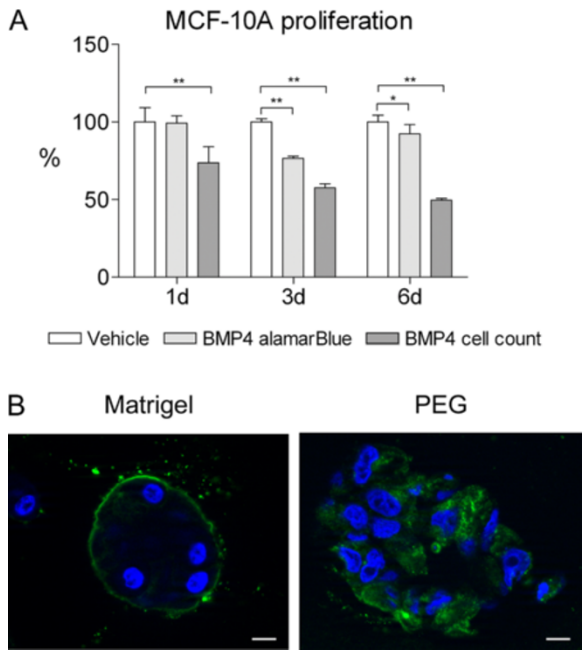

Figure 1 Characterization of MCF-10A cells in 2D and 3D culture. (A) BMP4 treatment significantly reduces the proliferation of MFC-10A cells in 2D culture. Cells were grown in the presence of 100 ng/ml BMP4 or vehicle and proliferation was measured using the alamarBlue reagent and by counting the cells at indicated time points. Relative proliferation (mean + s.d.) compared to vehicle is shown. *$P < 0.05$, **$P < 0.01$. **(B)** MCF-10A cells form polarized structures in Matrigel but not in PEG gel. The cells were grown in Matrigel for 14 and in PEG gel for 11 days, fixed, and immunofluorescently labeled with polarization marker α6-integrin antibody (green). The nuclei were stained with DAPI (blue). Images were taken with Zeiss Axio Imager.M2 microscope. Scale bar 10 μm.

In PEG gel, vehicle-treated MCF-10A cells mainly formed round cell clusters with occasional protrusions whereas BMP4-treated cells formed irregularly shaped elongated structures with high numbers of protrusions (Figure 2D). In addition, BMP4 inhibited the proliferation of the MCF-10A cells by 69% at day 11 as compared to the vehicle ($P < 0.005$, Figure 2E). Analysis of the area covered by cells revealed a maximum reduction of 51% at day 7 after BMP4 treatment ($P < 0.05$, Figure 2F).

BMP4 induces different phenotypes in breast cancer cells in 3D

Next we examined the effects of BMP4 in 3D cultures of four breast cancer cell lines. The cell lines were chosen based on our previous data showing a prominent

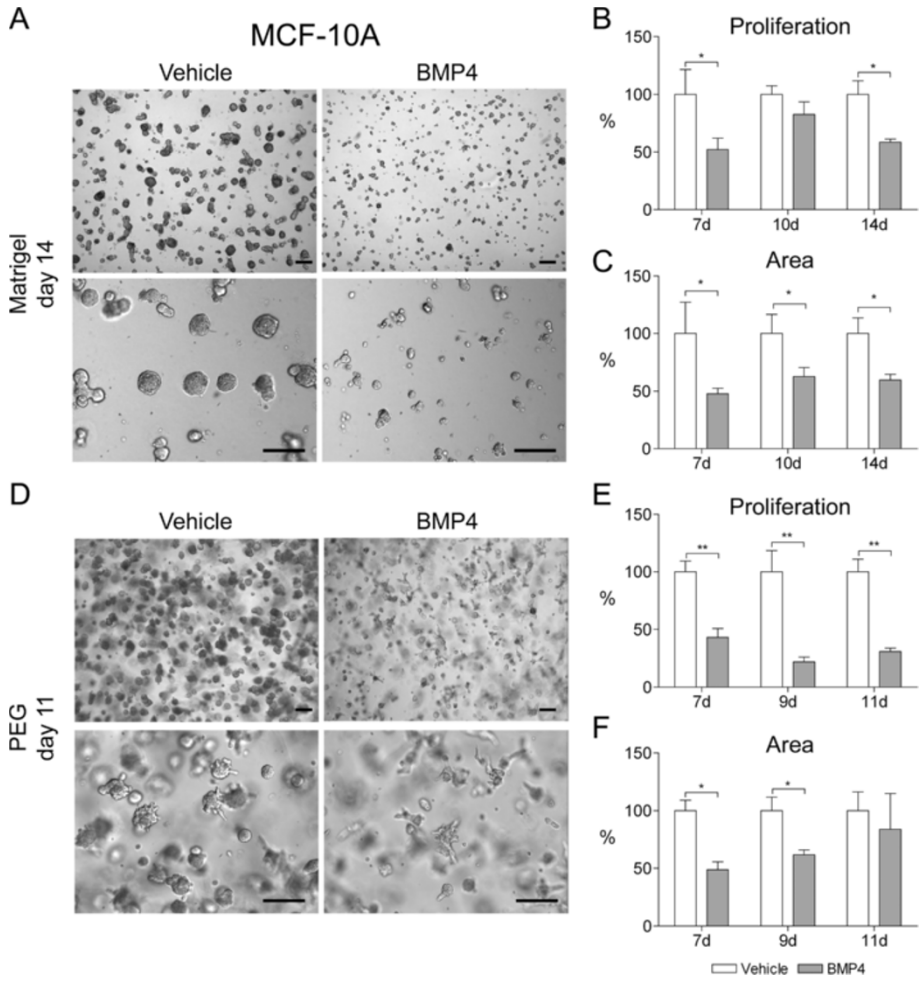

Figure 2 BMP4 inhibits MCF-10A cell growth in 3D cell culture. Cells were grown in Matrigel **(A-C)** or in PEG gel **(D-F)** supplemented with 100 ng/ml BMP4 or vehicle. Images were captured with Olympus IX71 microscope and representative examples from day 14 (Matrigel, panel **A**) and day 11 (PEG gel, panel **D**) are shown. Scale bars 200 μm. (b, e) Cell proliferation was measured using the alamarBlue reagent at indicated time points and relative proliferation (mean + s.d.) compared to vehicle is presented. **(C, F)** The area covered by cell clusters was measured from images taken at indicated time points using ImageJ and the relative mean area and s.d. compared to vehicle is shown. *P < 0.05, **P < 0.01.

phenotype upon BMP4 stimulation in 2D; either G1 cell cycle arrest and growth inhibition (T-47D, BT-474, MDA-MB-361) and/or increased migration (MDA-MB-231, MDA-MB-361) [10, unpublished]. T-47D cells formed irregular raft-like structures in Matrigel (Figure 3A). BMP4 treatment did not induce any obvious changes in the morphology of the cell clusters but inhibited cell proliferation (29% at day 7, 41% at day 10 and 10% at day 14 as compared to vehicle, $P < 0.05$, Figure 3A-B). The size of the area covered by cells was similarly reduced by 43% and 39% at days 7 and 10, respectively ($P < 0.05$, Figure 3C). At day 14 the difference was 28% but just failed to reach statistical significance (Figure 3C). In PEG gel, the T-47D cell structures were either round or polygonal in shape, in both BMP4- and vehicle-treated samples (Figure 3D). BMP4 induced a distinct decrease in cell proliferation at days 11 and 14 (30% and 51%, respectively, as compared to vehicle, $P < 0.01$, Figure 3E). Consequently, there was a significant reduction in the size of the cell area, ranging from 64% at day 7 to 79% at day 14 ($P < 0.05$, Figure 3F).

For BT-474 cells, the consequences of BMP4 treatment were first examined in 2D culture due to lack of previous information. A significant decrease in cell count was detected in BMP4-treated cells as compared to vehicle (30% at day 3 and 70% at day 6, $P < 0.01$, Additional file 2: Figure S1). In Matrigel the cells formed dense, mostly round structures (Figure 4A). Proliferation was reduced by 26% already at day 7 and continued to decrease up to 36% at day 14 after BMP4-treatment ($P < 0.05$, Figure 4B). A concomitant reduction of 40% to 50% on average could be seen in the area measurements ($P < 0.05$, Figure 4C).

MDA-MB-361 cells grew very slowly in both 3D environments and therefore were allowed to grow up to

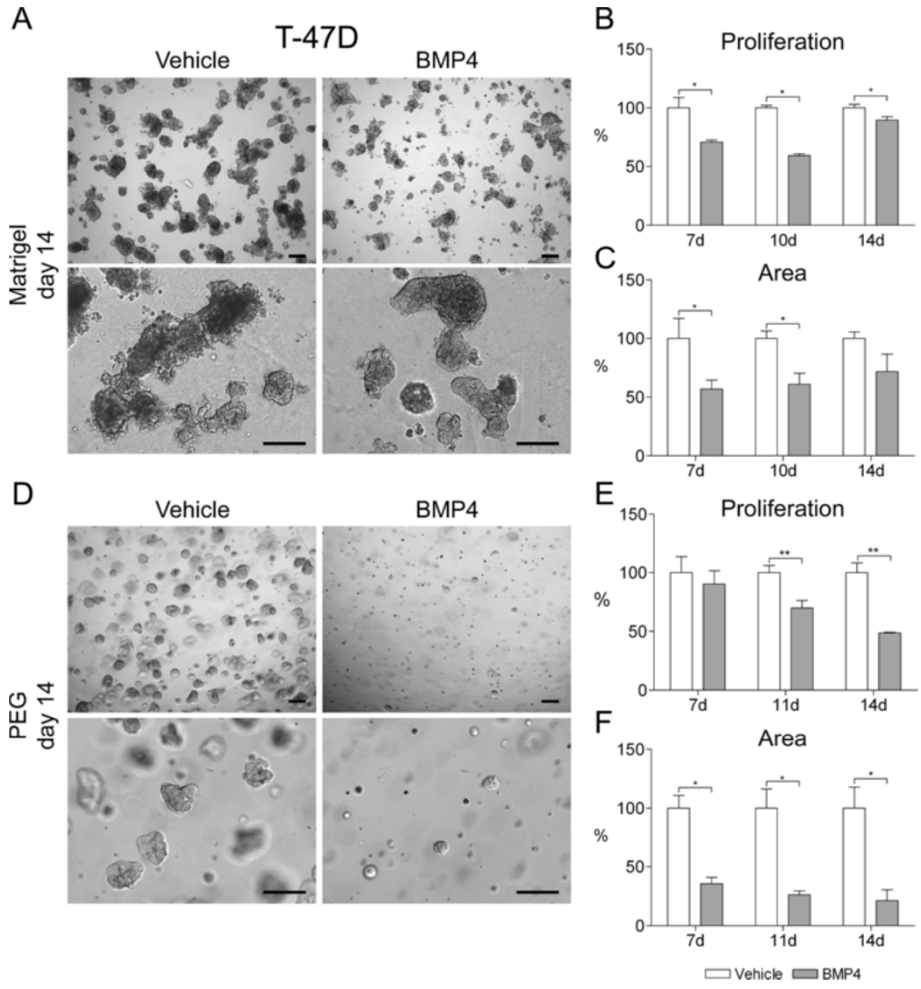

Figure 3 BMP4 inhibits T-47D cell growth in 3D cell culture. Cells were grown in Matrigel **(A-C)** or in PEG gel **(D-F)** and supplemented with 100 ng/ml BMP4 or vehicle. Images were taken as indicated in Figure 2 and representative examples from day 14 are shown. Scale bars 200 μm. **(B, E)** Cell proliferation and **(C, F)** area covered by cell clusters were measured and are presented as in Figure 2, *P < 0.05, **P < 0.01.

18 days (Additional file 3: Figure S2). In Matrigel, the cells formed small mostly round masses, and BMP4 treatment induced no consistent changes in proliferation, area or morphology of the cells (Additional file 3: Figure S2A-C). In contrast, in PEG gel BMP4 significantly decreased proliferation at day 11 through day 18 (15% and 28%, respectively, as compared to vehicle, $P < 0.01$, Additional file 3: Figure S2E). In addition, BMP4 decreased the size of the area covered by cells, with a maximum reduction of 48% at day 11 ($P < 0.05$, Additional file 3: Figure S2F). However, no changes in the morphology of the cell structures were observed in PEG gel with both BMP4 and vehicle treatments resulting in round cell clusters.

MDA-MB-231 cells formed mostly dense and compact round or oval structures in Matrigel with occasional branches (Figure 5A). Interestingly, BMP4 had a major impact on the morphology of the cells. It induced the formation of large branching stellate structures, which extended over large areas of the gel (Figure 5A). The first evidence on this effect was seen already at day 7, but it became prominent after 10 days in culture (Figure 5A). On the other hand, BMP4 did not have an effect on the proliferation of the MDA-MB-231 cells as measured by alamarBlue or the area covered by the cells (Figure 5B and 5C). It should be noted that the latter result is hindered by the difficulties in accurately measuring the area of the BMP4-induced stellate structures. In PEG gel, no branching was observed and the MDA-MB-231 cell masses were typically round or irregularly shaped in both BMP4- and vehicle-treated samples (Figure 5D). Interestingly, BMP4 significantly inhibited proliferation of the MDA-MB-231 cells in PEG gel, with a 36% reduction by day 14 ($P < 0.01$, Figure 5E). Similarly, the area covered by the cells was diminished by a maximum of 36% at day 11 ($P < 0.05$, Figure 5F).

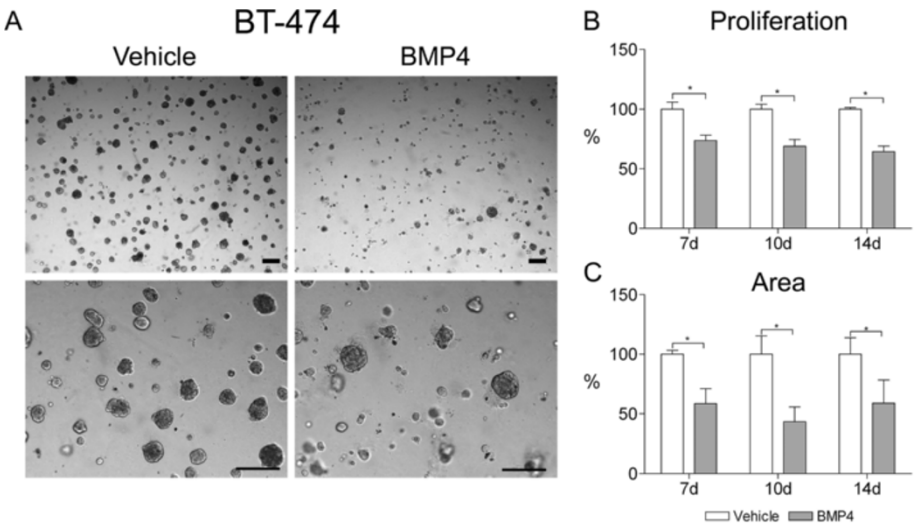

Figure 4 BMP4 inhibits BT-474 cell growth in 3D cell culture. (A) Cells were grown in Matrigel and supplemented with 100 ng/ml BMP4 or vehicle. Images were taken as indicated in Figure 2 and representative examples from day 14 are shown. Scale bars 200 μm. **(B)** Cell proliferation and **(C)** area covered by cell clusters were measured and are presented as in Figure 2, *P < 0.05.

BMP4-induced growth arrest is partly explained by induction of p21 expression

We have previously shown that the growth inhibition caused by BMP4 in breast cancer cell lines growing in monolayer culture is due to a G1 cell cycle arrest [10]. To investigate this further, the effect of BMP4 on the expression of 11 known cell cycle regulators was measured in T-47D and MDA-MB-361 cells grown for 24 hours in 2D. A change in the expression of the cell cycle inhibitor p21, phosphorylated CDC2 and Cyclins B1 and B2 was seen in both cell lines, with at least a 2-fold difference in one of the cell lines (Additional file 4: Figure S3). Among these, induction of p21 was the most prominent (4.1-fold in MDA-MB-361 and 2.2-fold in T-47D) and was thus selected for further evaluation. We verified that p21 expression was also induced by BMP4 in 2D culture of MDA-MB-231 and BT-474 cells (Figure 6A). In MCF-10A cells, distinct p21 induction (1.8-fold) was evident only after a prolonged (5 days) BMP4 treatment (Figure 6A) and was accompanied by a G1 cell cycle arrest (G1 phase fraction 80% vs. 69% in BMP4- and vehicle-treated cells, respectively, $P < 0.05$, Figure 6B). In Matrigel, the p21 levels were determined at day 4 or 7 after BMP4 treatment. BMP4 had no effect on p21 expression in MCF-10A cells whereas it did induce p21 expression in T-47D, BT-474, MDA-MB-361 and MDA-MB-231 cells (Figure 6A).

Induction of a stellate phenotype in MDA-MB-231 cells is MMP-dependent

To confirm that the stellate phenotype induced in the MDA-MB-231 cells in Matrigel was indeed dependent on BMP4, the cells were treated with BMP4 together with a BMP antagonist Gremlin, which inhibits the actions of BMP2, -4 and –7 [28]. Gremlin (1 μg/ml) alone had no effect on the morphology of the cells (Figure 7A). The cells treated with both Gremlin and BMP4 had similar morphology than vehicle-treated cells and thus Gremlin was able to reverse the stellate phenotype (Figure 7A).

We then speculated that the stellate phenotype may require the action of matrix metalloproteinases (MMPs). A broad-spectrum MMP inhibitor Batimastat was employed to test its potential in inhibiting the BMP4-induced phenotype. Batimastat (10 μM) alone resulted in a moderate reduction of growth of the cells as compared to vehicle-treated cells (Figure 7B). However, Batimastat was able to inhibit the formation of BMP4-induced stellate structures and, somewhat surprisingly, the combination of Batimastat and BMP4 resulted in a pronounced reduction in the size of the cell structures (Figure 7B).

As the stellate phenotype was reversed by an MMP inhibitor, we next examined the contribution of individual MMPs to this phenotype. Using quantitative RT-PCR, the expression levels of seven *MMP*s known to be targeted by Batimastat were measured in BMP4- and vehicle-treated MDA-MB-231 cells grown in Matrigel for 14 days. *MMP2*, *MMP7* and *MMP9* were not expressed in the MDA-MB-231 cells at a sufficient level to allow accurate measurements and there was no difference in *ADAM17* expression between BMP4-and vehicle-treated cells (data not shown). In contrast, there was a dramatic 19-fold increase in *MMP3* expression ($P < 0.005$) and a 3.7-fold increase in *MMP14* expression ($P < 0.05$) in BMP4-treated cells as compared to vehicle-treated cells. In addition, *MMP1* expression was 4.3 times higher in BMP4-treated cells but the

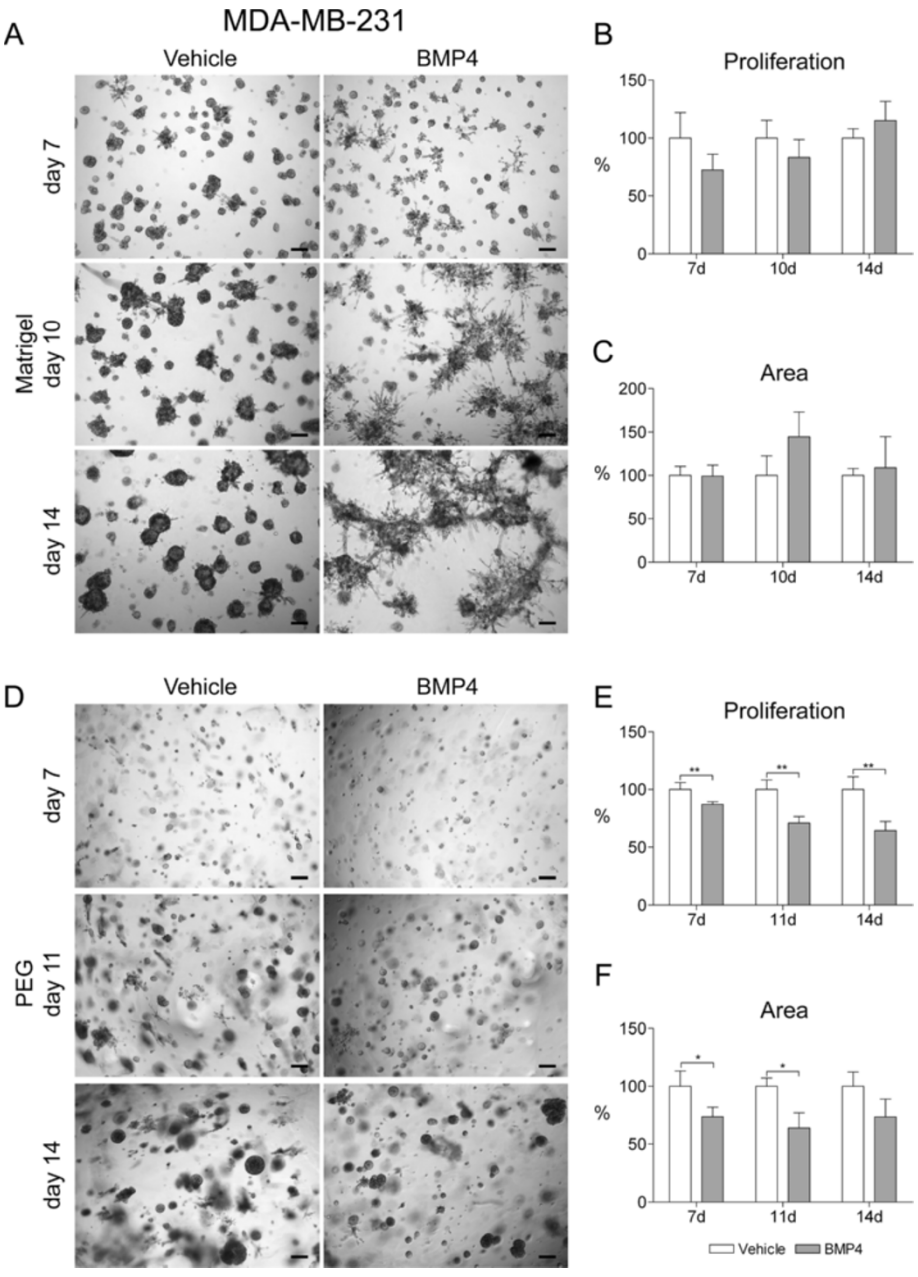

Figure 5 BMP4 induces a stellate phenotype and reduces the growth of the MDA-MB-231 cells in 3D cell culture. Cells were grown in Matrigel **(A-C)** or in PEG gel **(D-F)** supplemented with 100 ng/ml BMP4 or vehicle. Images were taken as indicated in Figure 2 and representative examples from days 7, 10 and 14 for Matrigel and days 7, 11 and 14 for PEG gel are shown. Scale bars 200 μm. **(B, E)** Cell proliferation and **(C, F)** area covered by cell clusters were measured and are presented as in Figure 2, *P < 0.05, **P < 0.01.

difference was not statistically significant. To further verify that the induction of *MMP3* and *MMP14* was exclusively related to the BMP4-induced stellate phenotype in MDA-MB-231 cells, we measured *MMP3* and *MMP14* mRNA levels in one of the non-stellate cell lines, BT-474, under similar conditions and found that in this case BMP4 did not induce the expression of these *MMP*s (data not shown).

Discussion

We have previously shown that BMP4 reduces proliferation and increases migration of breast cancer cells *in vitro* [10]. As these results were derived from cells grown in 2D monolayer culture, we set out to analyze the effect of BMP4 in a more physiological setting by employing 3D culture systems. We approached this issue by using both a biological gel (Matrigel, the standard 3D

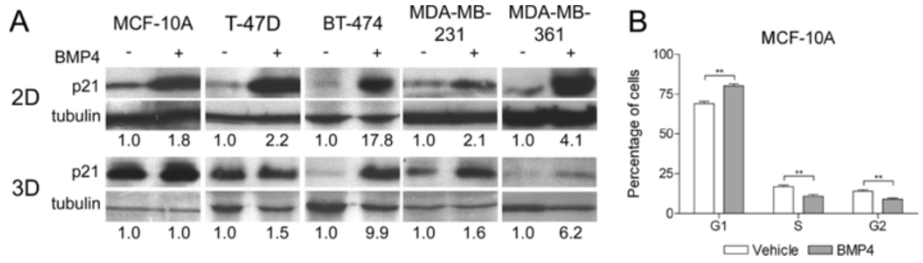

Figure 6 The expression of cell cycle inhibitor p21 is altered by BMP4. (A) MCF-10A cells were treated with 100 ng/ml BMP4 (+) or vehicle (–) for 5 days and the cancer cell lines for 24 hours when grown as monolayers (2D). In Matrigel (3D), the cells were grown and treated for 4 (MDA-MB-361) or 7 days. The expression of p21 was analyzed by western blot. Tubulin was used as a loading control and relative expression levels were calculated with ImageJ. **(B)** BMP4 treatment leads to G1 arrest of MCF-10A cells. The cell cycle was determined by flow cytometry at day 5 after the beginning of the treatments. The fraction (mean + s.d.) of cells in phases G1, S and G2 are shown. **P < 0.01.

culture environment) and a synthetic material with RGD peptides and MMP-degradable peptide links (PEG gel).

The two materials studied provided dissimilar 3D environments as first evidenced by differences in the morphology of the normal and cancer cell clusters. The MCF-10A normal mammary epithelial cells had a polarized acini structure in Matrigel, as previously shown [17], while in PEG gel the cells formed irregular non-polarized structures. Similarly, the morphology of the different cancer cells varied between the two 3D models, with the structures formed in Matrigel again corresponding to those previously reported [18]. On a functional level, the growth response of cells to BMP4 treatment in PEG gel mirrored the 2D data, whereas in Matrigel more diverse effects were observed. These data could be explained by several factors. Matrigel contains multiple biologically active molecules, such as laminin, collagen IV and many growth factors [15], that are likely to impact the results obtained. Of these biologically active molecules, e.g. laminin-1 has been shown to be essential for correct polarization of primary luminal epithelial cells in collagen gels [29]. It has also been reported that 50 mM RGD peptide is an optimal concentration for acinar growth of MCF-10A cells in polyethylene glycol tetravinyl sulfone (PEG-VS) gel [30]. A lower concentration of RGD (50 μM) was present in the PEG gel used here, possibly explaining the lack of acinar formation. In addition, the stiffness and elasticity of the matrix is known to influence the cellular phenotype, including proliferation, differentiation and migration, in 3D environments [31-33]. To summarize, the differences in cell morphology and BMP4 response between the two materials tested demonstrate that the mere 3D architecture is not sufficient to mimic the biological effects of tissue environment. Based on the morphological characteristics, Matrigel seems to provide a more appropriate milieu for breast epithelial cells. While many synthetic 3D materials are entering the market, they should be used cautiously until their biological properties have been explored.

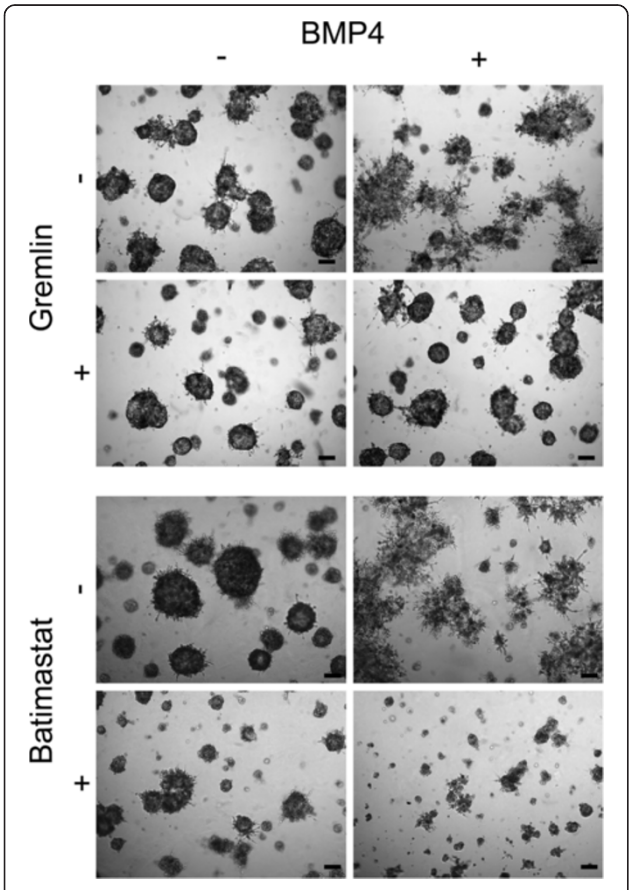

Figure 7 BMP4 antagonist Gremlin and MMP inhibitor Batimastat reverse the stellate phenotype of MDA-MB-231 cell clusters in Matrigel. The cells received 1 μg/ml Gremlin, 10 μM Batimastat and/or 100 ng/ml BMP4. Vehicle-treated cells were used as a control. Images were taken as indicated in Figure 2 and representative examples from day 14 are shown. Scale bar 200 μm.

Previous data from us and others [6,10] clearly demonstrate that BMP4 reduces the proliferation of breast cancer cells in 2D culture, and similar results have been reported in other tumor types [5,34-37]. Here we extend these findings and first show the same growth suppressive effect of BMP4 in MCF-10A normal immortalized breast epithelial

cells both in 2D and 3D environment. The 3D data from the breast cancer cell lines were more diverse. In PEG gel, BMP4 administration led to reduced cell proliferation for all cell lines tested, whereas in Matrigel two out of four cell lines (MDA-MB-231 and MDA-MB-361) did not display growth inhibition upon BMP4 treatment. In the case of MDA-MB-361, the very slow growth rate of the cells in 3D may have contributed to these findings, although the difference between responses in PEG gel and Matrigel implies an actual effect triggered by the different environments. Furthermore, the growth suppressive action of BMP4 seen in MDA-MB-231 cells in 2D [10] disappeared in 3D Matrigel and was overcome by a migratory phenotype. The response of the cells to biological molecules is known to change drastically in 3D, for example, many anticancer drugs are less effective in 3D culture [38]. Our data now suggest that the ability of BMP4 to reduce cell growth in 3D strongly depends on the material used. Nevertheless, cell line specific differences also exist and further highlight the importance of testing the impact of biological factors, including BMP4, in a proper environment.

BMP4 has been reported to induce G1 cell cycle arrest in cancer cells [10,39-41]. We now show for the first time that the mechanism behind this cell cycle arrest in breast cancer cells is the increased expression of the cell cycle inhibitor p21. This result is in concordance with previous reports in 2D culture of various normal and neoplastic cells [41-45]. Additionally, BMP2 has been shown to induce p21 expression in breast cancer cells [39,40,46]. Interestingly, BMP4 induced p21 expression in MDA-MB-231 and MDA-MB-361 cells in 3D even in the absence of growth inhibition, suggesting that p21 alone is not sufficient to induce growth arrest in these cells in 3D. Furthermore in MCF-10A cells, p21 induction and G1 cell cycle arrest were not evident until day 5 in 2D culture, even though a significant growth reduction was seen already at day 3. Likewise, in MCF-10A 3D culture no p21 induction was observed even after 7 days of BMP4 treatment. Therefore it seems likely that other factors are involved in the BMP4-mediated growth regulation in MCF-10A cells. Examination of a panel of cell cycle regulators in T-47D and MDA-MB-361 cells in 2D showed that BMP4 influenced the expression of multiple cell cycle proteins, including pCDC2, Cyclin B1 and Cyclin B2. These or other cell cycle regulators could thus contribute to the observed growth inhibition in MCF-10A cells as well. Previous studies have reported dysregulation of several cell cycle associated proteins, including Cyclin B1, CDC2, Rb, and E2F, after different stimuli in MCF-10A cells [47,48], emphasizing the fact that multiple factors may be simultaneously involved. Further research is needed to identify the specific cell cycle regulators influenced by BMP4 treatment in MCF-10A cells.

In most cases, BMP4 had no effect on the morphology of the cells grown in 3D environment, with the exception of MDA-MB-231 cells and MCF-10A cells. In PEG gel, MCF-10A cells formed irregular structures with small protrusions, the number of which increased upon BMP4 stimulation, indicating increased migration and/or invasion. This is consistent with previous results showing BMP4-induced invasive properties in mouse mammary epithelial cells in collagen gels [49]. In Matrigel, MDA-MB-231 cells formed stellate, branching structures in response to BMP4, which is in concert with previous observations of increased migration and invasion in 2D experiments [6,10]. Such structures were not observed in PEG gel, highlighting again the variation between the different 3D materials.

The MDA-MB-231 cells are known to be triple negative and represent the so-called basal subtype, whereas the remaining breast cancer cell lines used in this study are of luminal type [50]. We thus speculated whether the molecular subtype could explain the migratory response to BMP4 treatment seen only in MDA-MB-231 cells. To address this issue, we examined another triple negative basal breast cancer cell line, MDA-MB-436. However, the MDA-MB-436 cells were inherently migratory in Matrigel and BMP4 did not induce any additional effects (data not shown). Thus we conclude that the effects of BMP4 cannot be simply explained by the molecular subtype of the cell line. Neither could we link the BMP4-induced phenotypes to other known cell line characteristics, such as the histological type, mutational status, or tumorigenicity [18].

The BMP antagonist Gremlin was able to reverse the MDA-MB-231 stellate phenotype, demonstrating that the effect is truly due to the action of BMP4. Similarly, a broad spectrum MMP inhibitor Batimastat was able to inhibit the BMP4-induced branching of the MDA-MB-231 cells, indicating that the phenomenon required the action of matrix metalloproteinases (MMPs). Unexpectedly, Batimastat also reduced the growth of the cells, both with and without BMP4. MMPs have been shown to cleave intracellular or transmembrane proteins, thereby releasing factors that regulate cell proliferation, apoptosis, invasion and angiogenesis [51-54]. MMP9 has been particularly shown to possess growth-promoting effects [55,56]. Shon et al. [12] found BMP4 to suppress the activity of MMP9 in MDA-MB-231 cells, albeit in 2D culture, but in our 3D experiments the expression level of *MMP9* was too low to allow accurate measurements and thus MMP9 is unlikely to explain the growth suppressive effects of Batimastat. Nevertheless, examination of the expression of *MMP*s targeted by Batimastat revealed upregulation of *MMP3* and *MMP14* in BMP4-treated compared to vehicle-treated cells. Similar induction of *MMP3* or *MMP14* expression was not seen in the non-

migratory BT-474 cells, further suggesting a mechanistic link between these *MMPs* and the stellate phenotype in MDA-MB-231 cells. A recent study also showed that BMP4 induces the expression of multiple MMPs, including *MMP3* and *MMP14*, in mouse mammary fibroblasts and it also modestly induces the expression of *MMP3* in cancer associated human mammary fibroblasts and to a greater degree in normal human mammary fibroblasts [57]. In contrast, Otto et al. [58] found BMP4 to inhibit *MMP3* mRNA and protein expression in C3H10T1/2 stem cells, and this inhibition was related to adipogenetic differentiation. These opposing results are likely to reflect cell-type and context-specific differences.

The exact mechanisms behind *MMP3* and *MMP14* induction upon BMP4 treatment in MDA-MB-231 cells remain to be revealed. *MMP3* has in its promoter a binding element for AP-1, which is in turn known to be regulated by BMP4 [59,60], thereby representing a likely link between BMP4 and MMP3. However, previous data from other BMP/TGF-β family members suggest that additional signaling pathways may also contribute to the MMP induction. In MDA-MB-435 melanoma cells, TGF-β-induced upregulation of MMP14 has been shown to be dependent on the ERK1/2, PI3K, and JNK pathways [61] and in MDA-MB-231 cells TGF-β induced the expression of many *MMPs*, including *MMP14*, through the p38 MAP kinase [62]. Similarly, BMP2 has been shown to increase the expression of *MMP9* in gastric cancer cells through AKT, ERK and NF-κB signaling cascades [63]. Taken together, multiple signaling pathways may be involved in the BMP4-induced upregulation of MMP expression.

Conclusions

In conclusion, the data provided in this study demonstrate that Matrigel provides a more relevant environment to study the effects of biological factors on breast cancer cell behavior than the synthetic PEG gel. The responses of MDA-MB-231 and MDA-MB-361 cells to BMP4 were partly different in 2D than in 3D culture, thus strongly arguing for validation of 2D data in an appropriate 3D environment. Nevertheless, BMP4 retained its bifunctional role of reducing cell proliferation and inducing migration in 3D, albeit not in the same cell line. Finally, this study also delivered further evidence on the molecular mechanisms behind the BMP4-induced phenotypes.

Additional files

Additional file 1: Table S1. Gene specific primers and probes. UPL (Universal Probe Library) probes were purchased from Roche.

Additional file 2: Figure S1. BMP4 treatment reduces BT-474 cell growth in 2D cell culture. Cells were grown in the presence of 100 ng/ml BMP4 or vehicle and proliferation was measured using the alamarBlue reagent and by counting the cells at indicated time points. Relative proliferation (mean + s.d.) compared to vehicle is shown. *P < 0.05, **P < 0.01.

Additional file 3: Figure S2. BMP4 does not influence MDA-MB-361 cells grown in Matrigel but decreases cell proliferation in PEG gels. Cells were grown in Matrigel (a—c) or PEG gel (d—f) supplemented with 100 ng/ml BMP4 or vehicle. Images were taken as indicated in Figure 2 and representative examples from day 14 are shown. Scale bars 200 μm. (b, e) Cell proliferation and (c, f) area covered by cell clusters were measured and are presented as in Figure 2, *P < 0.05, **P < 0.01.

Additional file 4: Figure S3. BMP4 influences the expression of cyclin B1, cyclin B2, pCDC2 and p21. The expression levels of a set of known cell cycle regulators were examined using western blotting. MDA-MB-361 and T-47D cells were grown as monolayers and harvested 24 hours after the treatment with 100 ng/ml BMP4 (+) or vehicle (–). Tubulin was used as a loading control and relative expression levels were calculated with ImageJ.

Abbreviations

2D: Two-dimensional; 3D: Three-dimensional; BMP4: Bone morphogenetic protein 4; MMP: Matrix metalloproteinase; PEG gel: Polyethyleneglycol gel; TGF-β: Transforming growth factor β.

Competing interests

The authors declare that they have no competing interests.

Authors' contributions

MA and RJ conducted the experiments and wrote the manuscript. KJU consulted on the 3D culture experiments and participated in their design. ARM conducted initial experiments and helped in drafting the manuscript. EA and AK conceived of the study, participated in the design and helped to draft the manuscript. All authors approved the final version of the manuscript.

Acknowledgements

This study was supported by grants from the Finnish Cancer Organizations and the Competitive State Research Financing of the Expert Responsibility area of Tampere University Hospital (the unit of FimLab, grants 9 N021 and 9P003). We are grateful to Kati Rouhento for her skilful technical assistance and to Anni Järvinen and Anniina Brofeldt for their contribution in the experiments.

Received: 19 June 2013 Accepted: 17 September 2013
Published: 22 September 2013

References

1. Bragdon B, Moseychuk O, Saldanha S, King D, Julian J, Nohe A: **Bone morphogenetic proteins: a critical review.** *Cell Signal* 2011, **23:**609–620.
2. Winnier G, Blessing M, Labosky PA, Hogan BL: **Bone morphogenetic protein-4 is required for mesoderm formation and patterning in the mouse.** *Genes Dev* 1995, **9:**2105–2116.
3. Sadlon TJ, Lewis ID, D'Andrea RJ: **BMP4: its role in development of the hematopoietic system and potential as a hematopoietic growth factor.** *Stem Cells* 2004, **22:**457–474.
4. Cho KW, Kim JY, Song SJ, Farrell E, Eblaghie MC, Kim HJ, Tickle C, Jung HS: **Molecular interactions between Tbx3 and Bmp4 and a model for dorsoventral positioning of mammary gland development.** *Proc Natl Acad Sci U S A* 2006, **103:**16788–16793.
5. Kallioniemi A: **Bone morphogenetic protein 4-a fascinating regulator of cancer cell behavior.** *Cancer Genet* 2012, **205:**267–277.
6. Guo D, Huang J, Gong J: **Bone morphogenetic protein 4 (BMP4) is required for migration and invasion of breast cancer.** *Mol Cell Biochem* 2012, **363:**179–190.
7. Alarmo EL, Kuukasjarvi T, Karhu R, Kallioniemi A: **A comprehensive expression survey of bone morphogenetic proteins in breast cancer highlights the importance of BMP4 and BMP7.** *Breast Cancer Res Treat* 2007, **103:**239–246.
8. Davies SR, Watkins G, Douglas-Jones A, Mansel RE, Jiang WG: **Bone morphogenetic proteins 1 to 7 in human breast cancer, expression pattern and clinical/prognostic relevance.** *J Exp Ther Oncol* 2008, **7:**327–338.

9. Alarmo EL, Huhtala H, Korhonen T, Pylkkanen L, Holli K, Kuukasjarvi T, Parkkila S, Kallioniemi A: **Bone morphogenetic protein 4 expression in multiple normal and tumor tissues reveals its importance beyond development.** *Mod Pathol* 2013, **26:**10–21.
10. Ketolainen JM, Alarmo EL, Tuominen VJ, Kallioniemi A: **Parallel inhibition of cell growth and induction of cell migration and invasion in breast cancer cells by bone morphogenetic protein 4.** *Breast Cancer Res Treat* 2010, **124:**377–386.
11. Pal A, Huang W, Li X, Toy KA, Nikolovska-Coleska Z, Kleer CG: **CCN6 Modulates BMP signaling via the smad-independent TAK1/p38 pathway, acting to suppress metastasis of breast cancer.** *Cancer Res* 2012, **72**(18):4818–4828.
12. Shon SK, Kim A, Kim JY, Kim KI, Yang Y, Lim JS: **Bone morphogenetic protein-4 induced by NDRG2 expression inhibits MMP-9 activity in breast cancer cells.** *Biochem Biophys Res Commun* 2009, **385:**198–203.
13. Pampaloni F, Reynaud EG, Stelzer EH: **The third dimension bridges the gap between cell culture and live tissue.** *Nat Rev Mol Cell Biol* 2007, **8:**839–845.
14. Tibbitt MW, Anseth KS: **Hydrogels as extracellular matrix mimics for 3D cell culture.** *Biotechnol Bioeng* 2009, **103:**655–663.
15. Kleinman HK, Martin GR: **Matrigel: basement membrane matrix with biological activity.** *Semin Cancer Biol* 2005, **15:**378–386.
16. Cushing MC, Anseth KS: **Materials science, Hydrogel cell cultures.** *Science* 2007, **316:**1133–1134.
17. Debnath J, Muthuswamy SK, Brugge JS: **Morphogenesis and oncogenesis of MCF-10A mammary epithelial acini grown in three-dimensional basement membrane cultures.** *Methods* 2003, **30:**256–268.
18. Kenny PA, Lee GY, Myers CA, Neve RM, Semeiks JR, Spellman PT, Lorenz K, Lee EH, Barcellos-Hoff MH, Petersen OW, Gray JW, Bissell MJ: **The morphologies of breast cancer cell lines in three-dimensional assays correlate with their profiles of gene expression.** *Mol Oncol* 2007, **1:**84–96.
19. Schindler M, Ahmed I, Kamal J, Nur-E-Kamal A, Grafe TH, Young Chung H, Meiners S: **A synthetic nanofibrillar matrix promotes in vivo-like organization and morphogenesis for cells in culture.** *Biomaterials* 2005, **26:**5624–5631.
20. Mahoney MJ, Anseth KS: **Three-dimensional growth and function of neural tissue in degradable polyethylene glycol hydrogels.** *Biomaterials* 2006, **27:**2265–2274.
21. Salinas CN, Anseth KS: **The enhancement of chondrogenic differentiation of human mesenchymal stem cells by enzymatically regulated RGD functionalities.** *Biomaterials* 2008, **29:**2370–2377.
22. Ridky TW, Chow JM, Wong DJ, Khavari PA: **Invasive three-dimensional organotypic neoplasia from multiple normal human epithelia.** *Nat Med* 2010, **16:**1450–1455.
23. Ghosh S, Spagnoli GC, Martin I, Ploegert S, Demougin P, Heberer M, Reschner A: **Three-dimensional culture of melanoma cells profoundly affects gene expression profile: a high density oligonucleotide array study.** *J Cell Physiol* 2005, **204:**522–531.
24. Le Beyec J, Xu R, Lee SY, Nelson CM, Rizki A, Alcaraz J, Bissell MJ: **Cell shape regulates global histone acetylation in human mammary epithelial cells.** *Exp Cell Res* 2007, **313:**3066–3075.
25. Blum JL, Zeigler ME, Wicha MS: **Regulation of rat mammary gene expression by extracellular matrix components.** *Exp Cell Res* 1987, **173:**322–340.
26. Parssinen J, Alarmo EL, Karhu R, Kallioniemi A: **PPM1D silencing by RNA interference inhibits proliferation and induces apoptosis in breast cancer cell lines with wild-type p53.** *Cancer Genet Cytogenet* 2008, **182:**33–39.
27. Parssinen J, Kuukasjarvi T, Karhu R, Kallioniemi A: **High-level amplification at 17q23 leads to coordinated overexpression of multiple adjacent genes in breast cancer.** *Br J Cancer* 2007, **96:**1258–1264.
28. Gazzerro E, Canalis E: **Bone morphogenetic proteins and their antagonists.** *Rev Endocr Metab Disord* 2006, **7:**51–65.
29. Gudjonsson T, Ronnov-Jessen L, Villadsen R, Rank F, Bissell MJ, Petersen OW: **Normal and tumor-derived myoepithelial cells differ in their ability to interact with luminal breast epithelial cells for polarity and basement membrane deposition.** *J Cell Sci* 2002, **115:**39–50.
30. Weiss MS, Bernabe BP, Shikanov A, Bluver DA, Mui MD, Shin S, Broadbelt LJ, Shea LD: **The impact of adhesion peptides within hydrogels on the phenotype and signaling of normal and cancerous mammary epithelial cells.** *Biomaterials* 2012, **33:**3548–3559.
31. Huang G, Wang L, Wang S, Han Y, Wu J, Zhang Q, Xu F, Lu TJ: **Engineering three-dimensional cell mechanical microenvironment with hydrogels.** *Biofabrication* 2012, **4:**042001.
32. Lance A, Yang CC, Swamydas M, Dean D, Deitch S, Burg KJ, Dreau D: **Increased extracellular matrix density decreases MCF10A breast cell acinus formation in 3D culture conditions.** *J Tissue Eng Regen Med* 2013. e-pub ahead of print 12 February 2013.
33. Storm C, Pastore JJ, MacKintosh FC, Lubensky TC, Janmey PA: **Nonlinear elasticity in biological gels.** *Nature* 2005, **435:**191–194.
34. Shirai YT, Ehata S, Yashiro M, Yanagihara K, Hirakawa K, Miyazono K: **Bone morphogenetic protein-2 and −4 play tumor suppressive roles in human diffuse-type gastric carcinoma.** *Am J Pathol* 2011, **179:**2920–2930.
35. Virtanen S, Alarmo EL, Sandstrom S, Ampuja M, Kallioniemi A: **Bone morphogenetic protein −4 and −5 in pancreatic cancer–novel bidirectional players.** *Exp Cell Res* 2011, **317:**2136–2146.
36. Zhou Z, Sun L, Wang Y, Wu Z, Geng J, Miu W, Pu Y, You Y, Yang Z, Liu N: **Bone morphogenetic protein 4 inhibits cell proliferation and induces apoptosis in glioma stem cells.** *Cancer Biother Radiopharm* 2011, **26:**77–83.
37. Hjertner O, Hjorth-Hansen H, Borset M, Seidel C, Waage A, Sundan A: **Bone morphogenetic protein-4 inhibits proliferation and induces apoptosis of multiple myeloma cells.** *Blood* 2001, **97:**516–522.
38. Smalley KS, Lioni M, Herlyn M: **Life isn't flat: taking cancer biology to the next dimension.** *In Vitro Cell Dev Biol Anim* 2006, **42:**242–247.
39. Ghosh-Choudhury N, Ghosh-Choudhury G, Celeste A, Ghosh PM, Moyer M, Abboud SL, Kreisberg J: **Bone morphogenetic protein-2 induces cyclin kinase inhibitor p21 and hypophosphorylation of retinoblastoma protein in Estradiol-treated MCF-7 human breast cancer cells.** *Biochim Biophys Acta* 2000, **1497:**186–196.
40. Ghosh-Choudhury N, Woodruff K, Qi W, Celeste A, Abboud SL, Ghosh Choudhury G: **Bone morphogenetic protein-2 blocks MDA MB 231 human breast cancer cell proliferation by inhibiting cyclin-dependent kinase-mediated retinoblastoma protein phosphorylation.** *Biochem Biophys Res Commun* 2000, **272:**705–711.
41. Brubaker KD, Corey E, Brown LG, Vessella RL: **Bone morphogenetic protein signaling in prostate cancer cell lines.** *J Cell Biochem* 2004, **91:**151–160.
42. Chang SF, Chang TK, Peng HH, Yeh YT, Lee DY, Yeh CR, Zhou J, Cheng CK, Chang CA, Chiu JJ: **BMP-4 induction of arrest and differentiation of osteoblast-like cells via p21 CIP1 and p27 KIP1 regulation.** *Mol Endocrinol* 2009, **23:**1827–1838.
43. Jeffery TK, Upton PD, Trembath RC, Morrell NW: **BMP4 inhibits proliferation and promotes myocyte differentiation of lung fibroblasts via Smad1 and JNK pathways.** *Am J Physiol Lung Cell Mol Physiol* 2005, **288:**L370–8.
44. Su D, Zhu S, Han X, Feng Y, Huang H, Ren G, Pan L, Zhang Y, Lu J, Huang B: **BMP4-smad signaling pathway mediates adriamycin-induced premature senescence in lung cancer cells.** *J Biol Chem* 2009, **284:**12153–12164.
45. Zhu D, Wu J, Spee C, Ryan SJ, Hinton DR: **BMP4 mediates oxidative stress-induced retinal pigment epithelial cell senescence and is overexpressed in age-related macular degeneration.** *J Biol Chem* 2009, **284:**9529–9539.
46. Pouliot F, Labrie C: **Role of Smad1 and Smad4 proteins in the induction of p21WAF1, Cip1 during bone morphogenetic protein-induced growth arrest in human breast cancer cells.** *J Endocrinol* 2002, **172:**187–198.
47. Hawkes WC, Wang TT, Alkan Z, Richter BD, Dawson K: **Selenoprotein W modulates control of cell cycle entry.** *Biol Trace Elem Res* 2009, **131:**229–244.
48. Hsieh TC, Wijeratne EK, Liang JY, Gunatilaka AL, Wu JM: **Differential control of growth, cell cycle progression, and expression of NF-kappaB in human breast cancer cells MCF-7, MCF-10A, and MDA-MB-231 by ponicidin and oridonin, diterpenoids from the Chinese herb rabdosia rubescens.** *Biochem Biophys Res Commun* 2005, **337:**224–231.
49. Montesano R: **Bone morphogenetic protein-4 abrogates lumen formation by mammary epithelial cells and promotes invasive growth.** *Biochem Biophys Res Commun* 2007, **353:**817–822.
50. Kao J, Salari K, Bocanegra M, Choi YL, Girard L, Gandhi J, Kwei KA, Hernandez-Boussard T, Wang P, Gazdar AF, Minna JD, Pollack JR: **Molecular profiling of breast cancer cell lines defines relevant tumor models and provides a resource for cancer gene discovery.** *PLoS One* 2009, **4:**e6146.
51. Patel TR, Butler G, McFarlane A, Xie I, Overall CM, Stetefeld J: **Site specific cleavage mediated by MMPs regulates function of agrin.** *PLoS One* 2012, **7:**e43669.
52. Meighan PC, Meighan SE, Rich ED, Brown RL, Varnum MD: **Matrix metalloproteinase-9 and −2 enhance the ligand sensitivity of photoreceptor cyclic nucleotide-gated channels.** *Channels (Austin)* 2012, **6:**181–196.
53. Egeblad M, Werb Z: **New functions for the matrix metalloproteinases in cancer progression.** *Nat Rev Cancer* 2002, **2:**161–174.

54. Hua H, Li M, Luo T, Yin Y, Jiang Y: **Matrix metalloproteinases in tumorigenesis: an evolving paradigm.** *Cell Mol Life Sci* 2011, **68:**3853–3868.
55. Coussens LM, Tinkle CL, Hanahan D, Werb Z: **MMP-9 supplied by bone marrow-derived cells contributes to skin carcinogenesis.** *Cell* 2000, **103:**481–490.
56. Dufour A, Sampson NS, Li J, Kuscu C, Rizzo RC, Deleon JL, Zhi J, Jaber N, Liu E, Zucker S, Cao J: **Small-molecule anticancer compounds selectively target the hemopexin domain of matrix metalloproteinase-9.** *Cancer Res* 2011, **71:**4977–4988.
57. Owens P, Polikowsky H, Pickup MW, Gorska AE, Jovanovic B, Shaw AK, Novitskiy SV, Hong CC, Moses HL: **Bone morphogenetic proteins stimulate mammary fibroblasts to promote mammary carcinoma cell invasion.** *PLoS One* 2013, **8:**e67533.
58. Otto TC, Bowers RR, Lane MD: **BMP-4 treatment of C3H10T1/2 stem cells blocks expression of MMP-3 and MMP-13.** *Biochem Biophys Res Commun* 2007, **353:**1097–1104.
59. Piperi C, Papavassiliou AG: **Molecular mechanisms regulating matrix metalloproteinases.** *Curr Top Med Chem* 2012, **12:**1095–1112.
60. Lee SY, Yoon J, Lee MH, Jung SK, Kim DJ, Bode AM, Kim J, Dong Z: **The role of heterodimeric AP-1 protein comprised of JunD and c-Fos proteins in hematopoiesis.** *J Biol Chem* 2012, **287:**31342–31348.
61. Kuo YC, Su CH, Liu CY, Chen TH, Chen CP, Wang HS: **Transforming growth factor-beta induces CD44 cleavage that promotes migration of MDA-MB -435s cells through the up-regulation of membrane type 1-matrix metalloproteinase.** *Int J Cancer* 2009, **124:**2568–2576.
62. Gomes LR, Terra LF, Wailemann RA, Labriola L, Sogayar MC: **TGF-beta1 modulates the homeostasis between MMPs and MMP inhibitors through p38 MAPK and ERK1/2 in highly invasive breast cancer cells.** *BMC Cancer* 2012, **12:**26–2407. 12-26.
63. Kang MH, Oh SC, Lee HJ, Kang HN, Kim JL, Kim JS, Yoo YA: **Metastatic function of BMP-2 in gastric cancer cells: the role of PI3K/AKT, MAPK, the NF-kappaB pathway, and MMP-9 expression.** *Exp Cell Res* 2011, **317:**1746–1762.

doi:10.1186/1471-2407-13-429
Cite this article as: Ampuja *et al.*: BMP4 inhibits the proliferation of breast cancer cells and induces an MMP-dependent migratory phenotype in MDA-MB-231 cells in 3D environment. *BMC Cancer* 2013 **13**:429.

Cancer Letters 375 (2016) 238–244

Contents lists available at ScienceDirect

Cancer Letters

journal homepage: www.elsevier.com/locate/canlet

Original Articles

The impact of bone morphogenetic protein 4 (BMP4) on breast cancer metastasis in a mouse xenograft model

M. Ampuja [a], E.L. Alarmo [a], P. Owens [b], R. Havunen [a], A.E. Gorska [b], H.L. Moses [b], A. Kallioniemi [a,*]

[a] University of Tampere, BioMediTech, Tampere, Finland
[b] Department of Cancer Biology, Vanderbilt Ingram Cancer Center, Vanderbilt University, Nashville, TN, USA

ARTICLE INFO

Article history:
Received 8 January 2016
Received in revised form 3 March 2016
Accepted 3 March 2016

Keywords:
Bone morphogenetic protein
BMP4
Breast cancer
In vivo metastasis model
Bioluminescence imaging

ABSTRACT

Bone morphogenetic protein 4 (BMP4) is a key regulator of cell proliferation and differentiation. In breast cancer cells, BMP4 has been shown to reduce proliferation *in vitro* and interestingly, in some cases, also to induce migration and invasion. Here we investigated whether BMP4 influences breast cancer metastasis formation by using a xenograft mouse model. MDA-MB-231 breast cancer cells were injected intracardially into mice and metastasis formation was monitored using bioluminescence imaging. Mice treated with BMP4 developed metastases slightly earlier as compared to control animals but the overall number of metastases was similar in both groups (13 in the BMP4 group vs. 12 in controls). In BMP4-treated mice, bone metastases were more common (10 vs. 7) but adrenal gland metastases were less frequent (1 vs. 5) than in controls. Immunostaining revealed no differences in signaling activation, proliferation rate, blood vessel formation, EMT markers or the number of cancer-associated fibroblasts between the treatment groups. In conclusion, BMP4 caused a trend towards accelerated metastasis formation, especially in bone. More work is needed to uncover the long-term effects of BMP4 and the clinical relevance of these findings.

Introduction

Bone morphogenetic protein 4 (BMP4) is a member of the transforming growth factor β (TGFβ) superfamily of extracellular signaling molecules. BMP4 is one of 20 BMPs that were first identified based on their ability to form bone at extraskeletal sites but are now known to have multiple roles both during development and in adult tissues [1,2]. In the cellular context, BMPs regulate fundamental processes such as cell proliferation, differentiation, migration and survival, i.e. characteristics that are of great relevance also in cancer pathogenesis [3]. The versatile functions of BMPs are conveyed through the canonical SMAD pathway where the extracellular ligands first bind to specific cell surface serine-threonine kinase receptor dimers [4]. Intracellular SMAD proteins, which include receptor-regulated SMADs (SMAD1/5/9) and SMAD4, transmit the BMP signal by forming a complex that translocates to the nucleus in order to control the expression of BMP target genes [2,5]. The signals generated by BMPs may also be transferred via ERK, JNK and p38 mitogen-activated protein kinases (MAPKs) [6]. In addition, there is evident crosstalk between BMP and other signaling pathways, such as Wnt, JAK/STAT and Notch [5].

In breast cancer, the expression of several BMPs is deregulated [7,8]. In the case of BMP4, overexpression as compared to normal mammary gland has been described both in cancer cell lines [9,10] and in primary tumors [11,12]. Functional assays in multiple breast cancer cell lines implicated BMP4 as a strong inhibitor of cell proliferation through the induction of G1 cell cycle arrest [9,10]. Interestingly, BMP4 also influenced the migratory properties of breast cancer cells. BMP4 treatment increased migration and invasion of a subset of breast cancer cell lines either directly or via the functions of cancer-associated fibroblasts [9,10,12,13]. The MDA-MB-231 cells demonstrated an especially prominent increase in migration and invasion upon BMP4 stimulation. However, in a study by Shon and colleagues [14], MDA-MB-231 was reported to respond to BMP4 stimulation with reduced migration and invasion. Yet, data from 3D breast cancer cell models, which better mimic the *in vivo* environment, further sustained that BMP4 indeed enhances the migratory capacity of MDA-MB-231 cells [15]. The functional role of BMP4 as an inhibitor of cell growth and promoter of cell migration and invasion is further supported by breast cancer patient data. Strong BMP4 protein expression, which was detected in 25% of breast tumors, associated with low proliferation index and increased frequency of tumor recurrence [11].

The impact of BMP4 on breast cancer formation *in vivo* has been studied surprisingly little, but results from other tissue types mainly point to its role in tumor suppression [16]. For example, direct

* Corresponding author. Tel.: +358 50 437 2645.
E-mail address: anne.kallioniemi@uta.fi (A. Kallioniemi).

http://dx.doi.org/10.1016/j.canlet.2016.03.008
0304-3835/

manipulation of BMP4, either through overexpression or administration of recombinant protein, led to reduced tumor growth in xenograft models of brain, colorectal and lung cancers [17–21], whereas enhanced proliferation was seen in hepatocellular carcinoma [22]. Using mouse mammary cancer cells and an orthotopic xenograft model, Cao and colleagues [23] showed that overexpression of BMP4 had no effect on either *in vitro* cell proliferation or primary tumor growth. Nevertheless, BMP4 inhibited the metastatic ability of mouse mammary cancer cells in this model [23]. Other *in vivo* experiments in breast cancer have not focused on direct effects of BMP4 but have instead used manipulation of the BMP pathway and thus these data might not exclusively reflect BMP4 activity. For example, administration of DMH1, a BMP antagonist, and deletion of BMP receptor BMPR1A resulted in reduced mammary tumor growth in MMTV.PyVmT mouse model [24,25]. Furthermore, expression of dominant negative BMPR1A in a mouse model of breast cancer bone metastasis resulted in smaller osteolytic lesions and improved survival [26]. Manipulation of upstream regulators implicated BMP4 as a metastasis promoter in two breast cancer xenograft models [12,27] and a metastasis suppressor in one study [14]. Taken together, *in vivo* data on the functional effects of BMP4 and especially its possible role in breast cancer metastasis formation are very limited and contradictory. Here we sought to address this issue using intracardiac injection of MDA-MB-231 cells into nude mice together with direct treatment of the animals with BMP4. The MDA-MB-231 cells were specifically selected for this study since they exhibit distinct increase in migration and invasion in response to BMP4 treatment *in vitro* [9,10,15]. Metastasis formation was followed with bioluminescence imaging (BLI) and the possible contribution of BMP4 to basic characteristic of the metastasis samples as well as the surrounding tumor stroma were evaluated using immunohistochemistry and immunofluorescence.

Materials and methods

Cell lines

Breast cancer cell line (MDA-MB-231) and embryonic kidney cells (293T) were obtained from American Type Culture Collection (ATCC, Manassas, VA, USA) and maintained under the recommended culture conditions.

Plasmids, virus production and transduction

Lentiviral plasmid vector pHIV-Luciferase (pHIV-Luc) that contains the firefly Luciferase as a reporter gene was obtained from Addgene (plasmid no. 21375 provided by Bryan Welms, Addgene, Cambridge, MA, USA). Plasmid identity was verified by sequencing with ABI3130xl Genetic Analyzers using vector specific primers. GenElute Endotoxin-free Plasmid Maxiprep kit (Sigma-Aldrich, St. Louis, MO, USA) was used for plasmid purification. Altogether, 7 μg of lentivector was used to produce concentrated lentiviruses in 293T cells according to instructions in Lenti-X Tet-On Advanced Inducible Expression System (Clontech, Mountain View, CA, USA). Concentrated lentivirus was used to transduce 8.0×10^4 of MDA-MB-231 cells (6-well plates) in the presence of 8 μg/ml polybrene and normal culture medium for 24 h. Transduction medium was discarded the next day and cells were passaged five times in a ratio of 1:4 to ensure that they were free of viral particles before performing any experiments. Luciferase expression was confirmed using Luciferase Assay System (Promega, Madison, WI, USA) and luminescence was measured with Luminoskan Ascent (Thermo Fisher Scientific, Waltham, MA, USA).

3D Matrigel assay

Recombinant human BMP4 (rhBMP4) was obtained from R&D Systems (Minneapolis, MN, USA). Cells were cultured on growth factor-reduced Matrigel (Corning, Corning, NY, USA) using the overlay method as described previously [15]. Briefly, 24-well plates were coated with Matrigel. Cells (1.0×10^4 cells/ml) suspended in 2.5% Matrigel solution containing 100 ng/ml BMP4 or vehicle control (4 mM HCl with 0.1% BSA) were added on coated wells. Medium with BMP4 or vehicle control was replenished every two to three days and the cells were allowed to grow up to 14 days.

BMP4 treatment for the in vivo *experiment*

Before intracardiac inoculation, MDA-MB-231/Luc cells were pretreated with rhBMP4 (100 ng/ml) or equivalent volume of vehicle control for seven days and fresh medium was replenished every third day. For the dosage of mice, rhBMP4 was diluted to a concentration of 20 μg/ml in PBS with pH ca. 3.8. The vehicle control stock solution was similarly diluted before dosage.

Mice

All experiments were performed by Pharmatest Services Ltd (Turku, Finland) that holds the ethical approval of the National Committee for Animal Experiments. Female athymic nude mice (athymic nude Foxn1nu, Harlan, The Netherlands) were used for this study. BMP4- or vehicle control-treated MDA-MB-231/Luc cells (2×10^5 cells in 0.1 ml of PBS) were inoculated into the left cardiac ventricle of the mice under anesthesia and analgesia at day 0. Mice were given 100 μg/kg rhBMP4 or vehicle control through tail vein injection starting at day 0, three times a week for seven weeks. Animal welfare was monitored daily. The animals were weighed before each dosing and appearances of any clinical signs were recorded. Four mice died or were euthanized due to complications related to the cell inoculation and one mouse due to a dosing-related complication. These animals were excluded from the analyses, thus leaving 10 mice in the BMP4 group and 11 in control group. There was no statistical difference in the weight of the animals between the groups either during or at the end of the study.

Bioluminescence imaging (BLI) and sample collection

Whole body tumor burden and the number of metastases were quantified by imaging the bioluminescence emitted by the MDA-MB-231/Luc cells using IVIS Lumina imaging system (PerkinElmer, Waltham, MA, USA). 100 mg/kg of D-luciferin (Gold Biotechnology, St Louis, MO, USA) was administered intraperitoneally and the animals were anesthetized and imaged within 10–30 minutes after the luciferin administration. Imaging was performed weekly from week 3 until sacrifice at 7 weeks after inoculation.

Gross necropsy was performed on all animals at the end of the study, and all macroscopic signs were recorded. Samples from all tissues with metastases as well as corresponding control tissues with no signs of metastases were harvested, and collected. The tissues were fixed in 10% formalin, bone tissues were decalcified with EDTA, and all were embedded on paraffin (BiositeHisto, Tampere, Finland). 5 μm slides were cut and the tissue sections were deparaffinized and rehydrated for subsequent analyses. Hematoxylin and eosin (H&E) staining was performed using routine procedures.

Immunostainings

Antigen retrieval using citrate buffer was performed. In immunohistochemistry (IHC) with mouse antibodies, M.O.M. kit was used (Vector laboratories, Burlingame, CA, USA). The following primary antibodies were used in IHC: Phospho-Smad1/5/9 (1:200, cat 9511, Cell Signaling Technology, Danvers, MA, USA), Ki67 (1:200, cat KI67-MM1-L-CE-S, Leica Biosystems, Nussloch, Germany) and MECA32 (1:100, cat 550563, BD Biosciences, Franklin Lakes, NJ, USA). The following primary antibodies were used in immunofluorescence (IF): vimentin (1:500, cat 919101, BioLegend, San Diego, CA, USA), keratin 5 (1:500, cat 905501, BioLegend), keratin 14 (1:500, cat 905301, BioLegend) and α-SMA (1:500, cat A2547, Sigma-Aldrich, St. Louis, MO, USA). Antibodies in IHC were diluted in goat or rabbit serum or Normal antibody Diluent (ImmunoLogic, Duiven, the Netherlands) and for IF the dilution was done in 12% BSA. Secondary antibodies for IHC stainings were biotinylated goat anti-rabbit IgG and biotinylated rabbit anti-rat IgG (both at a dilution of 1:100, from Vector laboratories) or Simple Stain MAX PO (MULTI) Universal Immunoperoxidase polymer (Nichirei biosciences, Tokyo, Japan). DAB based detection was used to visualize target proteins. The three secondary antibodies used in IF were goat anti-chicken, anti-rabbit or anti-mouse Alexa Fluor 488 antibody (at a dilution of 1:200, all from Thermo Fisher Scientific). The IHC slides were counterstained with hematoxylin. IF slides were mounted in SlowFade +DAPI (Molecular Probes/Invitrogen) and IHC slides in AquaPolyMount (Polysciences, Inc., Warrington, PA, USA) or dehydrated and mounted in DPX Mountant (VWR, Radnor, PA, USA). Stainings were performed as described [24].

Bone stainings

The tissues were stained with Toluidine blue for bone and cartilage visualization. TRAP (tartrate-resistant phosphatase) staining for osteoclasts was performed by incubation in naphthol AS-BI phosphate solution (cat N-2125, Sigma Aldrich) followed by color reaction in sodium nitrate and pararosaniline dye (cat P-3750, Sigma Aldrich).

Image analysis

IHC and H&E images were taken with an Olympus microscope (Olympus, Tokyo, Japan) connected to Surveyor software (Objective Imaging, Cambridge, UK) and IF images with Zeiss Axio Imager M2 microscope (Carl Zeiss, Oberkochen, Germany) connected to an ApoTome slider module (Carl Zeiss). Quantification of Ki67 data was

performed using the NIH ImageJ software (http://rsbweb.nih.gov/ij/docs/examples/stained-sections/index.html) by calculating the percentage of positively stained areas within the tumor masses.

Statistical analyses

Statistical analyses were performed with statistical software R (version 3.1.0 or newer, www.r-project.org). Linear mixed-effects models and model contrasts were used to evaluate the BLI data. Time to the first metastasis observation was examined using the Kaplan–Meier method and the log-rank test.

Results

MDA-MB-231 cells retain their BMP4-induced migratory capacity after introduction of a luciferase reporter gene

We have previously shown that MDA-MB-231 cells respond to BMP4 treatment with increased migration and invasion, both in 2D and 3D environments [9,15]. Here we used the 3D Matrigel assay, to confirm that this effect was maintained after lentiviral introduction of the luciferase reporter gene into the cells. Identical to the parental cells [15], the luciferase-expressing MDA-MB-231 cells responded to BMP4 administration by forming branching, stellate structures indicative of increased cell mobility (Fig. S1).

BMP4 treatment has a small impact on metastasis formation

Intracardiac injection of MDA-MB-231/Luc breast cancer cells was established to study the effect of BMP4 on metastasis formation. The mice were treated with BMP4 (n = 10) or vehicle control (n = 11) intravenously and metastasis formation was followed by weekly bioluminescence imaging (BLI), starting at week three. The first indications of metastases were observed at day 28 in both groups. There was a slight but non-significant trend of earlier metastasis occurrence in BMP4-treated mice compared to control-treated animals (Fig. 1). According to the BLI data, nine out of ten (90%) animals in the BMP4 group and eight out of eleven (73%) animals in the control group showed signs of metastasis during the course of the experiment.

BMP4 influences the pattern of metastasis sites

Tissues were collected after sacrifice based on BLI data and macroscopic inspection of the animals. Metastases were verified using hematoxylin and eosin (H&E) staining and immunostaining using a pancytokeratin antibody that identifies cells of epithelial origin (Fig. 2). In the BMP4 group, we were unable to histologically ascertain the presence of metastasis in one mouse with positive BLI signal. Thus, a total of 13 metastases were confirmed in the BMP4 treatment group with six animals having two metastases (Table 1). Twelve metastases were observed in the control group with two animals having two and one three metastases (Table 1). Most of the metastases occurred in bone or adrenal glands. Notably, in the BMP4 treatment group there was only one case of adrenal gland metastasis compared to five in the control mice (Table 1). In contrast, there were ten bone metastases in the BMP4 treatment group compared to seven in the control group (Table 1). Of these, the thigh bone was the most common location in both groups with eight metastases (on average 0.8 thigh bone metastases/mouse) in the BMP4 group and five metastases (on average 0.45 thigh bone metastases/mouse) in the control group (Table 1).

Treatment groups show similar tumor cell and stromal features

In order to find out if BMP4 had an effect on the characteristics of tumor cells and the surrounding stroma, the metastatic tissues were stained with a set of markers. SMAD pathway activation was

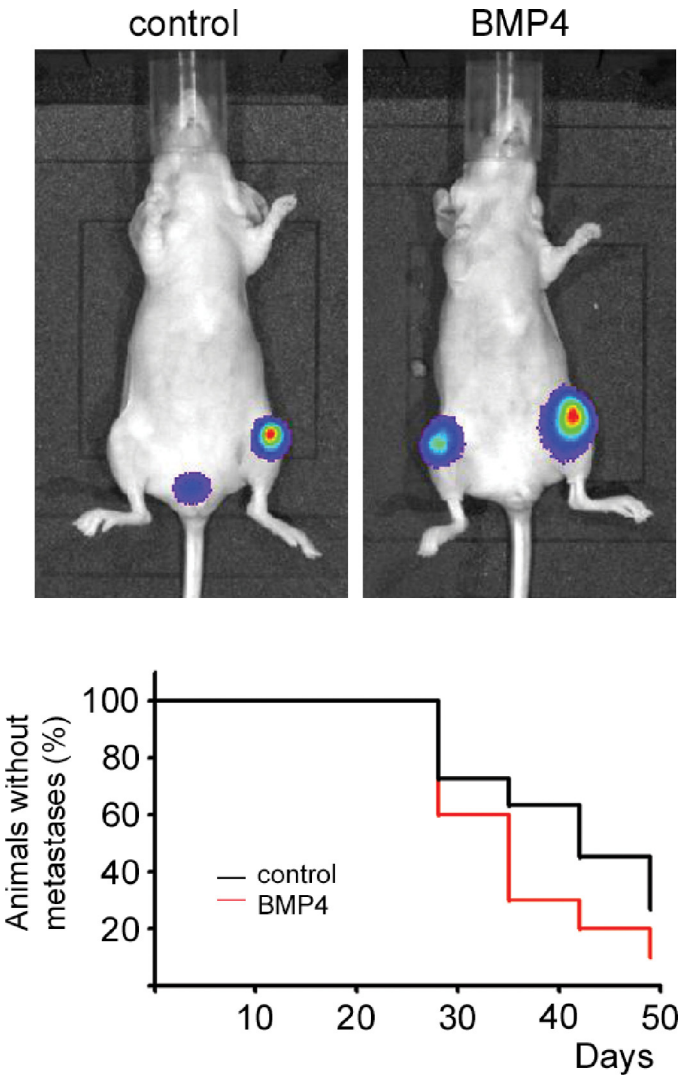

Fig. 1. Metastasis formation according to BLI data. Representative BLI images (top) of control- and BMP4-treated mice on day 49 (sacrifice). The measured photons are shown in a color scale with red as the highest value. The Kaplan–Meier plot (bottom) illustrates the time to first metastasis observation with BLI imaging in BMP4- and control-treated groups.

assessed with phospho-Smad1/5/9 antibody. Strong staining was seen in both BMP4 and control group, but there were no observable differences in the staining intensity (Fig. S2). Strong staining of Ki67 revealed similar proliferation activity in both groups (Fig. 3).

Staining for EMT markers vimentin and E-cadherin showed that, independent of BMP4 stimulation, MDA-MB-231/Luc cells expressed vimentin but not E-cadherin (Fig. 4, data not shown). Keratin 5 (K5, tumor cell marker) stained all MDA-MB-231/Luc cells in both BMP4 and control animals whereas basal cell marker keratin 14 positivity was observed in individual cells in both groups (Fig. 4).

To examine the metastases for possible presence of cancer-associated fibroblasts (CAF), alpha-smooth muscle actin (α-SMA) staining was used. In both treatment groups the α-SMA staining revealed that CAFs were present in the tumor mass but no change in the staining intensity or patterns were detected (Fig. 4).

We also wanted to examine possible changes in the stroma of the metastases. With MECA-32 staining of blood vessels, faint positive signal possibly representing incomplete vessels was observed in the tumor mass in the metastases, compared to regularly structured strongly stained blood vessels in the surrounding tissue.

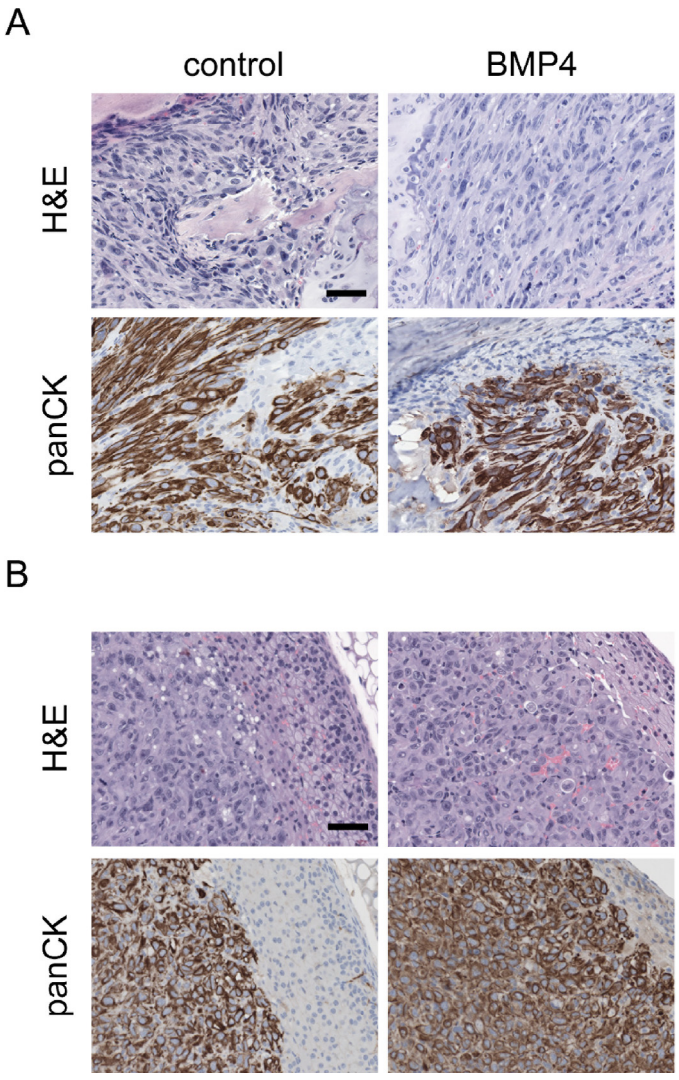

Fig. 2. Identification of tumor cells in mouse tissues using histological analyses. Representative examples of H&E staining and pancytokeratin (epithelial cell marker) IHC staining of (A) bone and (B) adrenal gland samples in control- and BMP4-treated mice. Scale bar 25 μm.

However, no apparent differences were seen between the treatment groups (Fig. 5).

BMP4 treatment does not influence bone morphology

Next we examined the possible effect BMP4 treatment might have had on bone health. Toluidine blue staining was used to visualize bone and cartilage in the epiphyseal plate. In both BMP4 and control groups, the cancer cells disturbed the epiphyseal plates in a similar

Table 1
Metastasis occurrence in BMP4 and control treatment groups.

Number of:	BMP4	Control
Mice	10	11
Metastases	13	12
Soft tissue	3	5
Adrenal gland	1	5
Bone tissue	10	7
Femur	8	5
Metastasis/mouse (max)	2	3
Mice without metastasis	2	3

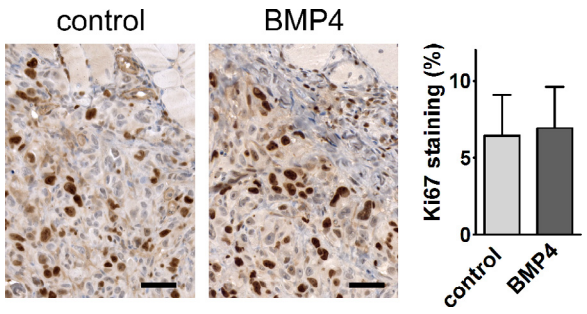

Fig. 3. Characterization of proliferation activity in the tumor samples. Representative images of proliferation marker Ki67 IHC staining (brown color) of bone tissue are shown for control and BMP4 treatment groups. ImageJ was used to quantify the percentage of positive staining within the tumor areas. Scale bar 25 μm.

manner, disrupting the integrity of the plate (Fig. S3). Unexpectedly, TRAP staining (marker for osteoclasts) was seen in the tumor mass in addition to bone tissue (Fig. S4) but again no change was observed between the treatment groups.

Discussion

Despite multiple *in vitro* studies indicating that BMP4 enhances breast cancer cell migration and invasion [9,10,12,13] as well as clinical data demonstrating an association between strong BMP4 expression in the primary tumor and increased frequency of recurrence [11], the specific impact of BMP4 on human breast cancer metastasis formation *in vivo* has not been adequately addressed. There is a single study reporting BMP4-mediated reduction of metastasis formation but using mouse mammary tumor cells [23]. Others have evaluated indirect manipulation of the BMP pathway with contradictory results regarding the effects on metastatic ability [12,14,26,27]. In this study a mouse xenograft model was utilized to evaluate the influence of BMP4 in the metastasis formation of MDA-MB-231 breast cancer cells. In terms of the experimental settings, we used BMP4 pre-treatment of the MDA-MB-231 cells together with subsequent administration of BMP4 through tail vein throughout the course of the experiment. Similar methods with comparable doses have previously been successfully used in the evaluation of the *in vivo* effects of BMPs in other cancer types [18–20,28–31].

A tendency towards accelerated development of metastases was observed in BMP4-treated animals as compared to controls, although statistical significance could not be reached. In addition to this overall trend, there were noticeable differences in the metastasis sites. BMP4-treated mice developed more bone metastases and less adrenal gland metastases than control animals. Adrenal gland metastases are rare in breast cancer, although they do occur particularly in lobular breast carcinomas [32]. Yet, MDA-MB-231 cells were also previously found to form adrenal gland metastases in a rat xenograft model [33]. The fact that BMP4 may inhibit adrenal gland metastasis is intriguing; however, additional studies are needed to confirm this observation. In any case, the overall clinical relevance of this finding is minor. In contrast, the increase in the number of bone metastases after BMP4 treatment, although small, is highly interesting since bone is the most common site of metastasis in human breast cancer. Importantly, our previous clinical data indicated that, in addition to the overall increase in tumor recurrence, 28% of the patients with high BMP4 expression in primary tumor developed bone metastases compared to only 19% of those with low expression [11]. Together these findings may have clinical relevance in identification of breast cancer patients with an elevated risk of bone metastasis. However, while considering the applicability of the data obtained to human disease, one must take into

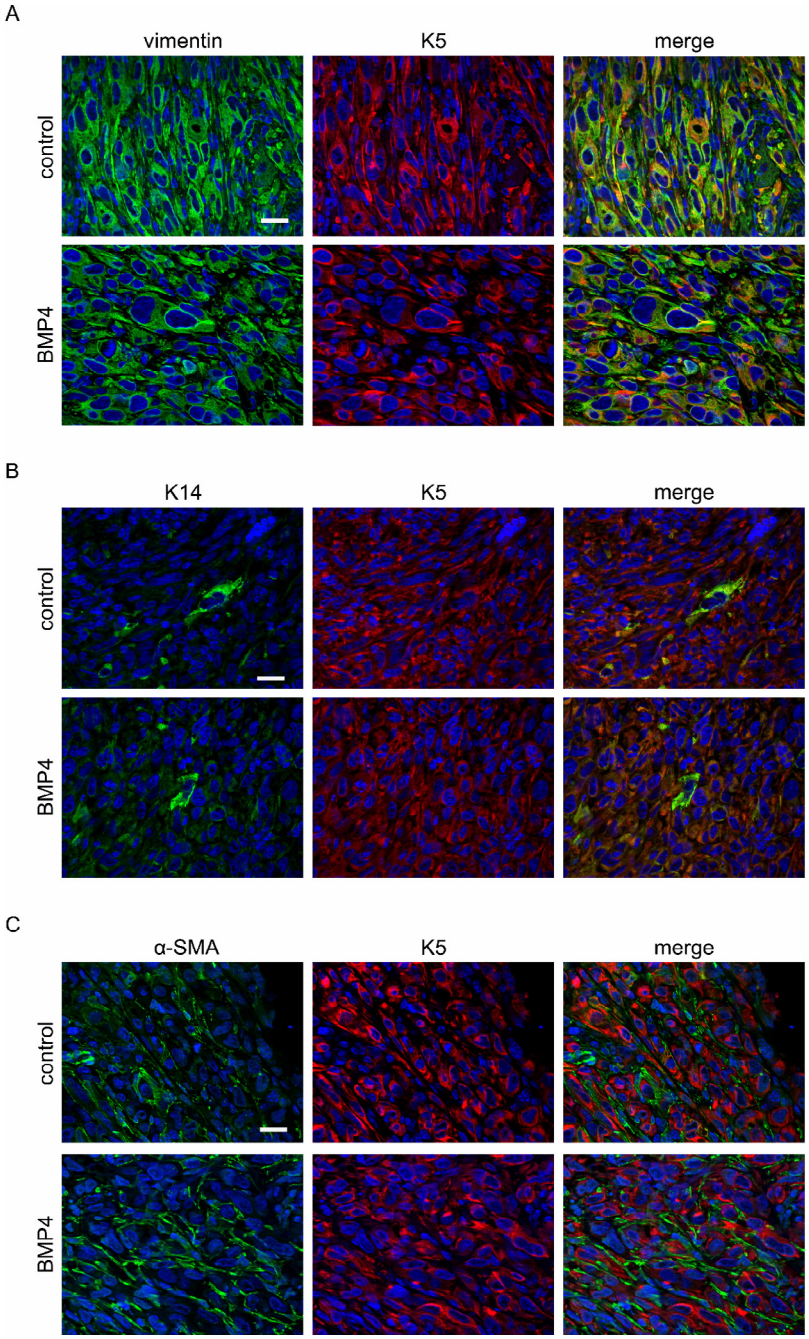

Fig. 4. Immunofluorescence analysis of EMT, basal and stromal cell markers in the control and BMP4 samples. (A) Vimentin (green) staining in bone, (B) K14 basal cell marker (green) staining in adrenal gland and (C) α-SMA cancer-associated fibroblast marker (green) staining in bone. Keratin A (K5, red) is a marker of the tumor cells. Representative images are shown. Scale bar 25 μm.

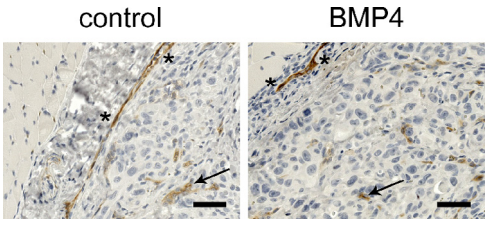

Fig. 5. Characterization of blood vessels in the tumor samples and surrounding stroma. Representative images of endothelial marker MECA32 IHC staining (brown color) of bone tissue are shown for control and BMP4 treatment groups. Asterisks indicate blood vessels in normal tissue and arrows point to irregular vascularization within the tumor tissue. Scale bar 25 μm.

account the short duration (seven weeks) of the study. Metastasis development is a long process and especially in breast cancer may take years, even decades. Unfortunately, it is impossible to fully assess such long-term effects using an animal model.

The intracardiac injection of tumor cells typically leads to bone metastases. Whether the slight elevation in the number of bone metastases in BMP4 treatment group is indicative of increased metastatic ability in general, increased ability to home to bone, or increased ability to survive in bone is presently unknown. Numerous genes or markers have been associated with bone-homing characteristics both in breast cancer and in other tumor types (reviewed in [34]) but the current literature on this subject is still incomplete and at the same time somewhat inconsistent. Our

previous data indicated that the expression levels of several MMPs, including MMP1, are increased in MDA-MB-231 cells upon BMP4 treatment in the 3D Matrigel model [15]. This finding is in line with data demonstrating increased MMP1 expression in MDA-MB-231 subpopulations with high metastatic potential to bone [35]. Recently, we have also shown that BMP4 induces the expression of several genes, such as PMEPA1, NOG, and CXCL1 ([36] and unpublished data), that have been likewise associated with bone metastasis formation [37–39].

BMPs, especially BMP2 and BMP7, are nowadays frequently used in the clinic to treat bone fractures in conjunction with surgery but there are some reservations due to their possible ability to induce cancer [40,41]. BMP4 has also been applied in bone regeneration, although with less efficient results than BMP2 [42,43]. In both BMP4 and control animals, the cancer cells caused massive distortion of the growth plate of the long bones. As already mentioned, slightly more bone metastases were observed upon BMP4 treatment, but BMP4 did not appear to influence the morphological features of the bone metastases. Altogether, the short duration of this study makes it impossible to conclude whether the use of BMP4 may attribute to cancer risk.

Immunostainings confirmed that MDA-MB-231 cells retained their characteristic proliferation rate in the *in vivo* environment, despite the BMP4 treatment. Our previous data showed a small reduction in the growth of MDA-MB-231 cells upon BMP4 treatment in standard 2D culture but no changes in 3D Matrigel, although distinct inhibition of proliferation was seen both in 2D and 3D in several other breast cancer cell lines [9,15]. These findings suggest that the antiproliferative effects of BMP4 are context dependent and, in the case of MDA-MB-231 cells, are counteracted by the cues present in 3D and *in vivo* environments. Previous studies have implicated BMP4 in the induction of EMT, for example, in ovarian and pancreatic cancer as well as in mammary epithelial cells [44–46]. The MDA-MB-231 cells are known to express vimentin and lack the expression of E-cadherin [47] and the *in vivo* environment or the BMP4 treatment did not change this typical mesenchymal phenotype. Thus our data does not provide any additional information on the possible EMT-inducing effects of BMP4 in breast cancer. Strong phospho-SMAD1/5/9 staining was observed in both BMP4 and control metastases. This observation likely reflects the fact that other BMPs also signal through the same pathway [4], which is therefore active irrespective of the BMP4 treatment.

We also assessed the effect of BMP4 on the stromal component of the metastases. Staining with MECA32 revealed structures that likely represent the formation of leaky, incomplete microvascularization in the tumor mass [48]. K14 is known to be expressed by basal myoepithelial and squamous epithelial cells [49] and K14 staining was seen in individual tumor cells in both treatment groups. α-SMA was used as a marker for cancer-associated fibroblasts (CAFs) [50] and the staining indicated that CAFs were equally present in both BMP4 and control samples. Positive staining for TRAP (an osteoclast marker) was seen in the lining of the bone epiphyseal plates but unexpectedly also inside the tumor mass in both BMP4 and control samples. There is some evidence that breast cancer cells express TRAP [51], but in our samples the staining pattern with random positive cells within largely negative tumor mass was quite different from that reported by Adams and colleagues. Thus our result may better correspond to another study reporting osteoclast giant cells in breast tumors [52]. Taken together, these data imply that the BMP4 treatment did not influence the tumor cell characteristics or the stromal composition of the metastases.

In conclusion, this is the first study to assess the direct impact of BMP4 on breast cancer metastasis formation using human cells. The data obtained point towards a slight trend towards accelerated metastasis formation upon BMP4 treatment, although statistical inferences could not be made. In concordance with our previous clinical data [11], BMP4 seemed to increase the occurrence of bone metastases. This finding may have direct clinical relevance since bone is the most common metastasis site for breast cancer. BMP4 treatment did not alter the tumor characteristics of the metastases. Further studies are needed to evaluate the possible long-term effects of BMP4 signaling in breast cancer metastasis formation.

Acknowledgments

We thank Kati Rouhento for her skillful technical aid and Johanna Lappeteläinen for her assistance with immunohistochemistry procedures. This study was supported by grants from the Finnish Cancer Organizations and the Competitive State Research Financing of the Expert Responsibility area of Tampere University Hospital (the unit of FimLab) and the Doctoral Programme in Biomedicine and Biotechnology to MA.

Conflict of interest

We hereby confirm that there are no conflicts of interest regarding our manuscript entitled: The impact of bone morphogenetic protein 4 (BMP4) on breast cancer metastasis in a mouse xenograft model.

Appendix: Supplementary material

Supplementary data to this article can be found online at doi:10.1016/j.canlet.2016.03.008.

References

[1] A.C. Carreira, F.H. Lojudice, E. Halcsik, R.D. Navarro, M.C. Sogayar, J.M. Granjeiro, Bone morphogenetic proteins: facts, challenges, and future perspectives, J. Dent. Res. 93 (2014) 335–345.
[2] C.C. Rider, B. Mulloy, Bone morphogenetic protein and growth differentiation factor cytokine families and their protein antagonists, Biochem. J. 429 (2010) 1–12.
[3] G.Q. Zhao, Consequences of knocking out BMP signaling in the mouse, Genesis 35 (2003) 43–56.
[4] A. Weiss, L. Attisano, The TGFbeta superfamily signaling pathway, Wiley Interdiscip. Rev. Dev. Biol. 2 (2013) 47–63.
[5] K. Miyazono, S. Maeda, T. Imamura, BMP receptor signaling: transcriptional targets, regulation of signals, and signaling cross-talk, Cytokine Growth Factor Rev. 16 (2005) 251–263.
[6] A. Nohe, E. Keating, P. Knaus, N.O. Petersen, Signal transduction of bone morphogenetic protein receptors, Cell. Signal. 16 (2004) 291–299.
[7] E.L. Alarmo, A. Kallioniemi, Bone morphogenetic proteins in breast cancer: dual role in tumourigenesis?, Endocr. Relat. Cancer 17 (2010) R123–R139.
[8] L. Ye, S.M. Bokobza, W.G. Jiang, Bone morphogenetic proteins in development and progression of breast cancer and therapeutic potential (review), Int. J. Mol. Med. 24 (2009) 591–597.
[9] J.M. Ketolainen, E.L. Alarmo, V.J. Tuominen, A. Kallioniemi, Parallel inhibition of cell growth and induction of cell migration and invasion in breast cancer cells by bone morphogenetic protein 4, Breast Cancer Res. Treat. 124 (2010) 377–386.
[10] D. Guo, J. Huang, J. Gong, Bone morphogenetic protein 4 (BMP4) is required for migration and invasion of breast cancer, Mol. Cell. Biochem. 363 (2012) 179–190.
[11] E.L. Alarmo, H. Huhtala, T. Korhonen, L. Pylkkanen, K. Holli, T. Kuukasjarvi, et al., Bone morphogenetic protein 4 expression in multiple normal and tumor tissues reveals its importance beyond development, Mod. Pathol. 26 (2013) 10–21.
[12] A. Pal, W. Huang, X. Li, K.A. Toy, Z. Nikolovska-Coleska, C.G. Kleer, CCN6 modulates BMP signaling via the smad-independent TAK1/p38 pathway, acting to suppress metastasis of breast cancer, Cancer Res. 72 (2012) 4818–4828.
[13] P. Owens, H. Polikowsky, M.W. Pickup, A.E. Gorska, B. Jovanovic, A.K. Shaw, et al., Bone morphogenetic proteins stimulate mammary fibroblasts to promote mammary carcinoma cell invasion, PLoS ONE 8 (2013).
[14] S.K. Shon, A. Kim, J.Y. Kim, K.I. Kim, Y. Yang, J.S. Lim, Bone morphogenetic protein-4 induced by NDRG2 expression inhibits MMP-9 activity in breast cancer cells, Biochem. Biophys. Res. Commun. 385 (2009) 198–203.
[15] M. Ampuja, R. Jokimaki, K. Juuti-Uusitalo, A. Rodriguez-Martinez, E.L. Alarmo, A. Kallioniemi, BMP4 inhibits the proliferation of breast cancer cells and induces an MMP-dependent migratory phenotype in MDA-MB-231 cells in 3D environment, BMC Cancer 13 (2013) 429.
[16] A. Kallioniemi, Bone morphogenetic protein 4-a fascinating regulator of cancer cell behavior, Cancer Genet. 205 (2012) 267–277.

[17] Y. Lombardo, A. Scopelliti, P. Cammareri, M. Todaro, F. Iovino, L. Ricci-Vitiani, et al., Bone morphogenetic protein 4 induces differentiation of colorectal cancer stem cells and increases their response to chemotherapy in mice, Gastroenterology 140 (2011) 297–309.
[18] S. Buckley, W. Shi, B. Driscoll, A. Ferrario, K. Anderson, D. Warburton, BMP4 signaling induces senescence and modulates the oncogenic phenotype of A549 lung adenocarcinoma cells, Am. J. Physiol. Lung Cell. Mol. Physiol. 286 (2004) L81–L86.
[19] T.G. Nishanian, J.S. Kim, A. Foxworth, T. Waldman, Suppression of tumorigenesis and activation of wnt signaling by bone morphogenetic protein 4 in human cancer cells, Cancer Biol. Ther. 3 (2004) 667–675.
[20] S.G. Piccirillo, B.A. Reynolds, N. Zanetti, G. Lamorte, E. Binda, G. Broggi, et al., Bone morphogenetic proteins inhibit the tumorigenic potential of human brain tumour-initiating cells, Nature 444 (2006) 761–765.
[21] H. Zhao, O. Ayrault, F. Zindy, J.H. Kim, M.F. Roussel, Post-transcriptional down-regulation of Atoh1/Math1 by bone morphogenic proteins suppresses medulloblastoma development, Genes Dev. 22 (2008) 722–727.
[22] C.Y. Chiu, K.K. Kuo, T.L. Kuo, K.T. Lee, K.H. Cheng, The activation of MEK/ERK signaling pathway by bone morphogenetic protein 4 to increase hepatocellular carcinoma cell proliferation and migration, Mol. Cancer Res. 10 (2012) 415–427.
[23] Y. Cao, C.Y. Slaney, B.N. Bidwell, B.S. Parker, C.N. Johnstone, J. Rautela, et al., BMP4 inhibits breast cancer metastasis by blocking myeloid-derived suppressor cell activity, Cancer Res. 74 (2014) 5091–5102.
[24] P. Owens, M.W. Pickup, S.V. Novitskiy, J.M. Giltnane, A.E. Gorska, C.R. Hopkins, et al., Inhibition of BMP signaling suppresses metastasis in mammary cancer, Oncogene 34 (2015) 2437–2449.
[25] M.W. Pickup, L.D. Hover, Y. Guo, A.E. Gorska, A. Chytil, S.V. Novitskiy, et al., Deletion of the BMP receptor BMPR1a impairs mammary tumor formation and metastasis, Oncotarget 6 (2015) 22890–22904.
[26] Y. Katsuno, A. Hanyu, H. Kanda, Y. Ishikawa, F. Akiyama, T. Iwase, et al., Bone morphogenetic protein signaling enhances invasion and bone metastasis of breast cancer cells through smad pathway, Oncogene 27 (2008) 6322–6333.
[27] D.P. Hollern, J. Honeysett, R.D. Cardiff, E.R. Andrechek, The E2F transcription factors regulate tumor development and metastasis in a mouse model of metastatic breast cancer, Mol. Cell. Biol. 34 (2014) 3229–3243.
[28] J.T. Buijs, C.A. Rentsch, G. van der Horst, P.G. van Overveld, A. Wetterwald, R. Schwaninger, et al., BMP7, a putative regulator of epithelial homeostasis in the human prostate, is a potent inhibitor of prostate cancer bone metastasis in vivo, Am. J. Pathol. 171 (2007) 1047–1057.
[29] R.H. Farnsworth, T. Karnezis, R. Shayan, M. Matsumoto, C.J. Nowell, M.G. Achen, et al., A role for bone morphogenetic protein-4 in lymph node vascular remodeling and primary tumor growth, Cancer Res. 71 (2011) 6547–6557.
[30] A. Klose, Y. Waerzeggers, P. Monfared, S. Vukicevic, E.L. Kaijzel, A. Winkeler, et al., Imaging bone morphogenetic protein 7 induced cell cycle arrest in experimental gliomas, Neoplasia 13 (2011) 276–285.
[31] R. Tsuchida, T. Osawa, F. Wang, R. Nishii, B. Das, S. Tsuchida, et al., BMP4/thrombospondin-1 loop paracrinically inhibits tumor angiogenesis and suppresses the growth of solid tumors, Oncogene 33 (2014) 3803–3811.
[32] X.J. Liu, P. Shen, X.F. Wang, K. Sun, F.F. Sun, Solitary adrenal metastasis from invasive ductal breast cancer: an uncommon finding, World J. Surg. Oncol. 8 (2010) 7.
[33] T. Yoneda, P.J. Williams, T. Hiraga, M. Niewolna, R. Nishimura, A bone-seeking clone exhibits different biological properties from the MDA-MB-231 parental human breast cancer cells and a brain-seeking clone in vivo and in vitro, J. Bone Miner. Res. 16 (2001) 1486–1495.
[34] U.H. Weidle, F. Birzele, G. Kollmorgen, R. Ruger, Molecular mechanisms of bone metastasis, Cancer Genomics Proteomics 13 (2016) 1–12.
[35] Y. Kang, P.M. Siegel, W. Shu, M. Drobnjak, S.M. Kakonen, C. Cordon-Cardo, et al., A multigenic program mediating breast cancer metastasis to bone, Cancer Cell 3 (2003) 537–549.
[36] A. Rodriguez-Martinez, E.L. Alarmo, L. Saarinen, J. Ketolainen, K. Nousiainen, S. Hautaniemi, et al., Analysis of BMP4 and BMP7 signaling in breast cancer cells unveils time-dependent transcription patterns and highlights a common synexpression group of genes, BMC Med. Genomics 4 (2011) 80.
[37] P.G. Fournier, P. Juarez, G. Jiang, G.A. Clines, M. Niewolna, H.S. Kim, et al., The TGF-beta signaling regulator PMEPA1 suppresses prostate cancer metastases to bone, Cancer Cell 27 (2015) 809–821.
[38] M. Tarragona, M. Pavlovic, A. Arnal-Estape, J. Urosevic, M. Morales, M. Guiu, et al., Identification of NOG as a specific breast cancer bone metastasis-supporting gene, J. Biol. Chem. 287 (2012) 21346–21355.
[39] A.L. Hardaway, M.K. Herroon, E. Rajagurubandara, I. Podgorski, Marrow adipocyte-derived CXCL1 and CXCL2 contribute to osteolysis in metastatic prostate cancer, Clin. Exp. Metastasis 32 (2015) 353–368.
[40] K.W. Lo, B.D. Ulery, K.M. Ashe, C.T. Laurencin, Studies of bone morphogenetic protein-based surgical repair, Adv. Drug Deliv. Rev. 64 (2012) 1277–1291.
[41] K. Schmidt-Bleek, B.M. Willie, P. Schwabe, P. Seemann, G.N. Duda, BMPs in bone regeneration: less is more effective, a paradigm-shift, Cytokine Growth Factor Rev. 27 (2016) 141–148.
[42] X. Gao, A. Usas, A. Lu, Y. Tang, B. Wang, C.W. Chen, et al., BMP2 is superior to BMP4 for promoting human muscle-derived stem cell-mediated bone regeneration in a critical-sized calvarial defect model, Cell Transplant. 22 (2013) 2393–2408.
[43] A. Usas, A.M. Ho, G.M. Cooper, A. Olshanski, H. Peng, J. Huard, Bone regeneration mediated by BMP4-expressing muscle-derived stem cells is affected by delivery system, Tissue Eng. Part A 15 (2009) 285–293.
[44] K.S. Park, M.J. Dubon, B.M. Gumbiner, N-cadherin mediates the migration of MCF-10A cells undergoing bone morphogenetic protein 4-mediated epithelial mesenchymal transition, Tumour Biol. 36 (2015) 3549–3556.
[45] K.J. Gordon, K.C. Kirkbride, T. How, G.C. Blobe, Bone morphogenetic proteins induce pancreatic cancer cell invasiveness through a Smad1-dependent mechanism that involves matrix metalloproteinase-2, Carcinogenesis 30 (2009) 238–248.
[46] B.L. Theriault, T.G. Shepherd, M.L. Mujoomdar, M.W. Nachtigal, BMP4 induces EMT and rho GTPase activation in human ovarian cancer cells, Carcinogenesis 28 (2007) 1153–1162.
[47] L.A. Gordon, K.T. Mulligan, H. Maxwell-Jones, M. Adams, R.A. Walker, J.L. Jones, Breast cell invasive potential relates to the myoepithelial phenotype, Int. J. Cancer 106 (2003) 8–16.
[48] D. Mihic-Probst, K. Ikenberg, M. Tinguely, P. Schraml, S. Behnke, B. Seifert, et al., Tumor cell plasticity and angiogenesis in human melanomas, PLoS ONE 7 (2012).
[49] R. Kordek, P. Potemski, R. Kusinska, E. Pluciennik, A. Bednarek, Basal keratin expression in breast cancer by quantification of mRNA and by immunohistochemistry, J. Exp. Clin. Cancer Res. 29 (2010) 39.
[50] M. Augsten, Cancer-associated fibroblasts as another polarized cell type of the tumor microenvironment, Front. Oncol. 4 (2014) 62.
[51] L.M. Adams, M.J. Warburton, A.R. Hayman, Human breast cancer cell lines and tissues express tartrate-resistant acid phosphatase (TRAP), Cell Biol. Int. 32 (2007) 191–195.
[52] Y. Shishido-Hara, A. Kurata, M. Fujiwara, H. Itoh, S. Imoto, H. Kamma, Two cases of breast carcinoma with osteoclastic giant cells: are the osteoclastic giant cells pro-tumoural differentiation of macrophages?, Diagn. Pathol. 5 (2010) 55.